U.PORTO
FEUP FACULDADE DE ENGENHARIA
UNIVERSIDADE DO PORTO

Integrated Techno-Economic Model: Renewable Gas Integration in Hard-to-Abate Industrial Consumers under RED III and Stochastic EU ETS Evolution

João Santos

Master's Thesis

Supervisor at REN
Prof. Dr. Bruno Henrique Martins dos Santos

Supervisor at FEUP
Prof. Dr. José Luís Alexandre

Master's Degree in Mechanical Engineering
Department of Mechanical Engineering
Faculty of Engineering of the University of Porto
University of Porto

Porto, 5 July 2026

© João Costa Santos, 2026

Integrated Techno-Economic Model: Renewable Gas Integration in Hard-to-Abate Industrial Consumers under RED III and Stochastic EU ETS Evolution

João Santos

Master in Mechanical Engineering

July 5, 2026

Abstract

Renewable gas integration creates a dual challenge for hard-to-abate industrial consumers connected to gas distribution networks: delivered gas composition may trigger physical retrofit needs, while RED III and EU ETS compliance require contractual procurement of certified renewable attributes.

This dissertation develops integrated techno-economic framework that operationalises the physical and contractual dissociation between the gas blend delivered at the industrial site and the renewable content legally attributed through Guarantee of Origin certification. The framework is structured into three sequential models: Model 1 evaluates blend properties, interchangeability criteria, and retrofit triggers; Model 2 translates physical and contractual configurations into annual costs across energy procurement, renewable attributes, and EU ETS compliance; and Model 3 computes NPV, LCDE, CAC, and avoided emissions over a 20-year planning horizon. A Monte Carlo extension then propagates EU ETS carbon-price uncertainty through the full framework using 10,000 simulated trajectories. In addition, this research includes a gap analysis of network-injection perspectives and planning, linking installation-level results with broader renewable gas deployment constraints.

Applied to a continuous container-glass manufacturing facility connected to a (DSO) in northern Portugal, across three biomethane GO premium scenarios anchored to a national normative administrative act auction reference. Results demonstrate that the physical retrofit obligation is modest, a single combustion adaptation of 117 kEUR (thousand euros) triggered in 2037. The binding constraint is the price level at which certified biomethane becomes available domestically. The rationality under a determinist approach, threshold for voluntary procurement ranges from 247 EUR/tCO_2 under current high prices to 93 EUR/tCO_2 under the reference level, against an initial modelled ETS price of 75.36 EUR/tCO_2. Voluntary procurement, under stochastic approach, becomes economically rational between 2028 and 2039 depending on the scenario, with the probability of positive NPV ranging from 26.6% to 78.6% across scenarios. Carbon-price volatility is identified as the dominant source of economic uncertainty, exceeding the inter-scenario spread at the distribution level. Cumulative avoided emissions range from 297 to 1,137 ktCO_2 at the P50 level across scenarios, quantifying the environmental value of renewable gas market development for a single connected installation.

An extended scenario compares network-based RFNBO compliance with in-situ hydrogen electrolysis, demonstrating a capital commitment, or CAPEX differential of 56× and identifying a break-even hydrogen cost decline rate of 4.1%/yr, A framework that is positioned as a proof-of-concept for a DSO-led industrial decarbonisation advisory tool, transferable to any hard-to-abate installation connected to a gas distribution network

Keywords: Biomethane; Hydrogen; Hard-to-abate Industry; Guarantees of Origin; Dissociation; RED III; Monte Carlo simulation; Energy Markets.

Resumo

A integração de gases renováveis cria um duplo desafio para consumidores industriais difíceis de descarbonizar ligados a redes de distribuição de gás: a composição do gás entregue pode exigir retrofit físico, enquanto o cumprimento da RED III e do EU ETS exige a aquisição contratual de atributos renováveis certificados.

Esta dissertação desenvolve um modelo tecnoeconómico integrado que operacionaliza a dissociação físico–contratual entre a mistura gasosa entregue na instalação industrial e o conteúdo renovável legalmente atribuído através de Garantias de Origem. O modelo é estruturado em três componentes sequenciais: o Modelo 1 avalia propriedades da mistura, critérios de intercambiabilidade e triggers de retrofit; o Modelo 2 traduz configurações físicas e contratuais em custos anuais de energia, atributos renováveis e cumprimento do EU ETS; e o Modelo 3 calcula NPV, LCDE, CAC e emissões evitadas ao longo de 20 anos. Uma extensão de Monte Carlo propaga a incerteza do preço de carbono do EU ETS através de 10,000 trajetórias simuladas. Além disso, a investigação inclui uma análise de lacunas sobre perspetivas e planeamento de injeção na rede, ligando resultados ao nível da instalação com restrições mais amplas de implantação de gases renováveis.

Aplicado a uma instalação de produção contínua de vidro de embalagem ligada a um DSO no norte de Portugal, em três cenários de prémio de GO de biometano ancorados numa referência administrativa nacional de leilão, os resultados mostram que a obrigação física de retrofit é modesta: uma única adaptação de combustão de 117 kEUR (milhares euros), ativada em 2037. A restrição principal é o preço a que o biometano certificado se torna disponível domesticamente. Numa abordagem determinística, o limiar de racionalidade para aquisição voluntária varia entre 247 EUR/tCO_2, sob preços elevados, e 93 EUR/tCO_2, no nível de referência, face a um preço inicial modelado do EU ETS de 75.36 EUR/tCO_2. Numa abordagem estocástica, a probabilidade de NPV positivo varia entre 26.6% e 78.6% entre cenários. A volatilidade do preço de carbono é identificada como a principal fonte de incerteza económica, superando a diferença entre cenários ao nível da distribuição. As emissões acumuladas evitadas variam entre 297 e 1,137 ktCO_2 no percentil P50.

Um cenário alargado compara o cumprimento da certificação do RFNBO através da rede com eletrólise do hidrogénio in-situ, demonstrando um diferencial de CAPEX de 56× e identificando uma taxa de redução do custo do hidrogénio de 4.1%/ano como ponto de equilíbrio. O modelo é posicionado como prova de conceito para uma ferramenta de apoio à decisão liderada pelo DSO, transferível para outras instalações difíceis de descarbonizar ligadas a redes de distribuição de gás.

Palavras-chave: Biometano; Hidrogénio; Indústrias pesadas; Garantias de Origem; Dissociação; RED III; Simulação de Monte Carlo; Mercados de Energia.

Acknowledgements

As I reach the end of this very important stage of my life, I want to take a moment to thank all the people who were part of this journey and supported me along the way. Each of them contributed, in different ways, to making this work possible. To all of them, I express my deepest gratitude.

First, I would like to thank REN-Portgás for the excellent welcome and support provided during these months. A special thank you to Luís Duarte and Nelson Sousa for all their guidance, for the inputs provided throughout the development of this dissertation, and also for allowing me to take part in conferences and events that broadened my knowledge, my perspective, and my contact with the energy sector.

I would also like to thank FEUP for being the best academic home I could have chosen. It gave me the foundations, the discipline, and the work ethic that helped me become the dedicated and persistent person I am today.

To Bruno, one of the best people I had the privilege to meet in recent time. His humility, excellence, and dedication are qualities that I deeply admire. More than a supervisor, he became a friend and an example that I will carry with me. I am truly grateful for everything I learned from him, not only as a future professional, but also as a person.

To my FEUP supervisor, Prof. José Luís Alexandre, I would like to express my gratitude for the support provided throughout this work.

To all my friends, who know the important role they had in my life during this process. They were present in moments of anxiety, which are natural in a stage like this, but also in the moments of rest, laughter, and friendship that made everything lighter and more meaningful. Thank you all.

To my grandparents, for all the love, education, and support they have given me throughout this long stage of my life.

To Bruna, for being the closest person during this period and for having the patience to support me in all the small things, which often turn out to be the most important ones. Thank you for making difficult days easier, for believing in me, and for being by my side. Without you, this journey would have been much harder.

Finally, to the two most special people in my life, my mother and my sister. This work is dedicated to them. Without them, I would never have reached this point. They are my greatest support, my greatest example, and the people I know will always be there to share my next achievements.

João Santos

"Intelligence appears to be linked to the complexity with which we can simulate future scenarios."

Michio Kaku

Contents

Contents xi

List of Figures xiii

List of Tables xv

Notation xvii

1 Introduction 1
- 1.1 Context and Motivation . . . 1
  - 1.1.1 RED III Framework . . . 4
  - 1.1.2 Guarantees of Origin . . . 5
  - 1.1.3 Carbon Market Dynamics . . . 8
- 1.2 Case Study Selection and Justification . . . 10
- 1.3 REN-Portgás . . . 11
- 1.4 Research Objectives . . . 12
- 1.5 Dissertation Structure . . . 13

2 State of art 14
- 2.1 Mathematical Thermophysical Basis . . . 15
- 2.2 Biomethane . . . 17
- 2.3 Hydrogen Blending . . . 20
- 2.4 Combined Effects . . . 27
  - 2.4.1 Interchangeability . . . 28
- 2.5 Techno-Economic Models and Policy Instruments . . . 34
- 2.6 Overall Policy Benchmarking . . . 39
  - 2.6.1 National Context . . . 41

3 Methodology 42
- 3.1 Motivation and Analytical Framework . . . 43
- 3.2 Physical Baseline . . . 47
- 3.3 Network Physical Phase Composition . . . 48
- 3.4 Model 1 - Thermophysical Blend Characterisation . . . 49
  - 3.4.1 Gas Mixture Properties . . . 51
  - 3.4.2 Interchangeability Criteria . . . 52
  - 3.4.3 Retrofit Capital Expenditure . . . 52
- 3.5 Model 2 - Operational Expenditure and Renewable Attribute Coverage . . . 54
  - 3.5.1 Physical Energy Cost . . . 55
  - 3.5.2 Renewable Attribute Procurement Cascade . . . 56

3.6 Model 3 - Economic and Carbon Performance Indicators . . . 61
3.6.1 Discounted Cash-Flow Structure . . . 62
3.6.2 Levelised Cost of Decarbonised Energy . . . 62
3.6.3 Avoided Emissions . . . 63
3.6.4 Carbon Abatement Cost . . . 63
3.6.5 Investment Viability Metrics . . . 64
3.7 Market Scenarios Architecture . . . 65
3.8 Monte Carlo Simulations . . . 66
3.9 Model Limitations . . . 69

4 Case Study **71**
4.1 Case Study Overview . . . 71
4.1.1 Network Node Characterisation . . . 72
4.1.2 Installation Characterisation . . . 74
4.2 Model Parameterisation . . . 75
4.2.1 Combustion Retrofit Parameterisation . . . 76
4.2.2 Economic and Regulatory Parameters . . . 77
4.2.3 Market Assumptions . . . 78
4.2.4 Monte Carlo´s Parameterisation . . . 81
4.3 Model Results . . . 83
4.3.1 Deterministic Results . . . 83
4.3.2 Monte Carlo Simulation Results . . . 85
4.3.3 Extended Scenario . . . 88
4.4 Discussion and Validation . . . 92

5 Conclusions **96**
5.1 Policy Implications . . . 99
5.2 Future Works . . . 101

Appendix A– Fundamental Thermophysical and Combustion Properties **103**

Appendix B– Model 1 Computational Implementation **104**

Appendix C– Model 2 Computational Implementation **106**

Appendix D– Model 3 Computational Implementation **108**

Appendix E– Monte Carlo Computational Implementation **110**

Appendix F– EU ETS EUA Annual Volatility Statistics **112**

Appendix G– Deterministic Scenario Outputs **114**

Appendix H– Extended Scenario: Technical and Economic Assumptions **116**

Appendix I– Network Injection Perspectives and Deployment Gaps **119**

References **125**

List of Figures

1.1 Representative hard-to-abate industrial sectors and typical process temperatures [7][6] [8] [9] [10] [11] . . . 2
1.2 Conceptual representation of the Industrial Decarbonisation Trilemma. . . . 3
1.3 Illustration of the GO certification book-and-claim type system [19]. . . . 6
1.4 Scheduled phase-out trajectory of EU ETS free allowances for energy-intensive industries [28–30]. . . . 9
1.5 Evolution of specific energy consumption and crown temperatures in European container glass furnaces over the last century [35]. . . . 11

2.1 Typical biomethane production, certification, distribution, and industrial-use pathway [44]. . . . 17
2.2 Specific fuel consumption of natural gas and biomethane as a function of inlet gas temperature for fluidised-bed drying [17] . . . 18
2.3 Gas emissivity per furnace section for natural gas and biomethane combustion products [13]. . . . 19
2.4 Specific enthalpy of combustion gases as a function of temperature for natural gas and a biomethane-natural gas [13]. . . . 20
2.5 Effect of 0%, 10%, and 20% H_2 blending on Wobbe Index and relative density of Portuguese natural gas[39]. . . . 22
2.6 Laminar burning velocity and adiabatic flame temperature as a function of hydrogen volume fraction in natural gas blends [48]. . . . 24
2.7 Flashback index variation with hydrogen addition in NG–H_2 mixtures [48]. . . . 24
2.8 Evolution of Weaver-based interchangeability indices for natural gas-hydrogen blends as a function of hydrogen volume fraction, adapted from Shkarovskiy et al. [9]. . . 31
2.9 Renewable gas policy decision windows and compliance horizons . . . 40

3.1 Main drivers of the analytical framework. Source: own elaboration. . . . 44
3.2 Model architecture and sequential execution pipeline. . . . 46
3.3 Illustrative evolution of hydrogen and biomethane volume fractions across network phases P_0–P_3. . . . 49
3.4 Model 1 Flowchart . . . 50
3.5 Model 2 Flowchart . . . 55
3.6 Sequential renewable attribute procurement cascade combining eligible RFNBO coverage, mandatory biomethane procurement, and additional economically justified renewable coverage. . . . 57
3.7 Model 3 Flowchart . . . 61

4.1 Typical process chain in container-glass manufacturing [35]. . . . 71
4.2 Evolution of thermophysical properties across network phases. . . . 74

List of Figures

4.3 RED III compliance trajectories adopted in the case study, with the dashed extension beyond 2035 indicating uncertainty in future RFNBO targets [3]. 77
4.4 Simulated EU ETS carbon-price trajectories under the GBM parameterisation. . 82
4.5 Biomethane rationality thresholds under three scenarios compared with the mean EU ETS carbon-price trajectory. 84
4.6 Monte Carlo NPV distribution relative to Baseline $B0$ under scenarios S_1, S_2, and S_3. 85
4.7 Monte Carlo distribution of carbon abatement cost across biomethane scenarios. . 86
4.8 Monte Carlo distribution of cumulative avoided emissions over the 2026–2045 planning horizon. 87
4.9 Sensitivity of $\Delta LCDE$ to the annual decline rate of the total hydrogen contract price. 90

F.1 Historical evolution of EU Allowance prices between 2018 and 2025, based on the daily closing-price series used for the estimation of annualised carbon-price volatility. 112
G.1 Annual deterministic outputs for Scenario S_1. 114
G.2 Annual deterministic outputs for Scenario S_2. 115
G.3 Annual deterministic outputs for Scenario S_3. 115
I.1 Injection capacity vs RED III minimum obligation, H_2B subcenario. 120
I.2 Injection capacity vs RED III minimum obligation, H_2A subcenario. 120
I.3 Supply-demand gap decomposition, H_2B subcenario. 121
I.4 Supply-demand gap decomposition, H_2A subcenario. 121
I.5 Compliance gap summary at key horizons [TWh/yr]. 123

List of Tables

1.1 RED III provisions relevant to industrial renewable-gas compliance. 5

2.1 Methods and criteria used for gas interchangeability assessment [59]. 29
2.2 Summary of interchangeability criteria applicable to renewable gas blends in Group H distribution networks. 32

3.1 EU ETS free-allocation phase-out trajectory [82]. 59

4.1 Projected network phase composition for renewable gas injection. 73
4.2 Industrial installation specifications used for model parameterisation. 75
4.3 Specific combustion retrofit costs adopted in the case study. 76
4.4 Financial parameters adopted in the case study. 77
4.5 Regulatory and carbon-market parameters adopted in the case study. 78
4.6 Reference values for the deterministic network gas price trajectory. 79
4.7 Biomethane GO premium and rationality threshold by scenario and reference year. 80
4.8 Hydrogen GO premium and rationality threshold by reference year. 81

A.1 Fundamental thermophysical and combustion properties adopted for hydrogen, pure methane, and Portuguese natural gas. 103
F.1 Annual EU ETS EUA price statistics and realised volatility from 2018 to 2025 [87]. 113
H.1 Technical and economic parameters adopted in the extended scenario. 116

Notation

Acronyms and Abbreviations

BPA	Biomethane Purchase Agreement
CAC	Carbon Abatement Cost
CAPEX	Capital Expenditure
CBAM	Carbon Border Adjustment Mechanism
CCS	Carbon Capture and Storage
CfD	Contract for Difference
CF	Capacity Factor
CO_2	Carbon Dioxide
CO_2e	Carbon Dioxide Equivalent
CUI	Código Universal de Instalação
DCF	Discounted Cash Flow
DGEG	Direção-Geral de Energia e Geologia
DSO	Distribution System Operator
ENTSO-G	European Network of Transmission System Operators for Gas
EU	European Union
EUA	European Union Allowance
EU ETS	European Union Emissions Trading System
FID	Final Investment Decision
GBM	Geometric Brownian Motion
GO	Guarantee of Origin
H_2	Hydrogen
HHV	Higher Heating Value
IEA	International Energy Agency
IRENA	International Renewable Energy Agency
LCDE	Levelised Cost of Decarbonised Energy
LCOH	Levelised Cost of Hydrogen
LHV	Lower Heating Value
LNEG	Laboratório Nacional de Energia e Geologia
MSR	Market Stability Reserve
NPV	Net Present Value
OPEX	Operational Expenditure
PAB	Plano de Ação para o Biometano
PEM	Proton Exchange Membrane
PNEC	Plano Nacional Energia e Clima
PPA	Power Purchase Agreement

PRR	Plano de Recuperação e Resiliência
RED III	Renewable Energy Directive III
REN	Redes Energéticas Nacionais
RFNBO	Renewable Fuel of Non-Biological Origin
RMSA-G	Relatório de Monitorização da Segurança de Abastecimento do Sistema Nacional de Gás
TNAC	Total Number of Allowances in Circulation
TOTEX	Total Expenditure
TSO	Transmission System Operator
WACC	Weighted Average Cost of Capital
WI	Wobbe Index

Symbols and Subscripts

General symbols

A	Free allowances allocated under the EU ETS
$B0$	Physical fossil-exposure baseline
C	Annual cost component
DF	Discount factor
ΔEF	Emission-factor reduction
ΔEm	Avoided emissions
E	Energy quantity or annual energy demand
EF	Emission factor
Em	Emissions attributed to a pathway or baseline
f	Fraction of energy or coverage share
J_A	Primary-air ratio
J_H	Heat-input ratio
J_{HT}	Absolute hydrogen fraction threshold
k	Network phase index
L	Retrofit level
M	Molecular weight
p	Energy, certificate, or contract price
P	Price, installed capacity, or power-related variable
r	Discount rate
S	Biomethane market scenario
SG	Specific gravity
t	Year index
T	Planning horizon
V	Volume or molar volume
WI	Wobbe Index
x	Molar or volumetric fraction of a gas component

Subscripts and modifiers

a	Reference or admitted gas condition, where applicable
Bio	Biomethane
$comb$	Combustion system
$elec$	Electrolyser or electricity-related variable
eff	Effective value after renewable attribution

ETS	EU ETS carbon-compliance layer
$free$	Free allowances
gas	Network gas
GO	Guarantee of Origin
H_2	Hydrogen
i	Generic gas component or scenario index
k	Network phase index
$L1, L2, L3$	Retrofit levels
mix	Gas mixture
NG	Fossil natural gas
s	Substitute gas
t	Year index
$total$	Total contract price or total value
$uncov$	Energy not covered by renewable attributes
$util$	Useful energy demand

Greek Symbols

α	Contractual renewable coverage share or retrofit cost coefficient
η	Efficiency
λ	Renewable gas procurement rationality threshold
μ	Annual drift parameter of the GBM carbon-price process
ρ	Gas density
σ	Annual volatility parameter of the GBM carbon-price process
ϕ	Fraction of EU ETS free allowances retained

Chapter 1

Introduction

1.1 Context and Motivation

Over the last decade, European climate strategy has undergone a fundamental transformation. What was once largely framed as aspirational target-setting has progressively been replaced by binding, sector-specific obligations linked to enforceable timelines. Through the Fit for 55 package, adopted in 2021, the European Union (EU) defined a pathway towards climate neutrality by 2050 [1]. The 2022 energy crisis, triggered by Russia's invasion of Ukraine, accelerated this transition. Although long-term climate objectives remained unchanged, Europe's dependence on imported fossil fuels became increasingly visible as a structural vulnerability, turning energy security from a long-term planning concern into an immediate political priority [1].

REPowerEU (COM/2022/230) was introduced as a direct policy response. It mobilised close to 300 billion euros and positioned renewable gases, particularly biomethane and green hydrogen, as strategic energy carriers for industrial decarbonisation rather than short-term substitute fuels [2]. This policy direction was subsequently consolidated through binding provisions in the recast of the late Renewable Energy Directive III (RED III), translating political ambition into obligations that also apply to the industrial sector [3].

Against this regulatory backdrop, the most demanding decarbonisation challenge falls on hard-to-abate industries. Ceramics, glass, cement, and primary metals are particularly relevant, not only because they require very high process temperatures, but also because heat must be supplied with a specific thermodynamic grade and combustion profile. Kilns, furnaces, and high-temperature reactors often require tightly controlled radiative flame behaviour, defined combustion atmospheres, and high-exergy heat inputs, which direct electrification cannot provide without major equipment-level process modifications [4–6].

For these industrial users, electrification is therefore not always a practical near-term route under current regulatory timelines. Process temperatures commonly exceed 900 °C, plants are often designed for continuous operation, and product quality may depend directly on combustion-atmosphere composition. As a result, direct electrification can be technically constrained or economically disruptive in the short to medium term [5, 6].

1.1. Context and Motivation

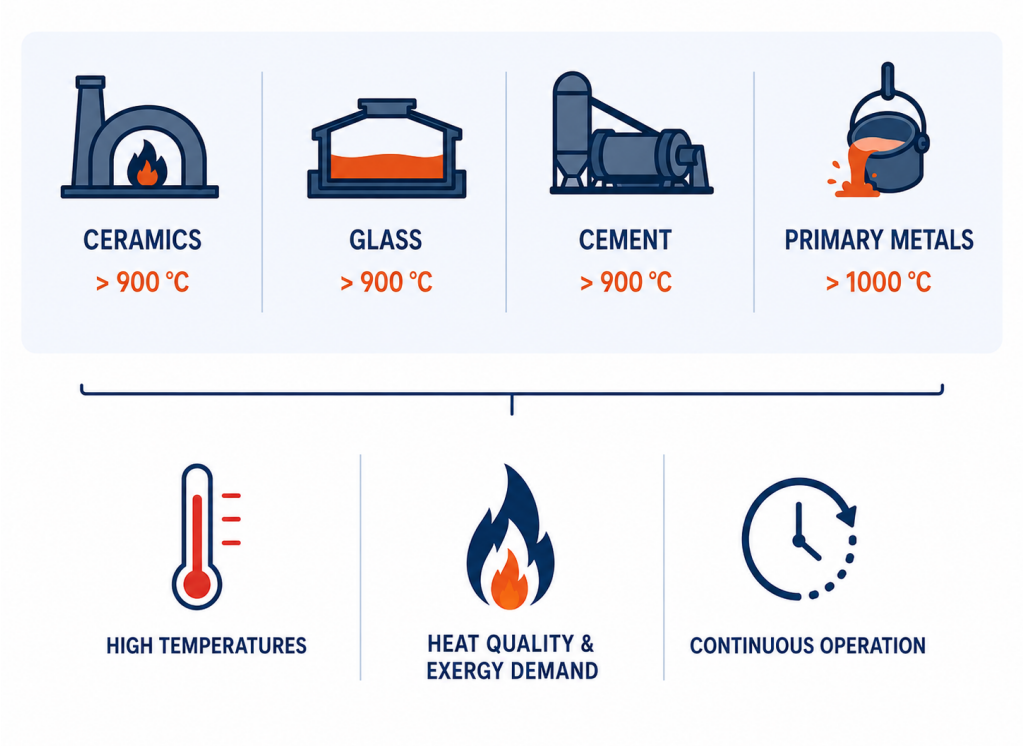


Figure 1.1: Representative hard-to-abate industrial sectors and typical process temperatures [7][6] [8] [9] [10] [11]

Renewable gases therefore occupy a central role in the decarbonisation of these sectors, mainly because they provide a technically continuous pathway that can operate within existing infrastructure constraints while responding to increasingly stringent regulatory timelines [12]. Biomethane is produced from organic residues and, once upgraded to grid-quality standards, can be injected into existing natural gas networks as a near drop-in substitute [7]. In practice, this allows combustion behaviour to remain largely compatible while reducing fuel carbon intensity [13]. Green hydrogen, produced through electrolysis using renewable electricity, can further reduce fossil carbon content in the delivered fuel, particularly as blending shares increase [14].

From this perspective, the natural gas distribution system, progressively supplied with renewable gases, becomes a practical decarbonisation pathway. It can support thermal process continuity while aligning with RED III requirements of the European Union Emissions Trading System (EU ETS) trajectory.[3, 15].

The set of conditions under which this gas-based pathway can remain technically admissible, regulatorily compliant, and economically viable for a hard-to-abate installation is defined in this thesis as the **Industrial Decarbonisation Trilemma**. This concept is based on three simultaneous constraints, none of which can be fully offset by overperformance in another dimension. **Regulatory compliance** requires progressive alignment with RED III renewable gas certification requirements while also accounting for rising carbon costs as EU ETS free allocations decline. **Physical continuity** requires injected blends to remain within admissible interchangeability boundaries, once these limits are exceeded, retrofits, operational changes, or equipment replacement may become unavoidable. **Economic competitiveness** requires total decarbonisation costs to remain compatible with prevailing market conditions, ensuring that compliance and fuel switching do not undermine the industrial site's ability to compete.[10]

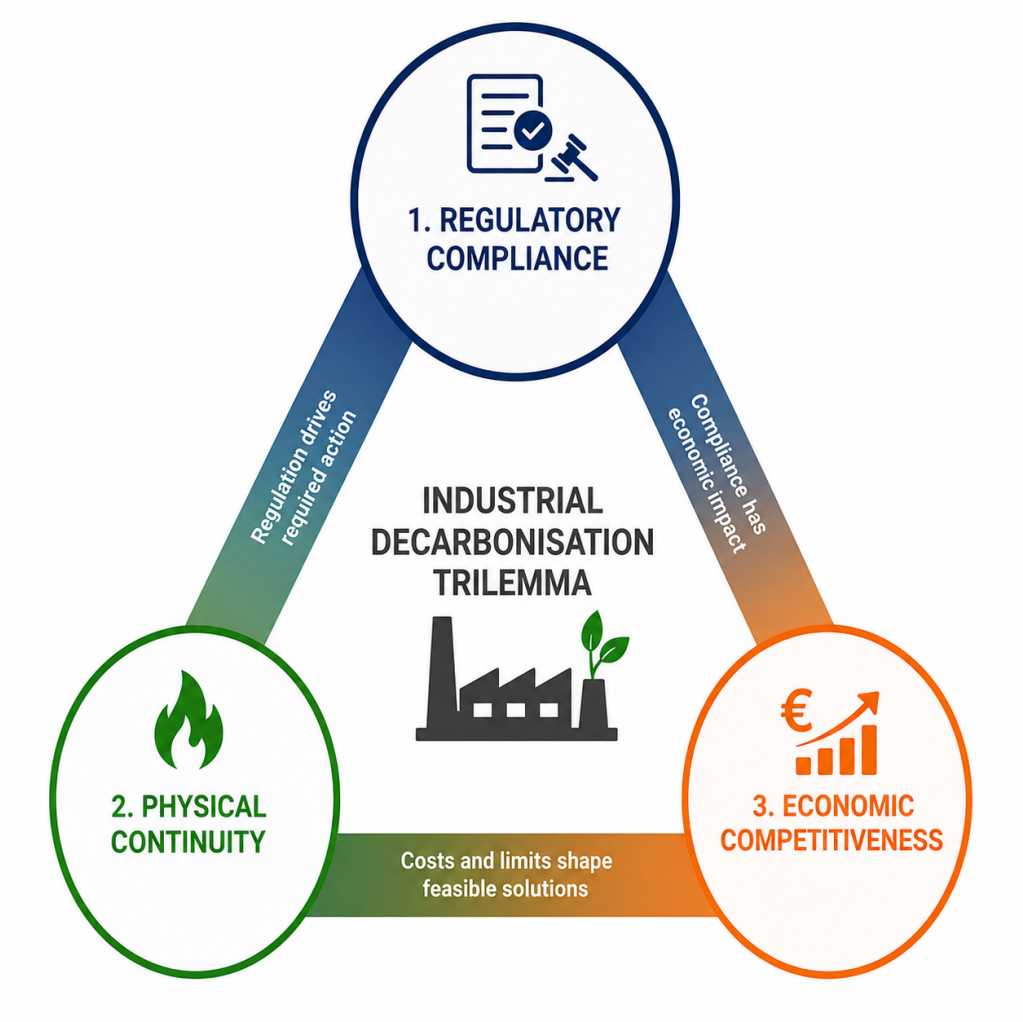


Figure 1.2: Conceptual representation of the Industrial Decarbonisation Trilemma.

Given the interdependence of these constraints, addressing them in isolation or sequentially is inadequate. To the best of the author's knowledge, existing literature does not provide a published model that explicitly captures these interactions at the level of an individual industrial site connected to a gas distribution network. Consequently, this study develops an integrated techno-economic framework that extends beyond cost estimation to offer a structured analytical basis for assessing industrial decarbonisation under concurrent physical, regulatory, and economic constraints.

The proposed methodology assesses the transition by initially identifying physical gas interchangeability limits that may necessitate equipment modifications. Subsequently, it estimates total decarbonisation costs over a specified time horizon, incorporating regulatory objectives and market uncertainties. In addition, a stochastic simulation framework is introduced to represent the uncertain evolution of key economic and regulatory drivers, thereby capturing the spectrum of future conditions that **industrial operators** and **network planners** must consider when making current investment decisions.

The methodology is subsequently applied to a case study within a distribution system operator (DSO) network, with a focus on hard-to-abate industrial gas consumers. Under RED III obligations and projected EU ETS carbon price trajectories, the framework offers practical guidance for

industrial decision-making and facilitates coordination between site-level decarbonisation strategies and long-term energy distributor planning.

1.1.1 RED III Framework

The Renewable Energy Directive III (RED III), established by Directive (EU 2023/2413), defines the revised European legal framework for accelerating renewable energy deployment across the Union. It raises the binding EU-wide renewable energy target to at least 42.5% of gross final energy consumption by 2030, with an indicative ambition of reaching 45%. RED III also introduces sector-specific provisions for key end-use sectors, including industry, heating and cooling, transport, and renewable fuels of non-biological origin (RFNBOs) [3].

RED III is particularly relevant for industrial applications because it links renewable energy deployment to both general industrial decarbonisation objectives and RFNBO-specific compliance requirements. One of the articles requires Member States to seek an indicative average annual increase of 1.6 percentage points in the share of renewable sources used for final energy and non-energy purposes in industry [3]. This provision establishes a regulatory basis for modelling a progressive renewable energy trajectory in industrial energy use, rather than treating renewable gas integration as a purely voluntary procurement decision [1]. Such a regulatory shift is especially important for hard-to-abate industries that rely predominantly on natural gas for high-temperature process heat, since compliance increasingly requires the integration, certification, or procurement of renewable energy carriers within industrial energy supply.

Beyond the broader industrial renewable energy trajectory, RED III introduces a specific sub-target for RFNBOs associated with hydrogen use in industry. Member States are required to ensure that RFNBOs account for at least 42% of hydrogen used for **final energy and non-energy purposes** in industry by 2030, increasing to 60% by 2035 [3]. This obligation applies exclusively to hydrogen and is examined further in Section 1.1.2. It refers to the energy content of eligible hydrogen use, rather than to total industrial energy demand or overall natural gas consumption.

The denominator of this obligation excludes specific hydrogen streams, including hydrogen used as an intermediate product in the production of conventional transport fuels and biofuels, hydrogen generated from the decarbonisation of industrial residual gases when substituting those gases, and hydrogen produced as a by-product or derived from by-products in industrial installations [3]. This distinction is particularly relevant for sectors such as fertiliser production and other agricultural value chains, where hydrogen already serves as a feedstock, as well as for hard-to-abate industries that may increasingly use hydrogen as an energy carrier to decarbonise high-temperature industrial processes [16].

This distinction is one of the central to the modelling framework adopted in this study, explicited later. Hydrogen contained in a distribution-network blend is first treated as a physical component of the gas mixture, affecting lower and higher heating values, specific gravity, Wobbe Index, volumetric flow requirements, combustion behaviour, and retrofit needs [7, 17]. Separately, where hydrogen is considered eligible under RED III accounting rules, the RFNBO requirement is represented as a regulatory constraint applied to the eligible hydrogen energy content. Therefore, physical hydrogen blending and RFNBO compliance are not assumed to be equivalent.

Table 1.1 summarises the RED III provisions most relevant to the proposed analytical framework.

Table 1.1: RED III provisions relevant to industrial renewable-gas compliance.

Provision	Legal basis	Requirement	Timeline
EU-wide renewable target	Art. 3	42.5% of gross final energy consumption	2030
Indicative EU ambition	Art. 3	45% of gross final energy consumption	2030
Industrial renewable ramp-up	Art. 22a	+1.6 pp/year in industrial renewable use	2021–2030
RFNBO hydrogen sub-target	Art. 22a	42% of eligible industrial H_2 use	2030
RFNBO hydrogen sub-target	Art. 22a	60% of eligible industrial H_2 use	2035
Guarantees of Origin	Art. 19	Certification of renewable energy attributes	–

At the time of writing, Portugal had not yet completed the full transposition of RED III into national law. The modelling framework therefore treats RED III as the European regulatory reference and assumes that the relevant industrial renewable-energy and RFNBO provisions will be implemented through national compliance, certification, procurement, and traceability mechanisms [3, 18].

This assumption is necessary to establish the regulatory baselines adopted in the case study. However, final allocation rules for network-blended renewable gases may depend on the Portuguese transposition process and on future regulatory guidance. Similarly, potential penalties or enforcement mechanisms are treated as sources of national regulatory uncertainty rather than fixed modelling inputs, since their design may only be defined through future legislation or regulatory decisions.

1.1.2 Guarantees of Origin

Building on the certification and traceability framework established under earlier EU renewable energy directives, RED III further reinforces the role of Guarantees of Origin (GOs) in renewable energy accounting, as a viable option to decarbonization these type of industries. GOs are standardised and tradable electronic certificates, each representing one megawatt-hour (MWh) of energy produced from renewable sources. Sustainability and greenhouse-gas saving criteria serve a distinct function, determining whether renewable fuels are eligible to contribute towards the renewable energy targets established under the Directive [3].

Within European gas networks, it is not possible to trace a specific renewable gas molecule from its injection point to an individual industrial consumer. The book-and-claim GO system illustrated in Figure 1.3 addresses this limitation by legally separating the physical gas flowing through the network from its associated renewable attributes. An industrial installation may therefore consume a mixed gas blend at the burner while purchasing GOs to certify that an equivalent share of its energy demand is covered by renewable energy attributes [3, 19].

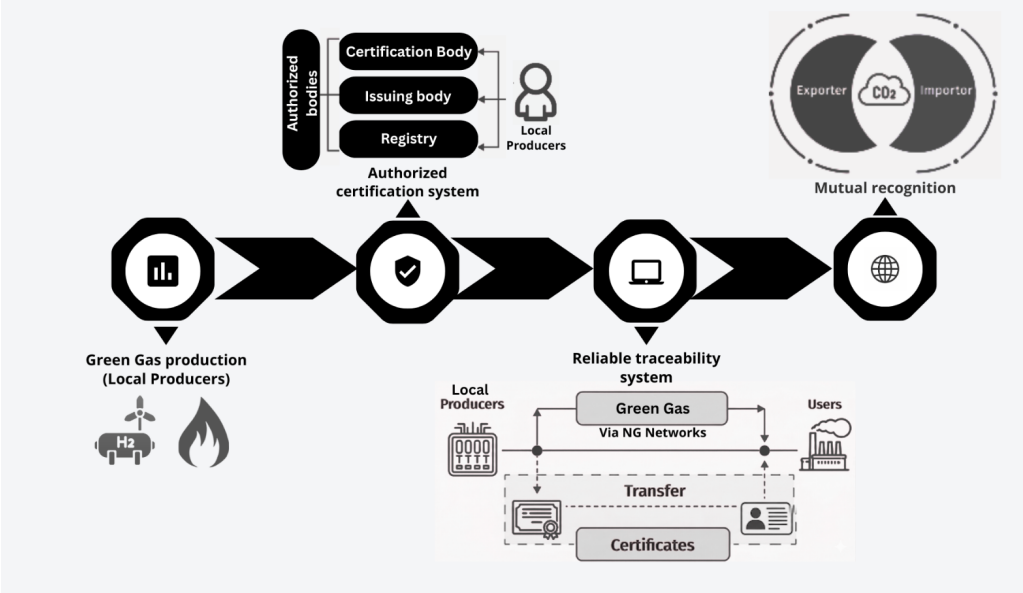


Figure 1.3: Illustration of the GO certification book-and-claim type system [19].

Beyond their accounting function, GOs can also operate through a registry-based market infrastructure that enables the issuance, transfer, import, export, and cancellation of renewable energy attributes. Within the European context, this creates an internal market for renewable attributes in which certified biomethane or renewable gas production in one location can be contractually allocated to a consumer in another location, subject to the rules of the relevant issuing body, registry, sustainability certification scheme, and national implementation framework [20].

This market-based transfer mechanism is essential for gas networks, since it allows industrial consumers to procure renewable gas attributes without requiring a direct physical connection to the specific production site. However, the credibility of such claims depends on robust certificate tracking, avoidance of double counting, and the cancellation of the GO once the renewable attribute has been claimed [20].

The treatment of guarantees of origin also draws on the more mature experience of the electricity sector, where renewable generation was integrated earlier and certificate-based accounting systems are already more established [21, 22].

However, the transfer of this logic from electricity to renewable gases is not straightforward. Electricity is physically indistinguishable once injected into the grid, and individual electrons cannot be traced from a specific generation asset to a final consumer. GOs therefore operate entirely as a contractual accounting mechanism that allocates renewable generation attributes independently of the physical electricity consumed [23].

Renewable gases differ fundamentally because they retain measurable physical properties after injection, including chemical composition, calorific value, density, and combustion behaviour. Their certification must therefore interact not only with registry, transfer, cancellation, and disclosure procedures, but also with fuel composition, sustainability criteria, network injection, mass-balance rules, gas-quality requirements, and carbon-accounting obligations [21]. As a result, the electricity GO model provides an important institutional precedent, but it cannot be transferred directly to biomethane or renewable hydrogen without additional technical and regulatory safeguards.

The application of certificate-based accounting to renewable hydrogen requires a separate qualification. Renewable hydrogen may be traced through different chain-of-custody approaches, in-

cluding physical segregation, mass balance, and book-and-claim systems [23]. Under physical segregation, renewable hydrogen remains separated from non-renewable hydrogen throughout the supply chain. Under mass-balance accounting, certified and non-certified hydrogen may be physically mixed, provided that the corresponding renewable quantities and attributes are consistently tracked across the relevant system boundary. Book-and-claim approaches allow the renewable attribute to be transferred independently of the physical hydrogen molecule [23].

In other side, a hydrogen guarantee of origin may provide evidence of renewable production, but it does not automatically demonstrate compliance with all RFNBO eligibility requirements under RED III. RFNBO recognition may also depend on additional criteria related to renewable electricity sourcing, temporal and geographical correlation, additionality, greenhouse-gas savings, and the applicable national implementation framework [3, 24].

The hydrogen fraction physically delivered through the gas network is treated as a component of the fuel blend and determines thermophysical properties, combustion behaviour, and equipment compatibility. By contrast, the renewable status attributed to that hydrogen is treated contractually through the applicable certification and RFNBO accounting requirements [24] **Physical hydrogen blending, hydrogen guarantees of origin, and RFNBO compliance are therefore non-equivalent dimensions.**

In conclusion, although renewable gas certification is more complex than electricity-based accounting, physical delivery and contractual attribution can still be separated through appropriate traceability and accounting mechanisms. For biomethane, book-and-claim systems allow renewable attributes to be allocated independently of the gas physically supplied to the industrial consumer. Renewable hydrogen may follow a similar approach, although recognition for compliance purposes depends on the applicable chain-of-custody method and on fulfilment of the additional RFNBO eligibility criteria.

Such mechanisms are particularly relevant under RED III, since dedicated renewable gas infrastructure for each industrial off-taker is unlikely to be feasible within European decarbonisation timelines. [19, 25].

Asymmetric Treatment of Biomethane and Hydrogen RFNBOs

As evidenced, biomethane and renewable hydrogen cannot be treated as equivalent renewable gas options under RED III. Although both may contribute to industrial decarbonisation, their certification, allocation, physical effects, and compliance functions differ substantially [3]. This asymmetry is particularly relevant for industrial facilities connected to gas distribution networks, where the physical composition of the delivered gas may not coincide directly with the renewable attributes recognised for compliance purposes.

For biomethane, certified renewable attributes may be allocated to downstream consumers through recognised chain-of-custody mechanisms, including guarantees of origin and mass-balance accounting, subject to the applicable national rules. Since biomethane is chemically equivalent to pure methane once it satisfies the relevant gas-quality requirements, its decarbonisation value is primarily established through certified origin and lifecycle greenhouse-gas accounting rather than through a distinguishable change in local combustion chemistry [26].

Renewable hydrogen requires a more restrictive treatment, since when injected into interconnected gas infrastructure may be traced through a mass-balance system, provided that the applicable certification and allocation requirements are satisfied. However, the sustainability and greenhouse-gas saving characteristics of RFNBO hydrogen cannot simply be reassigned to the nat-

ural gas fraction consumed by an industrial installation. Moreover, a hydrogen guarantee of origin does not, by itself, demonstrate compliance with all RFNBO eligibility requirements [24].

The distinction also extends to combustion. Biomethane and fossil methane produce similar combustion products at the point of use, although their lifecycle greenhouse-gas impacts differ according to feedstock, production, and certification conditions. Hydrogen combustion does not generate direct carbon dioxide emissions, but its renewable contribution depends on whether the hydrogen satisfies the applicable RFNBO production, certification, and accounting criteria [24, 26].

Consequently three RFNBO supply pathways may therefore be considered for industrial consumers [24, 27]:

- **On-site renewable hydrogen production.** Hydrogen is produced and consumed within the industrial site, establishing a direct connection between certified renewable production and final use.
- **Dedicated hydrogen supply.** Hydrogen is supplied through dedicated infrastructure connected to an eligible RFNBO producer, preserving a clearly identifiable physical hydrogen stream.
- **Blended network hydrogen with certified accounting.** Renewable hydrogen is injected into an interconnected gas network and delivered as part of a blended gas stream. Its recognition for compliance purposes depends on the applicable mass-balance, certification, and allocation rules, rather than solely on the presence of hydrogen within the physical blend [23].

The blended-network pathway is particularly relevant to this analysis because the hydrogen physically present in the gas supplied to an industrial consumer may not be fully recognised as RFNBO consumption. Therefore treating physical hydrogen blending and regulatory compliance separately, distinguishing the hydrogen fraction that can affect fuel properties and equipment operation from the certified renewable hydrogen considered for RED III compliance and procurement costs.

1.1.3 Carbon Market Dynamics

The European Union Emissions Trading System (EU ETS) is based on a cap-and-trade framework, which establishes an aggregate emissions ceiling for regulated installations. Allowances are allocated through a combination of free allocation and auctioning. Energy-intensive industries generally face high carbon-abatement costs and act as structural price takers in the allowance market [15]. The 2023 reform of the EU ETS, implemented through Directive (EU) 2023/959, strengthens the system by introducing an annual linear reduction factor of 4.3% until 2027 and 4.4% from 2028 to 2030. The reform aims to achieve a 65% reduction in covered emissions by 2030 relative to 2005 levels [28–30].

Free allowances for industrial installations will be gradually phased out between 2026 and 2034. Installations that previously operated under extensive free-allocation protection now face a narrowing transition period in which verified emissions may exceed allocated entitlements, turning carbon exposure into direct financial expenditure. Even installations currently receiving sufficient free allocation may experience implicit carbon costs, since surrendering allowances entails the opportunity cost of using tradeable assets [15]. The planned phase-out trajectory is shown in Figure 1.4.

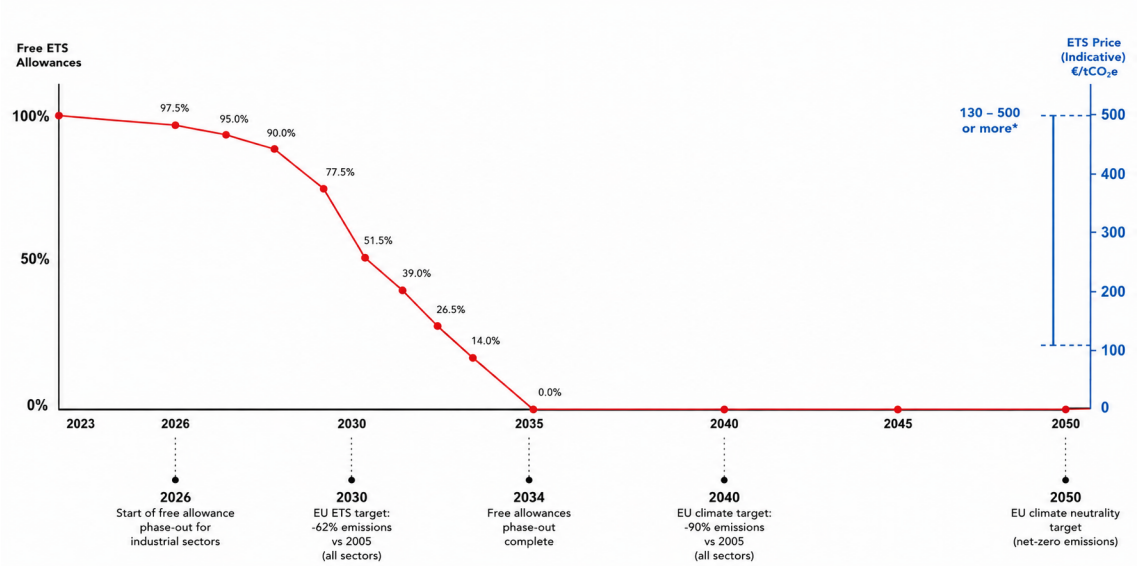


Figure 1.4: Scheduled phase-out trajectory of EU ETS free allowances for energy-intensive industries [28–30].

Total Number of Allowances in Circulation (TNAC) determines the effective market volume, including both free allocations and auctioned allowances. The Market Stability Reserve (MSR) was introduced to address structural oversupply in the EU ETS. If TNAC exceeds 833 million allowances, 24% of the surplus is transferred to the reserve. If TNAC falls below 400 million allowances, 100 million allowances are released back into the auction pool. Since 2023, any MSR volume exceeding the previous year's auction volume has been permanently invalidated [28]. This mechanism prevents the MSR from acting as a long-term storage buffer and ensures that accelerated decarbonisation does not generate excess allowances capable of weakening market prices [30].

The interaction between MSR dynamics and industrial decarbonisation trajectories may produce complex effects on carbon prices. As renewable gas integration reduces fossil gas consumption and, consequently, industrial demand for EU ETS allowances, a temporary surplus of EU allowances (EUAs) may emerge. Without corrective mechanisms, this surplus could exert downward pressure on carbon prices through the so-called "waterbed effect", whereby emissions reductions in one area release allowances that can be used elsewhere [15]. The MSR partially mitigates this effect by absorbing surplus allowances, while permanent invalidation reinforces scarcity and supports the long-term credibility of carbon pricing [15, 30].

Additionaly, Carbon Border Adjustment Mechanism (CBAM) introduces an extra competitiveness dimension. While EU producers internalise EU ETS costs, non-EU competitors may not face equivalent carbon constraints. CBAM seeks to equalise the carbon-cost burden on selected imports and reduce the risk of carbon leakage in import-intensive sectors [31, 32]. For hard-to-abate industrial installations, including, for now, sectors like ceramics, iron and fertilisers, the combined effects of the EU ETS free-allocation phase-out, MSR-enforced scarcity, and CBAM create a structural and escalating component of total industrial expenditure. As shown in Figure 1.4, the gradual phase-out of free allowances defines a strategic trajectory for industrial operators, indicating that carbon compliance will become an increasingly significant and unavoidable cost over time. Carbon compliance costs are therefore treated as a permanent, policy-driven factor shaping long-term industrial investment decisions [15].

1.2 Case Study Selection and Justification

The glass industry provides a representative case for evaluating the techno-economic implications of renewable gas integration in hard-to-abate industrial sectors. Container glass and related production lines are highly dependent on gaseous fuels, with approximately 80% of their energy demand supplied by natural gas [6, 33]. This reliance makes the sector a relevant testbed for assessing compliance pathways under the RED III framework introduced in Section 1.1.1.

Glass production is continuous and operates at high temperatures, with melting furnaces typically functioning between 1350 and 1650 °C, supported by feeders and annealing lehrs. The technical constraints inherent to these processes limit the feasibility of near-term electrification [6, 34]. In addition, the energy-intensive nature of glass furnaces increases the influence of fuel composition on operational safety, heat transfer, emissions, and product quality [6]. Figure 1.5 presents historical trends in specific energy consumption and crown temperatures in European container glass furnaces, illustrating efficiency improvements over the past century while reaffirming the predominant role of natural gas.

Examining the transition towards biomethane and green hydrogen injection through the existing distribution network allows for a systematic evaluation of compliance strategies, including guarantees of origin or GOs procurement, while maintaining uninterrupted industrial operation. Operational evidence from HyGlass and related projects [35, 36] indicates that hydrogen blending affects flame dynamics, NO_x formation, heat transfer, and product quality. The following sections review these technical implications, which are directly relevant for assessing the feasibility of renewable gas integration in hard-to-abate industrial processes.

Selected facility ranks among the largest industrial gas consumers connected to the DSO network, ensuring that the modelling exercise reflects economic and regulatory implications of renewable gas deployment at network level. Although glass products are not currently included within CBAM sectoral scope, this industry sector remains exposed to increasing carbon-cost pressure, progressive decarbonisation requirements, and industrial competitiveness concerns, since it is already covered by the EU ETS/CELE framework. Therefore it is a representive of a wider group of energy-intensive industries that must decarbonise before a fully protective border-adjustment framework is available for their products.

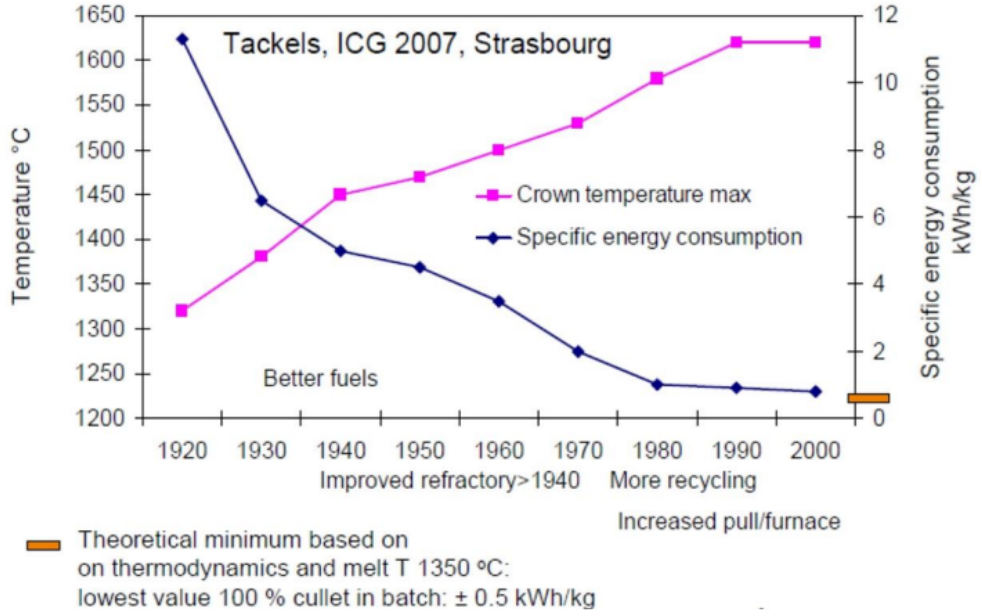


Figure 1.5: Evolution of specific energy consumption and crown temperatures in European container glass furnaces over the last century [35].

1.3 REN-Portgás

This research was conducted in collaboration with REN-Portgás, the DSO responsible for delivering natural gas and renewable gases in northern and coastal Portugal. REN-Portgás is a subsidiary of Redes Energéticas Nacionais (REN), which manages the national electricity transmission system and the national gas transmission network. The REN Group connects energy producers, particularly in the renewable energy sector, to consumption centres and ensures security of supply [37].

REN-Portgás plays a central role in renewable gas deployment by operating the distribution infrastructure through which biomethane and hydrogen-blended gas may progressively reach industrial end-consumers [37]. Distribution system operators therefore act not only as infrastructure operators but also as coordination agents. Their role is to ensure that renewable gas integration pathways remain compatible with network constraints and with the technical and operational requirements of industries that continue to rely predominantly on natural gas as an energy vector for production [37].

Initiated by REN in the first half of 2026, the H2 Braga pilot project represents the first operational test of hydrogen blending in Portugal. In this thesis, the project provides the empirical reference for the network phase scenarios analysed in the case study [38].

The collaboration facilitated access to operational and technical data on gas quality, network composition, and industrial consumption profiles. These data support the case study presented in Chapter 4, where the techno-economic model is applied to a representative hard-to-abate industrial installation and assessed for transferability to comparable contexts. Beyond its academic contribution, the analysis enables REN-Portgás to anticipate potential operational and economic impacts on industrial customers, increasing transparency and supporting stakeholder confidence under more stringent renewable gas targets and progressively stricter EU ETS obligations.

1.4 Research Objectives

Fundamentally, this dissertation aims to addresse the economic implications arising from the physical and contractual dissociation of renewable gas distribution, a dimension that remains insufficiently quantified in the existing literature. Industrial consumers supplied through gas distribution networks receive a physical gas blend at the meter, whereas the renewable content associated with their consumption may be legally attributed through (GOs), RFNBO certification, or other recognised accounting mechanisms. This creates a decoupling between physical delivery, contractual procurement, and regulatory recognition, which is not adequately represented in current techno-economic assessments.

This research is guided by **three specific objectives:**

- To develop an integrated techno-economic framework that links the thermophysical interchangeability constraints of biomethane and hydrogen blends to retrofit capital expenditure (CAPEX) requirements and industrial operational continuity.
- To operationalise the physical and contractual dissociation between delivered gas and certified renewable attributes as a quantifiable economic variable under stochastic carbon-market uncertainty.
- To evaluate alternative renewable gas procurement and compliance scenarios, considering biomethane cost and availability, hydrogen cost trajectories, and the potential role of on-site renewable hydrogen production.

Proposed framework captures the physical, contractual, regulatory, and economic interactions involved in renewable gas integration at industrial facilities. The decoupling discussed in Section 1.1.2, between gas physically delivered at the meter and renewable content legally attributed through GOs or RFNBO certification, is treated as a measurable economic variable rather than solely as a qualitative regulatory distinction.

Three analytical dimensions are integrated. **First**, thermophysical constraints associated with biomethane and hydrogen blends are translated into potential retrofit capital requirements. **Second**, RED III certification requirements and uncertain EU ETS carbon-cost trajectories are incorporated as regulatory drivers shaping long-term industrial decision-making. **Third**, renewable gas procurement is assessed across multiple scenario trajectories, reflecting uncertainty in domestic biomethane availability under national planning constraints, hydrogen market development, and their combined influence on renewable gas prices and associated GOs.

The original contributions of this thesis are threefold:

- It establishes a direct link between gas-blend interchangeability thresholds and retrofit CAPEX obligations within a unified discounted cash-flow structure.
- It operationalises physical and contractual dissociation as a measurable economic variable, enabling systematic evaluation of GO and RFNBO procurement strategies in relation to carbon-cost avoidance under uncertainty.
- It compares alternative renewable gas transition pathways, including network-based biomethane and hydrogen blending, procurement strategies under uncertain market evolution, and an extended scenario involving on-site renewable hydrogen production at the industrial installation.

Applied over a defined planning horizon, **this model should be able to provide a consistent**

method for evaluating technical admissibility, regulatory compliance, and economic rationality at installation level. In doing so, the thesis assesses whether renewable gas integration through existing distribution networks can provide a feasible decarbonisation pathway for hard-to-abate industrial consumers.

Beyond the development of the model itself, this thesis also adopts a **broader system perspective**. Renewable gas integration is not only an **installation-level decision** for industrial consumers, but also a transition process with implications for **distribution networks** and, indirectly, for the **transmission system** that supports national gas balancing and renewable gas injection. The framework therefore provides a basis for discussing whether, and under which conditions, **European renewable gas targets** can be translated into feasible **national decarbonisation pathways**. By connecting **installation-level economics** with network constraints, domestic supply limitations, certification mechanisms, and carbon-market exposure, the dissertation aims to support a more integrated view of industrial decarbonisation. This broader interpretation also creates the basis for the **policy implications** discussed at the end of the work, where the results are used to identify possible public-policy directions capable of improving renewable gas deployment, reducing compliance risk, and strengthening the role of **existing gas infrastructure** in Portugal's energy transition.

1.5 Dissertation Structure

This dissertation is organised into five chapters, moving from the regulatory and technical foundations of renewable gas integration to the development, application, and interpretation of the proposed techno-economic framework.

Chapter 1 introduces the industrial and regulatory context motivating the study. It presents the challenge faced by hard-to-abate industrial consumers connected to gas distribution networks and defines the physical-contractual dissociation between delivered gas composition and renewable attribute certification, which forms the central analytical basis of the thesis.

Building on this context, Chapter 2 reviews the state of the art on biomethane, hydrogen blending, gas interchangeability, renewable gas certification, and techno-economic modelling under RED III and EU ETS constraints. This chapter also discusses policy instruments and market conditions that influence renewable gas availability and price formation.

Chapter 3 then develops the integrated techno-economic framework. It presents the structure of the three sequential models and the Monte Carlo extension, defining the equations, decision rules, and indicators used to assess physical admissibility, operational costs, carbon exposure, and investment performance.

Chapter 4 applies the framework to a continuous container-glass manufacturing facility connected to the distribution network in northern Portugal. The chapter defines the case-study parameters, network phase schedule, and market scenarios, before presenting deterministic results, Monte Carlo outcomes, and an extended comparison with in-situ hydrogen production. The discussion also connects the installation-level results with the wider **(concession area)** context.

Finally, Chapter 5 summarises the main findings and discusses their implications. It highlights the technical, economic, environmental, and policy conclusions, with particular attention to biomethane market development, RFNBO certification, EU ETS uncertainty, the role of the DSO, and future extensions of the framework towards site-specific calibration and multi-installation deployment.

Chapter 2

State of art

This chapter reviews the scientific and technical literature relevant to the analytical dimensions underpinning the methodology developed in Chapter 3. The first dimension addresses the thermodynamic and interchangeability constraints of renewable gas blends, focusing on the physical boundaries that determine admissible biomethane and hydrogen mixture compositions in existing natural gas distribution infrastructure and their effects on industrial combustion equipment. The second dimension examines techno-economic models and policy instruments for industrial decarbonisation through renewable gases, including levelised cost frameworks, stochastic carbon-price modelling, renewable gas procurement mechanisms, and European policy benchmarking. These elements inform the scenario structure adopted in the Monte Carlo simulations. Together, both dimensions provide the analytical basis for the methodological choices presented in Chapter 3.

Multiple technological pathways can contribute to industrial decarbonisation, including electrification, energy-efficiency improvements, carbon capture, fuel switching, waste-heat recovery, and renewable gas integration [10]. This review focuses specifically on biomethane and green hydrogen, as these vectors are closely linked to the strategic role of gas distribution system operators in the near-term energy transition for industrial consumers. For industrial users already connected to natural gas distribution networks, renewable gas injection can reduce carbon exposure while preserving much of the existing gas infrastructure, operational practices, and combustion-based process architecture. This network-oriented perspective is particularly relevant for gas distribution companies seeking to define their role within an increasingly decarbonised energy system.

Biomethane and green hydrogen have emerged as the principal renewable gas vectors for decarbonising existing natural gas networks. Biomethane, produced through anaerobic digestion and subsequent upgrading of organic feedstocks, closely resembles natural gas chemically and can be injected into existing infrastructure when upgrading and gas-quality standards are satisfied [7]. Green hydrogen, produced through electrolysis using renewable electricity, provides a zero-carbon combustion option but has distinct thermophysical properties that constrain its admissible blending share with natural gas [9, 39]. The gradual integration of both vectors into distribution networks is recognised as a viable near-term decarbonisation strategy for hard-to-abate industrial sectors where direct electrification remains technically or economically constrained [16, 40].

2.1 Mathematical Thermophysical Basis

The thermodynamic characterisation of renewable gas blends injected into existing natural gas distribution networks follows the calculation procedures established in EN ISO 6976:2016 for calorific values, density, relative density, and Wobbe Index from gas composition under specified reference conditions [41]. EN 437:2021 is used as the appliance-testing and gas-family reference framework for interpreting gas interchangeability in Group H systems, particularly on a gross Wobbe Index basis [42]. It is not used in this thesis to define a fixed numerical retrofit threshold.

Unless otherwise stated, all gas properties are expressed at the adopted reference conditions of 15 °C and 1013.25 mbar. This convention is necessary because volumetric heating values, density, relative density, and Wobbe Index depend on the reference state. The same reference conditions are therefore maintained throughout the thermodynamic screening developed in this chapter and later operationalised in Chapter 3.

For a gas mixture composed of n species, the mixture molecular weight is obtained from the molar-weighted sum:

$$M_{\text{mix}} = \sum_{i=1}^{n} x_i M_i \qquad [\text{kg/kmol}] \tag{2.1}$$

where x_i is the mole fraction of component i, M_i is the molecular weight of component i, and $\sum_i x_i = 1$.

The relative density, or specific gravity, of the mixture with respect to dry air is:

$$SG_{\text{mix}} = \frac{M_{\text{mix}}}{M_{\text{air}}} \tag{2.2}$$

where $M_{\text{air}} = 28.97$ kg/kmol.

The volumetric density of the gas mixture at the adopted reference conditions is obtained from the ideal gas law:

$$\rho_{\text{mix}} = \frac{p_{\text{ref}} M_{\text{mix}}}{R T_{\text{ref}}} \qquad [\text{kg/m}^3] \tag{2.3}$$

where p_{ref} is the reference pressure, T_{ref} is the reference temperature, $R = 8314$ J/(kmol K) is the universal gas constant, and M_{mix} is the mixture molecular weight computed from Equation 2.1. At fixed reference conditions, this expression yields density as a function of gas composition alone [41].

Under the ideal-gas approximation, density ratios at identical pressure and temperature are directly proportional to molecular-weight ratios. The specific gravity in Equation 2.2 may therefore also be written as:

$$SG_{\text{mix}} = \frac{\rho_{\text{mix}}}{\rho_{\text{air}}} = \frac{M_{\text{mix}}}{M_{\text{air}}} \tag{2.4}$$

If the comparison is made relative to a reference gas, the corresponding density ratio is:

$$\frac{\rho_{\mathrm{mix}}}{\rho_{\mathrm{ref}}} = \frac{M_{\mathrm{mix}}}{M_{\mathrm{ref}}} \tag{2.5}$$

Heating values of the blend may first be calculated on a molar basis:

$$HHV_{m,\mathrm{mix}} = \sum_{i=1}^{n} x_i HHV_{m,i} \qquad [\mathrm{MJ/kmol}] \tag{2.6}$$

$$LHV_{m,\mathrm{mix}} = \sum_{i=1}^{n} x_i LHV_{m,i} \qquad [\mathrm{MJ/kmol}] \tag{2.7}$$

These molar heating values can be converted to a volumetric basis using the molar volume V_m at the adopted reference conditions:

$$HHV_{v,\mathrm{mix}} = \frac{HHV_{m,\mathrm{mix}}}{V_m} \qquad [\mathrm{MJ/m^3}] \tag{2.8}$$

$$LHV_{v,\mathrm{mix}} = \frac{LHV_{m,\mathrm{mix}}}{V_m} \qquad [\mathrm{MJ/m^3}] \tag{2.9}$$

When component calorific values are already available on a volumetric basis under the same reference conditions, as is common in gas-property databases, the equivalent expressions are:

$$HHV_{\mathrm{mix}} = \sum_{i=1}^{n} x_i HHV_i \qquad [\mathrm{MJ/m^3}] \tag{2.10}$$

$$LHV_{\mathrm{mix}} = \sum_{i=1}^{n} x_i LHV_i \qquad [\mathrm{MJ/m^3}] \tag{2.11}$$

A distinction that matters because volumetric heating values depend on the adopted reference conditions and, in rigorous gas-property calculations, on the treatment of real-gas behaviour. For screening-level blend comparison under distribution-network conditions, the ideal-gas approximation is retained, provided that the same reference state is used for all compositions.

The Wobbe Index is calculated as the ratio between the volumetric calorific value and the square root of relative density. The gross, or superior, Wobbe Index is given by:

$$WI_{\mathrm{gross}} = \frac{HHV_{v,\mathrm{mix}}}{\sqrt{SG_{\mathrm{mix}}}} \qquad [\mathrm{MJ/m^3}] \tag{2.12}$$

A corresponding net Wobbe Index can be defined using the lower heating value:

$$WI_{\mathrm{net}} = \frac{LHV_{v,\mathrm{mix}}}{\sqrt{SG_{\mathrm{mix}}}} \qquad [\mathrm{MJ/m^3}] \tag{2.13}$$

2.2 Biomethane

Biomethane is produced by upgrading raw biogas generated through the anaerobic digestion of organic residues, including agricultural waste, sewage sludge, landfill gas, and food-processing effluents [43]. During anaerobic digestion, complex organic molecules are broken down in the absence of oxygen, producing a raw gas mixture composed primarily of methane and carbon dioxide, with secondary components such as nitrogWhen both renewable gases are present, their combined effect on molecular weight, specific gravity, heating values, and Wobbe Index depends on the molar fractions of all components, as calculated using en, hydrogen sulphide, water vapour, and trace siloxanes [13, 43].

Before injection into natural gas networks or direct industrial use, raw biogas must be upgraded to remove non-combustible and corrosive components. Common upgrading technologies include pressure swing adsorption, water scrubbing, membrane separation, and cryogenic separation. These processes primarily target CO_2 removal, together with drying, H_2S removal, and siloxane elimination [13].

Once upgraded, grid-quality biomethane typically contains more than 95–97% methane by volume. Figure 2.1 illustrates the typical biomethane value chain, linking organic feedstock supply, biogas production, upgrading, grid injection, GO issuance, and final industrial use.

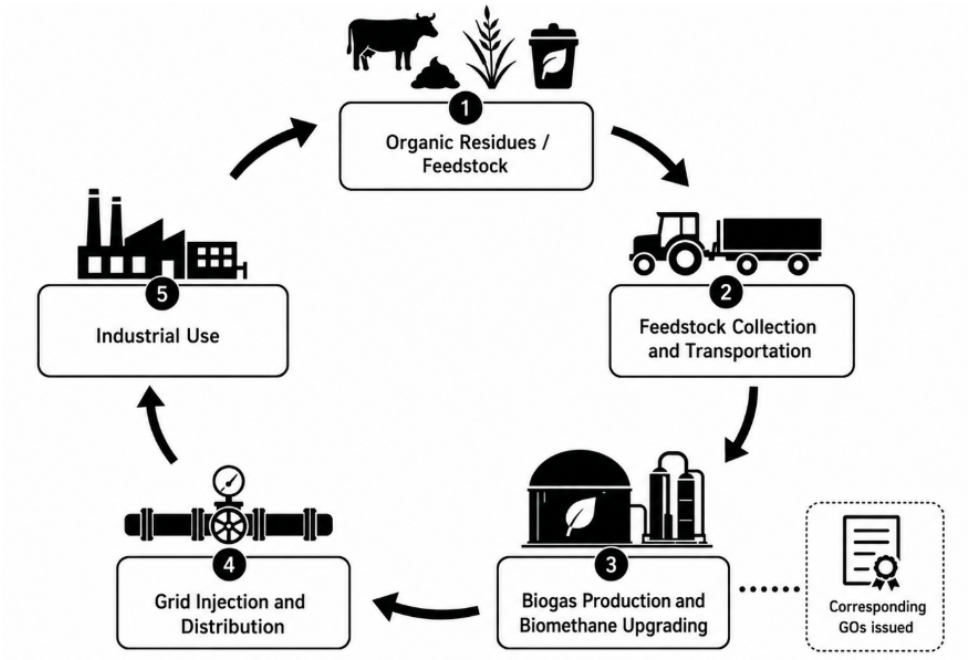


Figure 2.1: Typical biomethane production, certification, distribution, and industrial-use pathway [44].

Grid-quality biomethane exhibits thermophysical differences from fossil natural gas that, although quantitatively modest, may have relevant operational implications. Since biomethane consists primarily of methane, it contains limited heavier hydrocarbon fractions, such as ethane C_2H_6, propane C_3H_8, and butane C_4H_{10}, which are commonly present in fossil natural gas and contribute to its higher volumetric heating value and specific gravity [13].

A 24-month statistical analysis of gas distributed in the Portuguese national network, covering the period from October 2023 to September 2025, indicates that the natural gas composition

envelope yields LHV values between 37.5 and 40.3 MJ/Nm^3 and gross Wobbe Index values within an operational range of 48.2 to 53.2 MJ/Nm^3 [39]. By contrast, grid-quality biomethane typically exhibits LHV values between 34.1 and 34.4 MJ/Nm^3 and Wobbe Index values between 45.3 and 47.5 MJ/Nm^3, reflecting its predominantly methane-based composition and the absence of heavier hydrocarbon fractions [7].

Evidence from a Brazilian industrial context, based on 92 consecutive days of supply, shows that the Wobbe Index of biomethane remains consistently below that of fossil natural gas, with an average deviation of 7.25% in the case analysed [13]. Although absolute values differ between the Brazilian and Portuguese contexts, these results reinforce the need to evaluate biomethane against the specific gas-quality envelope of each network. Biomethane generally should therefore be treated as a near drop-in renewable gas only when applicable upgrading, quality, and interchangeability requirements are satisfied, rather than as thermophysically identical to fossil natural gas [7].

The practical implications for industrial combustion equipment depend strongly on the specific process considered. In low- to medium-temperature applications, such as fluidised-bed sand drying, biomethane substitution primarily affects fuel consumption rather than combustion feasibility. Santos Machado et al. (2025) show that the specific fuel consumption of both natural gas and biomethane decreases as inlet gas temperature increases [17]. The consumption difference between both fuels becomes less pronounced at higher temperatures, as illustrated in Figure 2.2.

This behaviour suggests that biomethane substitution has a greater impact at lower operating temperatures, where higher volumetric fuel flow rates are required to compensate for its lower calorific value. At higher drying temperatures, the relative fuel-consumption penalty decreases, supporting the functional interchangeability of biomethane and natural gas in these processes, provided that the fuel supply system can accommodate the required flow-rate adjustment. Under such conditions, bubbling fluidisation is not adversely affected by fuel substitution, and the observed consumption difference is mainly attributable to the lower heating value (LHV) of biomethane rather than to any fundamental combustion incompatibility [17].

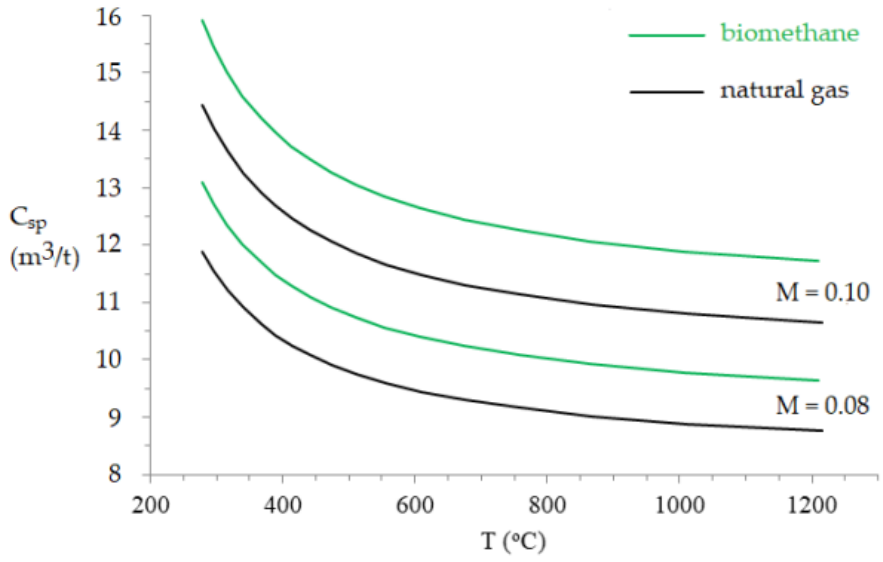


Figure 2.2: Specific fuel consumption of natural gas and biomethane as a function of inlet gas temperature for fluidised-bed drying [17]

In high-temperature processes, such as ceramic tile kilns operating at approximately 1200 °C and regenerative glass furnaces operating at around 1500 °C, Carvalho et al. [13] demonstrate that the commonly adopted ±5% Wobbe Index tolerance may be insufficient to ensure safe and stable operation.

If a burner operating at a constant air flow rate switches to a biomethane–natural gas blend with $WI_{\mathrm{mix}} = 0.95\,WI_{\mathrm{NG}}$, the additional fuel required to maintain the process temperature reduces the normalised air-to-fuel ratio and alters the furnace atmosphere. In the ceramic kiln case, this effect reduces the O_2 concentration from the required process minimum of 4% to approximately 2%, a condition that is incompatible with ceramic tile quality requirements [13]. This distinction between nominal gas interchangeability and actual high-temperature process compatibility is directly relevant to the characterisation of hard-to-abate industrial processes.

The radiative heat-transfer characteristics of biomethane combustion products are broadly comparable to those of natural gas under equivalent combustion conditions. The same study shows that the gas-phase emissivity profiles of biomethane combustion products remain close to those of natural gas across a furnace various sections analysed, with biomethane presenting only marginally higher emissivity values, as shown in Figure 2.3 [13]. This slight increase presented is mainly associated with the higher CO_2 contribution in the combustion products of biomethane-rich gases, rather than with fundamentally different combustion behaviour.

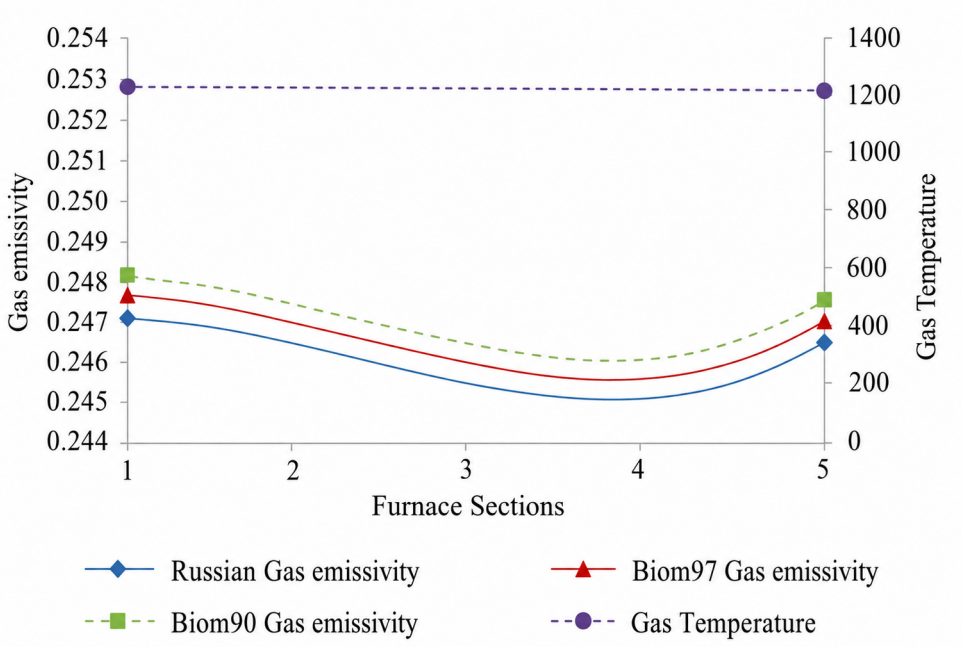


Figure 2.3: Gas emissivity per furnace section for natural gas and biomethane combustion products [13].

This limitation is quantified by the MIX case analysed by Carvalho et al. [13], corresponding to a blend of approximately 69.8% biomethane and 30.2% natural gas selected to satisfy the maximum admissible 5% Wobbe Index deviation.

As shown in Figure 2.4, even under this nominal interchangeability condition, the combustion-gas enthalpy requirement at $T_{\mathrm{furnace}} = 1200$ °C increases from 342.0 to 378.4 kJ/mol. This additional heat demand reduces the normalised air-to-fuel ratio and may compromise the oxygen availability required to maintain the appropriate furnace atmosphere for ceramic tile production [13].

The MIX (natural gas/biomethane) case, analysed on the study, provides a process-level illustration of why biomethane substitution from natural gas cannot be evaluated only through Wobbe Index deviation. For high-temperature furnaces, additional operational variables, including combustion-gas enthalpy, air-to-fuel ratio, oxygen concentration, and furnace-atmosphere requirements, must also be considered [13].

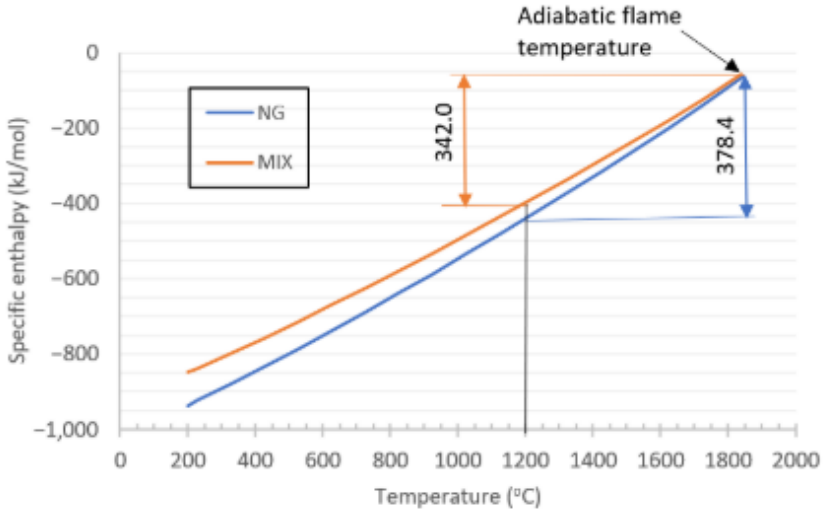


Figure 2.4: Specific enthalpy of combustion gases as a function of temperature for natural gas and a biomethane-natural gas [13].

Figure 2.4 highlights also the need to distinguish nominal gas interchangeability from process-level compatibility. Although the natural gas/biomethane blend was selected to remain within the permissible Wobbe Index deviation, the increased combustion-gas enthalpy requirement shows that additional operational variables must be considered in high-temperature furnaces, particularly air-to-fuel ratio, oxygen availability, and furnace-atmosphere specific requirements [13].

Such a result reinforces the interpretation of biomethane as a methane-rich renewable substitute whose integration remains technically less disruptive than hydrogen blending. Its practical suitability, however, remains conditional on compliance with upgrading, gas-quality, and process-control requirements [45].

This thermophysical similarity also supports the use of mass-balance and GO-based accounting for biomethane in interconnected gas networks, provided that sustainability criteria, certificate cancellation rules, and national implementation requirements are satisfied, as discussed in Section 1.1.2.

2.3 Hydrogen Blending

Green hydrogen is widely recognised as a strategic energy vector for decarbonising high-temperature industrial heat in sectors where direct electrification remains technically challenging or economically disruptive within relevant regulatory timescales [11]. In this context, blended combustion using existing gas infrastructure represents one of the most accessible near-term transition pathways for hard-to-abate industrial consumers [12]. However, a significant gap still persists between strategic ambition and operational deployment in the hydrogen sector.

Global hydrogen demand reached approximately 100 Mt in 2024, but demand remains concentrated almost exclusively in established applications, mainly refining and ammonia production. Emerging end-use applications, including industrial heat, power generation, and transport, still account for less than 1% of total hydrogen demand [16]. Low-emissions hydrogen, including hydrogen produced through electrolysis using renewable electricity, also represents less than 1% of global production, despite measurable growth in 2024 and a large project pipeline that has not yet fully translated into final investment decisions [16].

This structural immaturity, characterised by high policy ambition but limited operational deployment, defines the context in which the thermophysical properties, interchangeability constraints, and economic uncertainties of hydrogen blending must be evaluated for industrial applications.

Hydrogen differs fundamentally from methane and natural gas in its thermophysical and combustion properties. These differences have direct implications for gas distribution, metering, burner operation, and industrial process control.

On a mass basis, hydrogen H_2 has a lower heating value of approximately 120 MJ/kg, more than twice that of methane CH_4, at approximately 50 MJ/kg [11]. This high gravimetric energy density makes hydrogen attractive in applications where mass is the main constraint. Gas grids, industrial burners, and metering systems, however, operate primarily on a volumetric basis, where the comparison is reversed.

On the normal cubic metre basis adopted in the model property database, the volumetric lower heating value of hydrogen is 10.80 MJ/Nm^3, compared with 35.88 MJ/Nm^3 for methane. Hydrogen therefore provides less than one third of the energy per unit volume of methane. This volumetric energy deficit results from hydrogen's low density, approximately 0.090 kg/Nm^3, compared with 0.717 kg/Nm^3 for methane. These properties directly affect volumetric flow rates, metering, burner thermal input, and network energy-delivery capacity at constant pressure.

Beyond energy content and density, hydrogen also introduces a combustion regime that differs substantially from methane-rich natural gas. Its laminar burning velocity is several times higher than that of methane, depending on mixture fraction, pressure, and temperature, while its minimum ignition energy is considerably lower [7]. These characteristics increase flame reactivity and are directly relevant to flashback risk, ignition behaviour, and burner-stability assessment.

Hydrogen also has a much wider flammability range, extending from approximately 4% to 75% by volume in air, compared with approximately 5% to 15% for methane [7, 9]. These properties collectively extend the range of combustible mixtures and modify the safety and stability requirements of industrial combustion systems.

For a consistent comparison, the main thermophysical and combustion-property differences between hydrogen, pure methane, and Portuguese natural gas are summarised in Table A.1. All volumetric values used in the model are kept on the same normal cubic metre basis to avoid mixing values reported under different reference-state conventions.

The reduction in volumetric energy density associated with hydrogen blending has direct hydraulic implications for gas distribution systems and internal industrial gas installations. Delivering an equivalent energy content with pure hydrogen would require an approximately three-fold increase in volumetric flow rate relative to natural gas, while hydrogen blending at moderate fractions imposes a proportional flow-rate penalty that scales with the reduction in LHV_{mix} [46].

At network level, this penalty reduces pipeline energy transmission capacity at fixed operating

pressure. Maintaining constant energy delivery may therefore require increased compression, flow-rate adjustment, or pipe diameter adaptation [46]. At installation level, the same effect may also limit the hydraulic adequacy of existing internal gas pipework.

The Wobbe Index is the primary normative parameter for assessing gas interchangeability across European appliance standards, since it approximates the thermal input delivered through a fixed burner orifice at constant supply pressure. However, Wobbe Index compliance is a necessary but not sufficient condition for operational compatibility when hydrogen is introduced into a natural gas blend. Hydrogen also modifies density, flame speed, flammability limits, flashback tendency, material compatibility, and NO_x formation, all of which can affect burner operation even when the Wobbe Index remains within the admissible range [7].

Portuguese natural gas already exhibits measurable variability in methane content, heavier hydrocarbon fractions, and inert components, resulting in a range of Wobbe Index and relative density values across the national distribution network [39]. It is therefore methodologically necessary to assess hydrogen blending against the actual gas-quality envelope of the network rather than against pure methane alone.

Extreme compositions within the existing variability range may reach normative limits at lower hydrogen fractions than average compositions suggest. Analysis of Portuguese network gas-quality data shows that, at 10% H_2 by volume, the gross Wobbe Index of the blend remains within the national operational band of 48.2 to 53.2 MJ/m^3, while relative density decreases measurably compared with the base gas, as shown in Figure 2.5 [39].

At 20% H_2, the Wobbe Index generally remains within national limits, but mean relative density approaches 0.491. At this value, some compositions within the existing natural gas variability envelope may fall below the lower normative density threshold [39].

This finding indicates that relative density, rather than the Wobbe Index alone, becomes a key normative parameter as hydrogen fractions increase in the distribution network. Wobbe Index compliance at 20% H_2 should therefore not be treated as sufficient evidence of operational compatibility. Flame stability, safety margins, air-fuel mixing, and burner aeration may all be affected by reduced gas density and must be assessed independently [39].

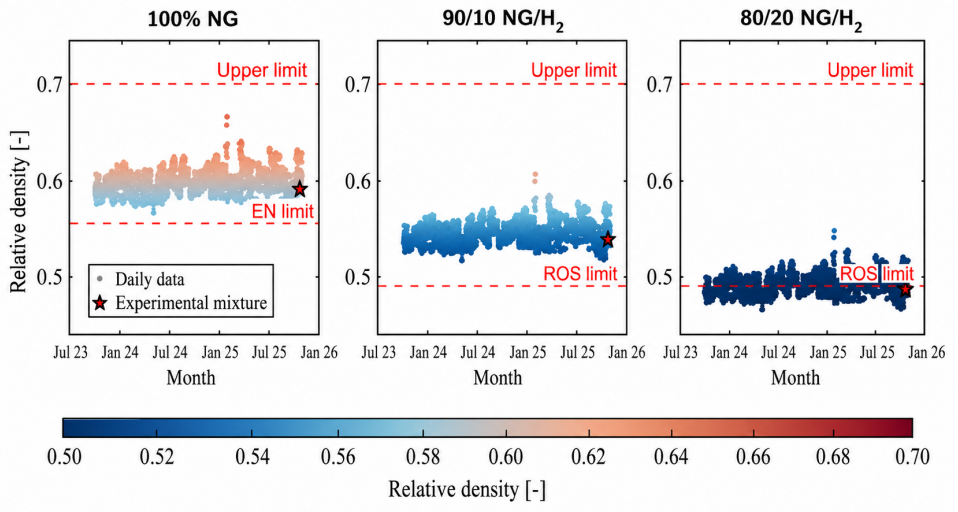


Figure 2.5: Effect of 0%, 10%, and 20% H_2 blending on Wobbe Index and relative density of Portuguese natural gas[39].

Blending hydrogen to natural gas produces changes in combustion kinetics that are substantially more pronounced than those observed with biomethane substitution. Hydrogen enrichment increases both the laminar burning velocity and the adiabatic flame temperature of the mixture, with the magnitude of these effects growing non-linearly with hydrogen fraction [47].

Through numerical simulation, Sun et al. (2022) show that laminar burning velocity increases from approximately 37.6 cm/s at 0% H_2 to 229.2 cm/s at 100% H_2 under the analysed conditions, representing an approximately six-fold increase driven by the different reaction kinetics of hydrogen combustion [48]. This acceleration is primarily attributable to enhanced production of highly reactive radical species, including H, O, and OH, whose molar fractions and production rates increase progressively with hydrogen content [48].

The chain-branching reactions central to this kinetic acceleration are represented by:

$$H + O_2 \rightarrow O + OH \tag{2.14}$$

$$OH + H_2 \rightarrow H + H_2O \tag{2.15}$$

Together, these reactions sustain a self-reinforcing radical pool that propagates the flame significantly faster than in pure methane combustion [48].

The adiabatic flame temperature also increases with hydrogen fraction, reflecting both the higher reaction intensity and the modified heat capacity of the combustion products. More importantly for burner operation, hydrogen addition substantially increases the burning velocity of the NG–H_2 mixture. As shown in Figure 2.6, burning velocity increases with hydrogen addition and is also influenced by the excess-air coefficient, indicating that the combustion response of NG-H_2 blends cannot be interpreted from fuel composition alone. This behaviour is directly relevant to burner stability because flashback occurs when the flame propagation velocity becomes higher than the velocity of the unburnt mixture leaving the burner ports [48].

2.3. Hydrogen Blending

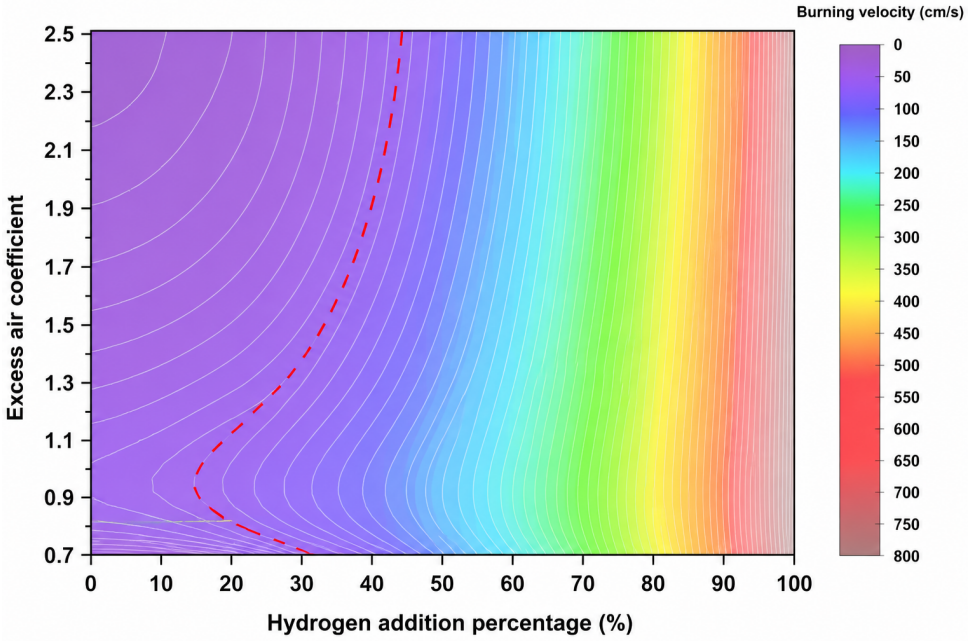


Figure 2.6: Laminar burning velocity and adiabatic flame temperature as a function of hydrogen volume fraction in natural gas blends [48].

These kinetic changes produce two competing practical effects for burner operation. On the one hand, hydrogen enrichment extends the lean flammability limit and can improve flame stability under fuel-lean conditions, reducing the risk of flame extinction at low thermal loads. Such behaviour may be advantageous for burner turndown performance. On the other hand, the higher burning velocity increases the risk of flashback, whereby the flame propagates upstream into the premixing zone faster than the flow velocity can prevent, potentially causing equipment damage or uncontrolled combustion [7, 9, 48]. This effect is illustrated in Figure 2.7, where the flashback index increases progressively with hydrogen addition and approaches the suitability thresholds reported by Sun et al. (2022) at hydrogen fractions above approximately 23–25% by volume.

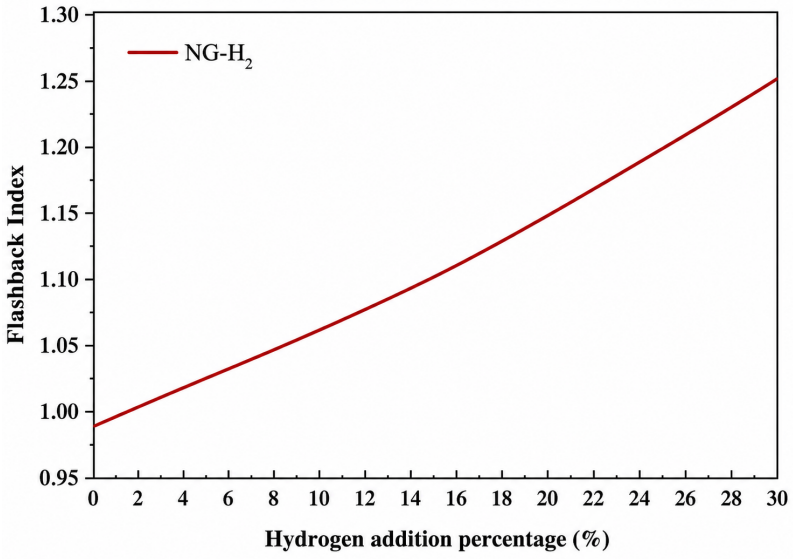


Figure 2.7: Flashback index variation with hydrogen addition in NG–H_2 mixtures [48].

This interpretation is consistent with experimental validation using real Portuguese network gas. Hydrogen additions up to 10% by volume produced no critical instability or flashback in the burner configurations tested, with the flame remaining compact and reactive without adverse morphological changes [39]. For hydrogen fractions in the 10–20% by volume range, the same experimental programme classifies behaviour as prospective and subject to **case-by-case evaluation**, since the combined effects of higher burning velocity, reduced density, altered air-to-fuel mixing, and increasing flashback propensity begin to approach the operational boundaries of standard burner designs [39].

The combined evidence therefore supports a conservative interpretation of hydrogen blending limits, on Wobbe Index compliance may indicate acceptable heat-input behaviour, but burning-velocity and flashback constraints require independent assessment [39].

The substitution of natural gas with hydrogen blends introduces a distinct industrial trade-off between reducing carbon emissions and increasing nitrogen oxide formation. Regarding carbon emissions, hydrogen enrichment reduces CO_2 emissions by displacing carbon-containing fuels and generally lowers CO emissions by promoting more complete combustion, due to higher flame temperatures and increased radical availability [48]. Franco and Rocca (2024) quantify these reductions, reporting approximately 7% lower CO_2 emissions at 20% H_2 and about 11% at 30% H_2 by volume [11]. However, these reductions remain limited because a given hydrogen volume fraction replaces a smaller share of the total thermal energy delivered, owing to hydrogen's low volumetric energy density. In the ceramic industry, 16% H_2 blending achieves an approximately 5% reduction in CO_2, increasing to 21% at 50% H_2 and 52% at 80% H_2. This demonstrates that substantial decarbonisation through blending requires hydrogen fractions well above those currently feasible within conservative interchangeability limits [11].

With respect to nitrogen oxide emissions, the same kinetic mechanisms that accelerate combustion and enhance flame stability also increase NO_x formation through the thermal pathway. Lan et al. (2024) provide computational fluid dynamics (CFD) evidence from an industrial furnace simulation at 60% H_2, showing an approximately 37.5% reduction in CO_2 and a 70% reduction in CO compared with the natural gas baseline, alongside an increase in NO of approximately 155% [49]. This increase is attributed to higher adiabatic flame temperatures and greater concentrations of reactive O and OH radicals, which promote thermal NO_x formation [48, 49].

In hard-to-abate industrial facilities, the balance between carbon-emission reduction and increased NO_x formation creates a constrained optimisation problem [48]. The thermodynamic benefits of hydrogen blending must therefore be assessed alongside local emissions compliance requirements under the applicable industrial emissions framework.

The ceramic sector provides a relevant applied context for assessing the industrial implications of hydrogen blending. Approximately 64% of its CO_2 emissions originate from fossil fuel combustion, primarily natural gas, with firing and drying operations constituting the most energy-intensive and emissions-critical stages of production [50, 51]. The high-temperature kiln firing stage, which is essential for product quality through precise atmosphere control and thermal management, remains structurally difficult to electrify within the regulatory timelines established by EU decarbonisation objectives [50, 51].

As a result, gaseous fuel substitution and incremental hydrogen blending represent viable transition pathways for ceramic manufacturing [10, 50]. Industry-level analysis of hydrogen blending in Portuguese ceramic production indicates that complete substitution of natural gas with hydrogen is not currently feasible as an immediate transition. A more practical near-term approach involves

gradual blending of natural gas with hydrogen, combined with burner modifications and the development of hybrid kiln systems capable of operating across a range of blend compositions [50].

Development pathways towards higher blend fractions are being addressed through dedicated demonstrator programmes. A laboratory-scale furnace with 10 kW nominal thermal input has been developed for the controlled characterisation of blend combustion behaviour across a range of hydrogen fractions. The results inform the design of a pre-industrial roller kiln demonstrator with an 11 m length and 200 kW nominal capacity, engineered for operation with up to 50% H_2 in an initial phase [50].

These demonstrator initiatives establish the technical feasibility of progressive hydrogen integration in ceramic kilns and highlight the substantial engineering modifications required to exceed current interchangeability thresholds. However, they also reveal the technological and market immaturity of high-hydrogen industrial combustion pathways[51]. At present, such solutions remain largely confined to pilot and demonstrator projects, rather than representing mature, standardised, and widely deployable industrial options [52].

In addition to combustion kinetics and gas interchangeability, hydrogen integration into existing natural gas infrastructure introduces material and infrastructure constraints. Metallic components such as pipelines, fittings, and pressure vessels may be vulnerable to hydrogen embrittlement, a degradation process in which hydrogen atoms diffuse into the metal lattice and reduce ductility, fatigue resistance, and fracture toughness. The severity of hydrogen embrittlement depends on factors such as steel grade, stress state, hydrogen partial pressure, and operating conditions [53, 54].

Polymeric and elastomeric materials used in seals, gaskets, and flexible connections are subject to distinct failure mechanisms, including hydrogen permeation, volumetric swelling, microcracking, and rapid gas decompression. In rapid gas decompression, dissolved hydrogen expands quickly when pressure is reduced, causing internal cavitation and subsequent seal failure [53, 55].

Composite materials and lined vessels used in high-pressure storage applications may also suffer matrix cracking, delamination, and progressive degradation under repeated pressure cycling, limiting service life under hydrogen-rich conditions [53, 55].

Although these material compatibility constraints do not apply equally across all blend fractions, their severity generally increases with hydrogen partial pressure, which depends on both blend fraction and absolute supply pressure. Consequently, interchangeability assessments for hydrogen blending must extend beyond combustion parameters and include the materials present throughout the distribution network and end-use installations [55].

At the infrastructure level, IEA *Global Hydrogen Review 2025* confirms that hydrogen distribution infrastructure remains limited globally, with pipelines, storage facilities, and distribution projects facing persistent delays. Certification standards and monitoring protocols for hydrogen-containing gas systems also remain under development in many jurisdictions [16]. This regulatory and infrastructure immaturity reinforces the conclusion that admissible hydrogen fractions in existing natural gas distribution networks are constrained not only by combustion and interchangeability thresholds, but also by the readiness of the surrounding infrastructure ecosystem [16].

In summary, hydrogen blending constitutes a constrained and process-specific decarbonisation strategy rather than a direct fuel substitution. Its technical feasibility depends on renewable hydrogen availability and combined compliance with gas-quality parameters, combustion stability, emissions control, heat-transfer requirements, infrastructure compatibility, and the operational constraints of the industrial user.

2.4 Combined Effects

Previous subsections addressed biomethane and hydrogen as distinct renewable gas pathways, reflecting the prevailing structure of the literature, where each vector is usually evaluated independently against a natural gas baseline. In practice, however, distribution networks transitioning towards renewable gases may simultaneously receive biomethane injections from decentralised production sites and hydrogen blending at network entry points. Industrial consumers may therefore receive a three-component mixture of natural gas, biomethane, and hydrogen at their consume point.

The properties of such ternary blends cannot be inferred by simply superimposing individual binary analyses, since biomethane and hydrogen modify the gas-quality envelope in fundamentally different and partially offsetting ways. As discussed in Section 2.2, grid-quality biomethane remains methane-rich and primarily affects the distributed gas by displacing heavier hydrocarbon fractions. This tends to reduce lower heating value (LHV) and specific gravity relative to fossil natural gas, while generally maintaining the Wobbe Index within an acceptable range when gas-quality requirements are satisfied [7]. By contrast, as established in Section 2.3, hydrogen reduces volumetric LHV and specific gravity more strongly, while also altering combustion kinetics through increased reactivity, flame speed, and flashback propensity [7, 11].

When both renewable gases are present, their combined effect on molecular weight, specific gravity, heating values, and Wobbe Index depends on the molar fractions of all components, as calculated using Equation 2.1 and Equation 2.11. This relationship has been demonstrated for Portuguese natural gas compositions by Quintino et al. (2021) and assessed against the national gas-quality envelope characterised by Mil-Homens et al. (2025) [7, 39]. The resulting gas-quality issue is therefore no longer defined by a single blending limit. Instead, it depends on the combined biomethane and hydrogen shares in the final mixture delivered to the industrial site.

This creates a coupled composition problem. Increasing the biomethane share modifies the methane-rich background composition by reducing the contribution of heavier hydrocarbons and lowering baseline density. Simultaneously, increasing the hydrogen share further reduces volumetric energy content and density, while increasing combustion reactivity. As a result, the impact of a given hydrogen fraction cannot be fully interpreted without accounting for the simultaneous biomethane fraction in the mixture, since both changes interact through the same thermophysical parameters [11]. Additional complexity arises from the actual compositional variability of Portuguese natural gas, which already exhibits variation in methane content, heavier hydrocarbon fractions, and inert components across the national network [39].

Consequently, a given biomethane/hydrogen combination should not be evaluated against a fixed reference composition alone, but against the full envelope of base gas compositions that may be present at a specific network node [47].

Existing literature on renewable gas integration into natural gas networks generally treats biomethane substitution and hydrogen blending as separate research problems, reflecting their different levels of technological maturity and deployment context. Studies on biomethane primarily focus on upgrading technologies, network gas-quality management, and interchangeability implications for industrial and domestic end-use equipment [13, 39]. Studies on hydrogen blending, in contrast, address gas-quality variation, laminar burning velocity, NO_x formation, flashback risk, and material compatibility [11, 39, 48, 49].

Although this separation is analytically useful for characterising each renewable gas individually, it creates a structural gap when both vectors coexist in the final blend delivered to an industrial

consumer. This combined-blending perspective is increasingly relevant as distribution networks may receive decentralised biomethane injections and hydrogen blending simultaneously [56, 57]. It therefore requires a formal discussion of interchangeability criteria and normative limits applicable to this ternary gas mixtures in existing distribution infrastructure.

The transition towards multi-gas networks also requires corresponding advances in network monitoring and planning practices. As renewable gas injections become more decentralised and compositionally variable, DSOs will require dynamic gas-quality tracking capabilities to estimate or directly measure the composition of distributed gas and the resulting quality parameters across the network [56, 57]. For industrial consumers, this information is essential for anticipating burner adjustments, combustion-control strategies, retrofit timing, contractual procurement, and regulatory compliance.

As renewable gas injection increases, DSOs must provide clear network transition plans, including expected blend ranges, gas-quality evolution, monitoring procedures, and implementation timelines [56, 57]. The following subsection therefore reviews the main interchangeability criteria and normative limits as technical parameters supporting transparent network planning. Well-defined planning is necessary to help industrial consumers align equipment adaptation and investment decisions with the progressive introduction of biomethane and hydrogen into distribution networks.

2.4.1 Interchangeability

Interchangeability is not simply a question of compositional similarity. It refers to whether a substitute gas can be used in existing appliances or industrial equipment without producing unacceptable deviations in heat input, combustion stability, air requirement, emissions, or safety. In the classical formulation proposed by Weaver, two gases are considered exactly interchangeable when substitution produces no observable or measurable change in key combustion phenomena, including heat input, flame stability, flashback tendency, yellow tipping, incomplete combustion, and primary air requirement [58].

In practice, exact interchangeability is rarely achieved between gases of different composition. The engineering question is therefore not whether two gases are identical, but whether the deviations introduced by the substitute gas remain within admissible tolerance bands for the specific equipment and application considered [59]. This distinction is particularly relevant for renewable gas integration, since biomethane and hydrogen affect gas quality through different mechanisms [7].

Several interchangeability methods have been proposed to evaluate these effects, each focusing on different combustion phenomena and equipment risks. Table 2.1 summarises the main methods and criteria commonly reported in the literature.

Table 2.1: Methods and criteria used for gas interchangeability assessment [59].

Method or index	Region / origin	Controlled combustion parameters
Knoy index	European Union	Flame lift
Dutton's criteria	Great Britain and Australia	Yellow tipping, soot formation, and complete combustion
Weaver method	United States	Complete combustion, flame lift, flashback, yellow tipping, heat input, and primary air requirement
AGA methods	United States	Flame lift, flashback, and yellow tipping
Delbourg method	France	Yellow tipping and soot formation

Gas interchangeability can be assessed through several national and regional approaches, each developed to address specific combustion phenomena and regulatory contexts. These include the Knoy factor in the European context, Dutton's criteria in Great Britain and Australia, the AGA method in the United States, the Delbourg method in France, and the Weaver method, also developed in the United States [9, 60].

Among the available interchangeability assessment approaches, the Weaver method remains one of the most comprehensive composition-based frameworks. Originally developed for fuel-gas interchangeability assessment, it evaluates several combustion-related phenomena within a single multi-index structure, including heat input rate, primary air requirement, flame lift, flashback tendency, yellow tipping, and incomplete combustion [9, 58, 60].

This multi-index structure makes the Weaver framework particularly relevant in contexts where a single aggregate indicator, such as the Wobbe Index, is insufficient to characterise operational compatibility. Rather than only indicating whether the overall thermal input remains within an admissible range, the Weaver method helps identify which specific combustion phenomenon is most affected by a change in gas composition. It is therefore especially useful for evaluating hydrogen-containing blends, where variations in flame speed, flashback tendency, and air requirement may become critical even when Wobbe Index limits are satisfied [59].

Recent studies have applied interchangeability indicators to hydrogen/natural gas blends in distribution-network contexts, showing that hydrogen addition affects not only heating value and Wobbe Index, but also density-related and combustion-stability parameters [9, 39, 61]. This is relevant because Wobbe Index compliance alone may not be sufficient to guarantee operational compatibility, especially when hydrogen fractions increase and burner aeration, flame stability, and safety margins become more sensitive to density and combustion-velocity changes [9].

These properties are particularly useful in the absence of a harmonised European standard directly applicable to large industrial combustion equipment above 300 kW, where process-specific combustion behaviour, safety margins, and operational continuity must be assessed beyond the conventional gas-appliance framework [42].

The first criterion is the heat-input ratio, J_H, which compares the gross Wobbe Index of the substitute gas with that of the reference gas [9]:

$$J_H = \frac{WI_{\text{gross},s}}{WI_{\text{gross},r}} \quad [-] \tag{2.16}$$

where $WI_{\text{gross},s}$ and $WI_{\text{gross},r}$ are the gross Wobbe indices of the substitute and reference gases, respectively.

2.4. Combined Effects

An index that quantifies whether the substitute gas maintains approximately the same thermal input to the burner under constant supply pressure and unchanged orifice geometry [9].

A value of $J_H = 1.0$ indicates heat-input equivalence between the two gases, while deviations from unity indicate that the substitute gas delivers a different thermal power under identical supply conditions. In practical interchangeability assessment, a tolerance band of approximately $\pm 5\%$ around the reference Wobbe Index is commonly used as an initial screening criterion, although this threshold should not be interpreted as sufficient evidence of full operational compatibility for all industrial combustion systems [9, 42, 58].

The second criterion is the primary air ratio, J_A, defined within the Weaver framework as [9]:

$$J_A = \frac{V_{t,s}}{V_{t,r}} \sqrt{\frac{SG_r}{SG_s}} \quad [-] \tag{2.17}$$

where $V_{t,s}$ and $V_{t,r}$ are the stoichiometric air-to-fuel volume ratios of the substitute and reference gases, respectively, expressed in $\mathrm{m}^3_{\mathrm{air}}/\mathrm{m}^3_{\mathrm{fuel}}$, and SG_s and SG_r are the specific gravities of the substitute and reference gases relative to air [9, 58, 60].

This index quantifies whether the substitute gas requires approximately the same primary air supply as the reference gas under unchanged burner geometry. A value of $J_A = 1.0$ indicates equivalence in the theoretical combustion-air requirement after accounting for the density-driven change in gas flow through the burner injector.

Deviations from this value indicate that the substitute gas may alter burner aeration, excess-air conditions, flame stability, furnace atmosphere composition, thermal NOx formation, and product quality [9, 60].

In practical interchangeability assessment, the admissible condition is commonly expressed as $J_A = 1.0 \pm 5\%$, corresponding to:

$$0.95 \leq J_A \leq 1.05. \tag{2.18}$$

Recent hydrogen-blending studies applying the Weaver framework show that the primary air ratio can become restrictive as hydrogen concentration increases, since hydrogen changes both the stoichiometric air demand and the density of the gas mixture [9, 61].

In addition to the Weaver-based indices, a complementary hydrogen-specific screening criterion is retained. This criterion is not a classical Weaver index, but a practical compatibility threshold based on the absolute hydrogen volume fraction in the blend:

$$J_{HT} = x_{H_2} \quad [-] \tag{2.19}$$

where $x_{\mathrm{H_2}}$ denotes the volumetric hydrogen fraction in the delivered gas blend. This criterion imposes a direct limit on hydrogen content independently of Wobbe Index compliance, reflecting that hydrogen affects combustion behaviour through mechanisms not fully captured by Wobbe-based indicators alone. These effects are discussed in detail in Section 2.3.

For this reason, several studies and network assessments treat approximately 20% $\mathrm{H_2}$ by volume as an upper screening threshold for the use of existing natural gas infrastructure and end-use

equipment without major modification. However, this value should not be interpreted as a universal technical limit, since admissibility depends on burner design, operating pressure, control strategy, materials compatibility, safety margins, and the specific industrial application considered [7, 39].

Shkarovskiy et al. [9] show that hydrogen addition affects the Weaver-based interchangeability indices in a non-equivalent way. As illustrated in Figure 2.8, both J_A and J_H decrease as the hydrogen fraction increases, but the primary air ratio presents a more restrictive behaviour. While J_H remains close to the lower admissible limit at 10% H_2, J_A decreases more sharply and breaches the lower tolerance threshold as the hydrogen fraction approaches approximately 20% by volume. This confirms that Wobbe-based heat-input equivalence alone is insufficient to assess hydrogen blending compatibility, since burner aeration may become limiting before other interchangeability criteria are violated.

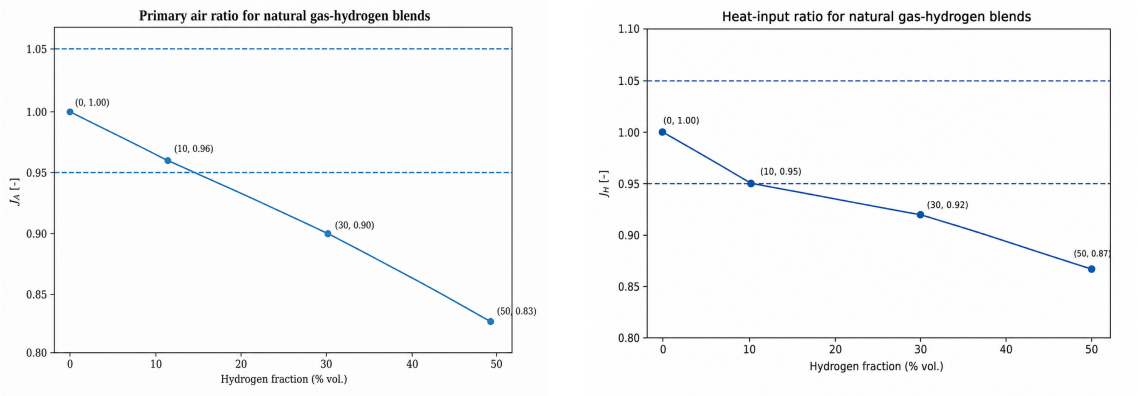


Figure 2.8: Evolution of Weaver-based interchangeability indices for natural gas-hydrogen blends as a function of hydrogen volume fraction, adapted from Shkarovskiy et al. [9].

This comparison indicates that J_A may become restrictive at blend compositions for which the Wobbe Index criterion still appears admissible. A mixture may therefore maintain J_H within the accepted tolerance band while simultaneously falling outside the admissible aeration envelope. For this reason, J_A should be treated as an independent and non-redundant criterion for equipment modification assessment, rather than as a parameter that can be replaced by Wobbe Index analysis alone [9].

The interchangeability criteria discussed in this subsection are consolidated in Table 2.2, together with their admissible limits, reference sources, and potential consequence of violation for industrial combustion equipment.

2.4. Combined Effects

Table 2.2: Summary of interchangeability criteria applicable to renewable gas blends in Group H distribution networks.

Criterion	Admissible limit	Reference source	Consequence of violation
J_H – Wobbe Index deviation	$0.95 \leq J_H \leq 1.05$	[41, 42]	Burner adjustment or retrofit assessment
J_{HT} – Absolute hydrogen fraction	$x_{H_2} \leq 20\%$ vol.	[7, 39]	Hydrogen-specific equipment compatibility assessment
J_A – Primary air ratio	$0.95 \leq J_A \leq 1.05$	[9, 58]	Air-fuel recalibration or combustion-system retrofit assessment

In addition to J_H, J_A, and the hydrogen-specific threshold J_{HT}, the full Weaver framework includes further indices that address specific combustion failure modes. The flame lifting index, J_L, assesses the likelihood of flame detachment from the burner port, which occurs when gas-flow velocity exceeds local burning velocity, causing the flame to stabilise downstream or extinguish. By contrast, the flashback index, J_F, evaluates the risk of upstream flame propagation into the premixing zone when burning velocity exceeds mixture flow velocity [9, 58, 60].

These failure modes are particularly relevant for hydrogen-enriched blends, since hydrogen addition increases laminar burning velocity and, consequently, flashback propensity, as discussed in Section 2.3. However, existing literature indicates that such effects remain relatively limited at low hydrogen blending levels and become operationally significant mainly as hydrogen fractions approach the upper limits considered in appliance and burner studies [7, 9, 39].

The yellow tipping index, J_Y, measures the tendency to form luminous yellow flame tips, which indicate incomplete hydrocarbon pyrolysis and soot formation. This phenomenon is typically less pronounced in hydrogen-enriched blends, since hydrogen addition reduces the hydrocarbon content of the fuel mixture. The incomplete combustion index, J_I, assesses the risk of carbon monoxide formation and unburnt fuel in combustion products, indicating whether the substitute gas may compromise combustion completeness under unchanged burner conditions [58, 60].

For natural gas/hydrogen blends, Shkarovskiy et al. [9] show that J_L and J_F are among the Weaver indices most responsive to hydrogen addition, reflecting the kinetic acceleration described in Section 2.3. By contrast, J_Y and J_I are less affected by hydrogen enrichment, as reduced hydrocarbon content suppresses soot formation and limits incomplete combustion risk under the evaluated conditions [9, 58, 60].

This selectivity shows that the main combustion risks associated with hydrogen blending extend beyond stoichiometric or energy-based considerations and include aerodynamic and kinetic effects. A blend may therefore satisfy heat-input requirements while still presenting challenges related to aeration, flame stabilisation, or flashback propensity.

Within the scope of this thesis, J_H, J_A, and J_{HT} are retained as the principal operational screening criteria because they are directly related to heat input, primary air requirement, and hydrogen-specific compatibility limits. The remaining Weaver indices provide valuable physical context for interpreting the combustion impacts of hydrogen enrichment. However, using them as definitive triggers for equipment modification would require burner-specific validation, operational

data, and safety assessments beyond the scope of a screening-level techno-economic model.

Although the full Weaver index set provides a comprehensive characterisation of combustion failure modes, the primary air ratio, J_A, has particular operational significance for industrial combustion equipment. In domestic and commercial appliances, gas interchangeability assessments are often linked to visible flame stability phenomena, such as lifting, flashback, and yellow tipping [9, 58, 60]. In industrial process furnaces, however, the combustion atmosphere inside the heating chamber is often the critical operational variable [9].

This atmosphere is directly influenced by the air-to-fuel ratio and resulting excess-air level. Key characteristics such as O_2 concentration, CO content, oxidising or reducing conditions, and thermal profile affect product quality, energy efficiency, NO_x formation, and equipment integrity. These factors are process-specific and may be more sensitive than the visible flame phenomena represented by J_L, J_F, and J_Y alone [9, 13].

The J_A index is directly linked to this operational context. Values of J_A below the lower admissible bound of 0.95 indicate that, under unchanged burner geometry and supply conditions, the substitute gas may entrain insufficient primary air compared with the reference gas. This reduction can lower the effective air-to-fuel ratio and shift the combustion atmosphere towards fuel-rich conditions, increasing the risk of incomplete combustion, CO formation, and product-quality deterioration in ceramic and glass processes where oxidising-atmosphere control is critical [9, 13].

Conversely, J_A values above the upper admissible bound of 1.05 indicate a tendency towards excess air, which can increase flue-gas losses, alter furnace thermal efficiency, and influence NO_x formation depending on flame temperature, oxygen availability, and burner configuration. For example, in the ceramic tile case reported by Carvalho et al. [13], biomethane substitution under constant air-flow conditions reduced the O_2 concentration in the furnace atmosphere. This demonstrates that gas substitution can affect industrial process quality through changes in air-to-fuel balance rather than solely through visible flame instability.

The mechanistic relationship between primary air requirement, combustion atmosphere, and industrial process outcomes confirms that J_A is more than an abstract interchangeability indicator. For hard-to-abate industrial consumers, it provides a practical warning signal for operational consequences related to furnace-atmosphere control, combustion efficiency, emissions, and product quality.

2.5 Techno-Economic Models and Policy Instruments

The integration of renewable gases into industrial energy systems involves both technical and economic considerations. Although the preceding sections addressed the physical and contractual dimensions of biomethane and hydrogen blending, a comprehensive evaluation of industrial renewable gas adoption must also account for the techno-economic frameworks and policy instruments that shape investment, procurement, and compliance decisions.

Quantitative indicators such as net present value (NPV), levelised costs, carbon abatement cost (CAC), and break-even analysis are widely used to assess the economic feasibility of renewable energy and industrial decarbonisation pathways [62, 63]. These indicators provide structured measures of cost, value creation, carbon-abatement performance, and threshold conditions. However, they differ in their ability to capture long-term uncertainty, technology-specific cost drivers, and exposure to carbon pricing.

For renewable hydrogen, the levelised cost of hydrogen (LCOH) remains a key reference indicator for comparing production pathways and informing policy-support mechanisms. However, this metric primarily reflects the economics of hydrogen production projects rather than the total cost incurred by industrial end-users [64]. LCOH estimates are highly sensitive to system boundaries and assumptions regarding electricity prices, full-load hours, electrolyser capital expenditure, cost of capital, efficiency, stack replacement, balance of plant, engineering, procurement and construction costs, and operating expenditure [64, 65].

Simplified LCOH values may therefore underestimate the effective cost of renewable hydrogen when site-specific infrastructure, financing conditions, compression, storage, transport, certification, and implementation risks are excluded [64, 65]. In the context of industrial renewable gas integration, this distinction is important because the relevant decision variable is not only the production cost of hydrogen, but the delivered and certified cost of renewable gas that satisfies the physical, contractual, and regulatory requirements of the industrial installation.

The following review provides an overview of current techno-economic modelling approaches and policy instruments for renewable gas integration. It identifies the limitations of conventional deterministic methods and establishes the rationale for adopting scenario-based and stochastic modelling under conditions of market, regulatory, and technical uncertainty.

Levelised Cost Frameworks and Stochastic Price Modelling

Levelised-cost frameworks are widely used to compare decarbonisation pathways across energy sources, technologies, and geographic contexts. In the context of industrial heat, a normalised cost metric expressed per unit of useful energy output enables alternative decarbonisation pathways to be compared on a common basis, accounting for capital expenditure, fuel costs, carbon-cost exposure, conversion efficiency, and utilisation assumptions.

Gilbert et al. [66] develop a generalised framework for decarbonised heat supply across multiple heat sources and industrial applications, covering process temperatures from approximately 80 °C to 1200 °C. Their analysis shows that the cost of delivering carbon-neutral heat depends strongly on the selected heat source, the required temperature level, and the local energy-system context. It also demonstrates that fuel and carbon costs may dominate total cost outcomes in several industrial heat applications.

In addition to this multi-source perspective, Zier et al. [6] employ a bottom-up sectoral model for the German glass industry, which is characterised by high-temperature melting processes and

limited short-term fuel-switching options. Their findings suggest that deep decarbonisation requires fuel switching to low-carbon energy vectors rather than relying solely on efficiency improvements, thereby identifying fossil gas substitution as a relevant transition pathway within the modelled timeframe [6].

Together, these studies position levelised-cost analysis and sectoral techno-economic modelling as key analytical references for industrial heat decarbonisation. Nevertheless, three structural limitations of conventional frameworks are particularly relevant when evaluating renewable gas integration through distribution networks.

First, deterministic cost metrics typically depend on fixed values or predefined trajectories for fuel prices, carbon allowance prices, and renewable attribute costs. While this approach facilitates comparison between pathways, it conceals the probability that a given option may become economically advantageous or disadvantageous under changing market conditions. This limitation is especially important when carbon-price uncertainty is a primary driver of economic outcomes, supporting the use of stochastic EU ETS price modelling in industrial decarbonisation assessment [64, 67].

Second, conventional frameworks often compare energy vectors on a EUR/MWh basis without explicitly accounting for the physical and combustion constraints that determine compatibility with existing equipment. In the context of biomethane and hydrogen blending within gas distribution networks, factors such as gas-quality admissibility, Wobbe Index compliance, primary air requirements, hydrogen content, burner compatibility, and retrofit needs influence both technical feasibility and cost [7, 9, 42, 58]. Retrofit costs arising from interchangeability violations may therefore fall outside the boundaries of conventional levelised-cost analyses.

Third, standard frameworks frequently assume a direct correspondence between the energy carrier physically consumed and the decarbonisation attribute assigned to that consumption. This assumption is problematic in renewable gas networks, where the physical gas composition delivered at the industrial meter may differ from the renewable content legally attributed through certification, or other contractual mechanisms [3, 24]. The distinction between physical and contractual attributes therefore requires an analytical framework that separately accounts for delivered energy cost, renewable attribute procurement, retrofit-related capital expenditure, and residual EU ETS compliance exposure.

Net present value (NPV) complements levelised-cost indicators by preserving the timing and magnitude of cash flows associated with an investment decision. While levelised-cost metrics normalise discounted costs over a physical output, such as useful heat or hydrogen produced, NPV evaluates whether a capital commitment generates net economic value over the project horizon. It is therefore widely used in renewable energy project appraisal and industrial decarbonisation assessment [62].

Within industrial decarbonisation studies, NPV is especially relevant because retrofit investments, renewable gas procurement costs, carbon-cost savings, and avoided fossil-fuel expenditures are distributed across different time periods. A pathway with a competitive levelised cost may remain unattractive if it requires substantial upfront capital expenditure, exposes operators to uncertain future fuel prices, or delays cost savings until later in the planning horizon. Conversely, a pathway with a higher apparent energy cost may be economically justified if it mitigates future carbon exposure or avoids more costly retrofit obligations [62].

A related application is break-even analysis, which determines the carbon price, renewable gas procurement cost, subsidy level, or investment horizon at which a decarbonisation option

reaches economic neutrality. Break-even indicators are therefore valuable for translating discounted cash-flow results into threshold values that are interpretable by industrial decision-makers and policymakers [62, 63].

However, conventional NPV analysis often relies on deterministic assumptions regarding future cash flows, discount rates, fuel prices, carbon allowance prices, and policy conditions. This produces a single point estimate and typically frames the investment decision as a binary accept-or-reject outcome. Although useful for transparent comparison, this approach does not adequately capture uncertainty in the main cost drivers of industrial decarbonisation, including EU ETS allowance prices, renewable gas procurement costs, certification costs, and technology costs [15, 67, 68].

This limitation is particularly significant for renewable gas integration, since the economic value of biomethane or hydrogen blending depends on variables that may change considerably over a multi-decade planning horizon. Among these variables, EU ETS carbon prices are especially influential because they affect both the operating cost of continued fossil natural gas use and the avoided-cost value associated with renewable gas adoption.

Abadie and Chamorro [67] illustrate this limitation by analysing carbon-constrained investments under stochastic EU ETS price dynamics. Their findings show that carbon-price volatility can significantly influence both investment timing and appraisal under uncertainty. Although their study focuses on carbon capture rather than renewable gas blending, the central insight is directly applicable to industrial renewable gas adoption that when carbon prices are uncertain, deterministic investment appraisal may provide an incomplete basis for decision-making [67].

Monte Carlo simulation offers a probabilistic extension to conventional techno-economic assessment by allowing uncertain variables to be sampled from defined distributions and generating a spectrum of possible economic outcomes rather than a single deterministic estimate. In the context of renewable gas integration, this approach is particularly relevant because EU ETS prices, renewable gas procurement costs, certification costs, and the phase-out of free allocations may evolve concurrently over the planning horizon [15, 67].

Additional economic indicators, such as carbon abatement cost (CAC), are also fundamental to industrial decarbonisation assessment. CAC quantifies the incremental cost of a decarbonisation pathway per tonne of CO_2 avoided relative to a fossil baseline, enabling direct comparison with carbon allowance prices under the EU ETS. A pathway is considered economically rational when its abatement cost is lower than the relevant carbon price or avoided carbon-compliance cost. Recent research by Shafiee and Schrag employs CAC as a primary metric to assess the economic viability of green hydrogen across end-use sectors, while biomethane-focused studies similarly use abatement-cost analysis to evaluate the cost-effectiveness of renewable gas in emission reduction pathways [63].

Avoided emissions provide a complementary physical metric, measuring the quantity of CO_2 emissions reduced relative to a fossil baseline independently of the cost structure used to achieve that reduction. In industrial decarbonisation assessment, avoided emissions are therefore useful for linking economic indicators such as NPV and CAC to the actual decarbonisation performance of each pathway [63, 66].

In summary, the reviewed literature supports the use of levelised-cost indicators, NPV, break-even analysis, stochastic carbon-price modelling, Monte Carlo simulation, CAC, and avoided emissions in industrial heat decarbonisation assessment. Nevertheless, these tools are often applied within frameworks that treat technical feasibility, carbon exposure, renewable procurement, and price uncertainty as separate dimensions. This separation becomes restrictive when renewable gas

blending is assessed at the scale of a specific hard-to-abate industrial installation, where physical blend admissibility, retrofit requirements, renewable attribute procurement, and EU ETS exposure converge within a single investment decision. This underscores the need for integrated techno-economic approaches that connect economic performance, carbon-abatement value, stochastic market uncertainty, and the technical constraints associated with renewable gas use in existing industrial combustion systems.

Renewable Gas Markets and Procurement Instruments

Assessing the role of renewable gases in industrial energy systems requires more than the comparison of economic indicators alone. Industrial consumers do not evaluate biomethane and green hydrogen only through the cost per unit of useful heat. They also consider market availability, contract duration, price risk, certification reliability, and policy-support mechanisms when deciding whether to adopt renewable gas procurement strategies.

Market-based procurement instruments play an important role in renewable gas adoption. Power purchase agreements (PPAs) and contracts for difference CfDs) are widely used in renewable energy markets to reduce investment risk, stabilise revenues, and improve price predictability [69]. Although these instruments are most commonly associated with renewable electricity, their underlying economic principles are also relevant to renewable gases, since biomethane and green hydrogen require contractual structures capable of supporting investment, bankability, and long-term industrial offtake.

Renewable gas procurement is therefore not determined by price alone. It also depends on how contracts allocate supply risk, price volatility, certification value, and long-term commitments among producers, suppliers, and industrial consumers. These instruments influence not only procurement costs, but also the ability of industrial operators to manage uncertainty, demonstrate compliance, and justify investments in fuel switching or equipment adaptation [62, 66].

Biomethane and green hydrogen should not be treated as interchangeable renewable gas markets. Biomethane is the more mature option, supported by commercially available technologies such as anaerobic digestion, upgrading, and grid injection. According to Gas for Climate, the EU could sustainably produce up to 41 bcm of biomethane by 2030 and 151 bcm by 2050, contributing to the REPowerEU target of 35 bcm per year by 2030 [70]. However, market expansion remains constrained by sustainable feedstock availability, the spatial dispersion of organic resources, permitting procedures, grid connection requirements, upgrading and injection capacity, and the effectiveness of national support and certification systems [70].

Biomethane purchase agreements (BPAs) allow industrial consumers to secure renewable gas volumes over periods aligned with their decarbonisation plans. Similarly to PPAs in the electricity sector, BPAs may define price, volume, delivery conditions, feedstock origin, certification requirements, and contract duration [69]. Long-term BPAs can reduce exposure to short-term price volatility and improve revenue certainty for new biomethane projects. However, they may also limit flexibility if prices decline, demand changes, or alternative compliance options become available. By contrast, spot-market procurement preserves flexibility but exposes industrial consumers to higher price and supply uncertainty, particularly in a market still constrained by feedstock availability and implementation capacity.

Green hydrogen presents a different procurement challenge. Although many projects have been announced globally, actual deployment has progressed more slowly than expected due to high costs, uncertain demand, infrastructure delays, and slow market formation [16]. Odenweller

and Ueckerdt also highlight the gap between ambitious hydrogen targets and realistic short-term deployment progress [71]. Green hydrogen should therefore not yet be regarded as a mature market with stable and transparent costs. Instead, it remains a strategic energy carrier whose deployment is shaped by implementation risk, uncertain demand, infrastructure readiness, and the need for public support.

Because of these constraints, green hydrogen generally requires stronger policy support than biomethane. CfDs, fixed-premium auctions, and similar schemes have become central instruments for reducing the cost gap between low-emission hydrogen and fossil alternatives. The European Hydrogen Bank supports renewable hydrogen producers through fixed-premium auctions, while the H2Global programme adopts a CfD-like structure in which public funds cover the difference between the price paid to hydrogen suppliers and the resale price achievable with industrial users [69].

Even though these mechanisms can reduce investment and revenue risks, they dont eliminate core uncertainties related to renewable electricity prices, electrolyser costs, infrastructure development, certification, and demand creation. Firm demand for low-emission hydrogen remains limited, and coordinated policy action is still required across offtake agreements, infrastructure planning, and demand-side measures to support market formation [16]. Odenweller and Ueckerdt further argue that realising the global green hydrogen project pipeline without carbon pricing would require substantially higher public support than currently planned [71]. Hydrogen CfDs and similar instruments should therefore be interpreted as risk-sharing tools for an early-stage market, rather than as evidence that green hydrogen is already mature, liquid, or price-transparent.

The procurement risks associated with biomethane and green hydrogen are therefore structurally different. For biomethane, the main uncertainties concern feedstock availability, national project implementation capacity, price formation in an emerging certificate market, and the reliability of RED III certification. These risks are significant, but they are associated with a comparatively mature technology and can be partially managed through long-term BPAs [69]. Green hydrogen faces broader implementation challenges, including uncertain production costs, exposure to renewable electricity prices, infrastructure readiness, demand creation, project-delivery risk, and compliance with RFNBO certification requirements [3, 16, 71].

This distinction directly informs the modelling approach developed in Chapter 3. In more mature renewable gas markets, biomethane procurement can be represented through contract structures that reduce price volatility and provide revenue certainty to producers [69, 70]. Green hydrogen, by contrast, is treated as a less mature market characterised by higher implementation risk, stricter physical constraints, stronger dependence on public support, and uncertainty around infrastructure readiness and RFNBO certification. The practical implementation of these requirements remains uncertain due to ongoing regulatory development, as discussed in Section 1.1.2 [3, 16, 71].

2.6 Overall Policy Benchmarking

The variation in renewable gas deployment across EU Member States cannot be explained by technical potential or stated political ambition alone. Countries with comparable feedstock availability, gas infrastructure, and REPowerEU-aligned objectives display markedly different injection volumes and market penetration rates, suggesting that policy-instrument design plays a decisive role in determining whether renewable gas targets are translated into operational capacity [1, 72].

However, technical admissibility does not by itself mobilise investment. Renewable gas projects require a policy architecture capable of creating bankable revenue conditions, credible certification mechanisms, and predictable market access sufficiently early to influence project development and industrial procurement decisions [1].

For this reason, policy benchmarking is used here not as a descriptive comparison of national strategies, but as a diagnostic tool for assessing whether policy instruments are capable of shaping market formation within the relevant investment window. The key question is not only whether a country has renewable gas targets, but whether the instruments supporting those targets become operational early enough to generate physical supply, contractual certainty, and recognised renewable attributes before industrial compliance horizons are reached [1].

Three instrument properties are particularly relevant for this assessment: tariff sufficiency, contract horizon, and temporal antecedence. All together, they determine whether a support mechanism provides an adequate price signal, enough revenue certainty, and sufficient lead time for renewable gas projects to move through permitting, financing, construction, network connection, certification, and offtake arrangements. This temporal dimension is particularly important, since biomethane and renewable hydrogen projects can require several years before reaching operational injection [1].

Main implication is temporal. The year in which a policy instrument becomes operationally effective determines which industrial compliance horizon it can realistically influence. A support scheme introduced too close to a regulatory deadline may be formally aligned with national or European objectives, while still being unable to affect physical renewable gas availability within that same horizon.

Assessed through tariff sufficiency, contract horizon, and temporal antecedence, current Portuguese policy architecture provides important legal and institutional foundations. However, it does not yet fully ensure that domestic renewable gas supply will be available early enough to support industrial decarbonisation decisions within the 2030, 2035, and 2040 compliance horizons [1].

2.6. Overall Policy Benchmarking

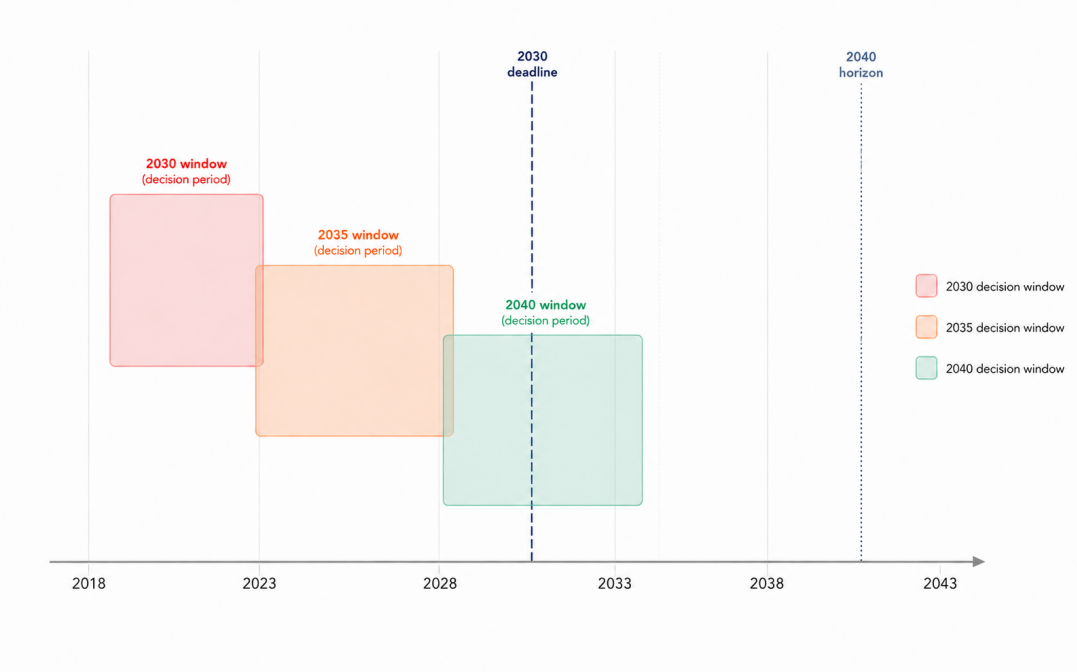


Figure 2.9: Renewable gas policy decision windows and compliance horizons

Figure 2.9 illustrates how policy timing interacts with industrial compliance horizons. The 2030 horizon is effectively constrained, since projects capable of contributing materially to domestic renewable gas availability by that date would have required investment decisions, permitting, financing, construction, network connection, and certification several years earlier. The 2035 window remains more actionable, but is narrowing rapidly as project-development lead times are considered. By contrast, the 2040 horizon still offers a more realistic opportunity for policy instruments adopted in the near term to influence physical injection capacity and certified renewable gas availability.

The earlier integration of renewable energy into the electricity sector provides a useful precedent for interpreting the decision windows associated with renewable gases [73]. The expansion of renewable electricity did not occur through a single policy intervention, but through successive phases involving target definition, support-scheme implementation, infrastructure adaptation, market development, technology cost reduction, and gradual investor confidence [74, 75]. Each phase depended on decisions taken sufficiently early to influence the following stage of deployment.

A similar temporal logic could apply to biomethane and renewable hydrogen, strategic targets must be followed by operational instruments, project development, network integration, certification systems, and market formation before meaningful industrial supply can emerge [74]. These decision windows presented in Figure 2.9 should therefore be interpreted as stages in a broader market-development process, in which delayed policy activation may postpone not only individual projects, but also the learning, liquidity, and institutional maturity required for the renewable gas market to evolve.

In the absence of such certainty, industrial consumers may be forced to rely on procurement from more mature European markets like, Germany, France or Denmark, the use of unbundled Guarantees of Origin, or even choose alternative decarbonisation pathways [10, 16]. These options may provide partial compliance flexibility, but they may also increase exposure to price volatility, weaken the link between physical gas delivery and renewable attribution, or even require technolo-

gies that are less compatible with existing high-temperature industrial processes [16]. The timing of policy implementation therefore becomes a central determinant of whether renewable gas can function as a practical decarbonisation route for hard-to-abate industries connected to distribution networks.

2.6.1 National Context

Portugal's biomethane market remains at an early stage of development. Registered injection capacity under DL 62/2020, as reported in RMSA-G 2025, amounts to approximately 0.546 TWh/yr accumulated through 2026 across national gas distribution and transmission networks [76]. This remains well below the renewable gas requirement implied by RED III **(Article 22)** for the Portuguese industrial sector, estimated at approximately 2.7 TWh/yr by 2030 using RMSA-G 2024 industrial demand projections [76, 77]. Such gap is structural rather than technical. Existing gas infrastructure can accommodate biomethane and limited hydrogen blending within established interchangeability thresholds [7], but a policy architecture capable of mobilising domestic supply at the required scale has not yet been fully implemented.

In March 2024, the Portuguese government presented the *Plano de Ação para o Biometano* (PAB), later summarised by *Laboratório Nacional de Energia e Geologia* (LNEG), which includes phased industrial incorporation obligations and a consolidated licensing guide [78, 79]. These measures provide an important institutional foundation for market development. However, they do not yet constitute a bankable price-support instrument with sufficient tariff certainty, contract duration, and temporal antecedence to mobilise the project pipeline implied by national targets.

A companion study to this dissertation, currently under submission, quantifies these deployment gaps and their supply–demand structure across alternative biomethane and hydrogen trajectories. Its principal results are reproduced in Appendix I for reference. A study that also develops a policy-implication framework based on support mechanisms adopted in more mature European renewable gas markets, mechanisms that are used as comparative references to assess which policy design elements could be relevant for emerging markets such as Portugal.

Chapter 3

Methodology

The modelling framework developed in this chapter examines the progressive decarbonisation of hard-to-abate industrial installations connected to gas distribution networks. During this transition, industrial consumers are affected by changes in the physical composition of the delivered gas, the cost and availability of certified renewable gases, renewable attribute procurement requirements, and exposure to the EU ETS carbon price.

Renewable gas integration differs fundamentally from electricity-based decarbonisation. Once electricity enters the grid, its physical characteristics do not vary according to the generation source. Gas networks, by contrast, may deliver fuels with changing chemical composition, energy density, combustion behaviour, and equipment compatibility [21]. The methodology therefore separates the analysis into two interconnected layers: **a physical layer and a contractual layer.**

Physical layer evaluates the gas mixture delivered to the installation, calculating the relevant thermophysical and combustion properties, assesses gas interchangeability, and identifies retrofit requirements whenever the admissible operating limits of the existing equipment are exceeded.

The contractual layer determines how renewable gas consumption is recognised for certification, emissions accounting, and regulatory compliance. It includes the procurement of guarantees of origin and RFNBO-certified hydrogen, the allocation of effective emission factors, and the resulting exposure to renewable energy obligations and EU ETS costs.

These layers are treated separately because physical delivery and contractual attribution do not necessarily evolve in parallel, as illustrated by book-and-claim arrangements. The composition of the gas delivered to the installation determines combustion performance and equipment operation, regardless of the certificates acquired by the consumer. Renewable attributes, by contrast, may change the installation's recognised emissions and compliance position without altering the physical properties of the gas entering the burners. The model therefore connects both dimensions while preserving the distinction between them.

The economic analysis combines deterministic market scenarios with stochastic carbon-price modelling. Although this hybrid approach may be criticised for bringing together two different forms of uncertainty treatment, it was adopted deliberately in response to the limited availability of robust data for modelling the future evolution of renewable gas markets. Introducing additional stochastic variables would have required assumptions that were difficult to calibrate and could have added considerable complexity to the interpretation of the results without materially improving the conclusions sought in this study.

Biomethane procurement is therefore represented through three deterministic contract-price trajectories, each anchored to the Portuguese renewable gas procurement mechanism established under portuguese auctions.

Renewable hydrogen follows a separate deterministic trajectory, reflecting its distinct certification requirements, supply conditions, and market-development pathway. Unlike biomethane, in our scenarios, its physical contribution is constrained by the hydrogen fraction made available through the network-transition schedule, while its recognition as renewable consumption depends on compliance with the applicable RFNBO requirements [24].

Uncertainty in the EU ETS carbon price is represented through Monte Carlo simulation. Alternative carbon-price trajectories are generated and propagated through the economic model, allowing the resulting indicators to be evaluated across a distribution of possible carbon-market outcomes rather than under a single deterministic pathway.

The framework consists of three sequentially connected models. Model 1 evaluates the physical properties and admissibility of the delivered gas blend. Model 2 calculates the corresponding energy, renewable attribute, and carbon-compliance costs. Model 3 integrates these outputs into the economic and environmental indicators used to compare the available decarbonisation pathways. The Monte Carlo extension introduces carbon-price uncertainty into this integrated structure.

All parameters are defined explicitly and may be adjusted to represent other hard-to-abate industrial installations connected to gas distribution networks. The framework is therefore intended not only as a case-specific calculation tool, but also as a transferable decision-support structure for industrial consumers operating under renewable gas, RED III, and EU ETS constraints.

The full computational framework was implemented in Python through a central control script that coordinates the sub-models and executes the calculations sequentially. The corresponding pseudocode is presented in Appendices B–F, covering Models 1 to 3 and the Monte Carlo extension.

Installation-specific parameters, market assumptions, and scenario calibration are presented in Chapter 4. There, the framework is applied to a hard-to-abate industrial consumer connected to the REN–Portgás distribution network in Portugal.

3.1 Motivation and Analytical Framework

The proposed methodology evaluates the techno-economic implications of progressive renewable gas integration for hard-to-abate industrial installations connected to gas distribution networks. Its structure is intentionally generic, allowing the framework to be transferred across different installations and network contexts, provided that the relevant regulatory conditions remain broadly consistent with RED III and the EU ETS.

A single cost comparison cannot adequately represent this transition. Differences expressed only in EUR/MWh overlook the interaction between fuel composition, equipment compatibility, renewable gas certification, carbon exposure, and long-term market development. A pathway that appears competitive on an energy-cost basis may still require substantial retrofit investment, fail to satisfy the applicable certification requirements, or expose the installation to increasing carbon costs over the planning horizon.

Four drivers structure the analysis, as illustrated in Figure 3.1. Regulatory compliance captures the renewable energy requirements established under RED III and the progressive reduction of free

allowance allocation under the EU ETS system. Physical admissibility covers gas composition, interchangeability limits, combustion compatibility, and the retrofit measures required when existing operating boundaries are exceeded. Procurement cost includes physical energy supply, renewable attribute acquisition, and the additional cost of certified biomethane and RFNBO hydrogen. Market uncertainty is represented through stochastic EU ETS price trajectories, while renewable gas costs are treated through deterministic market scenario assumptions, based on national reference values.

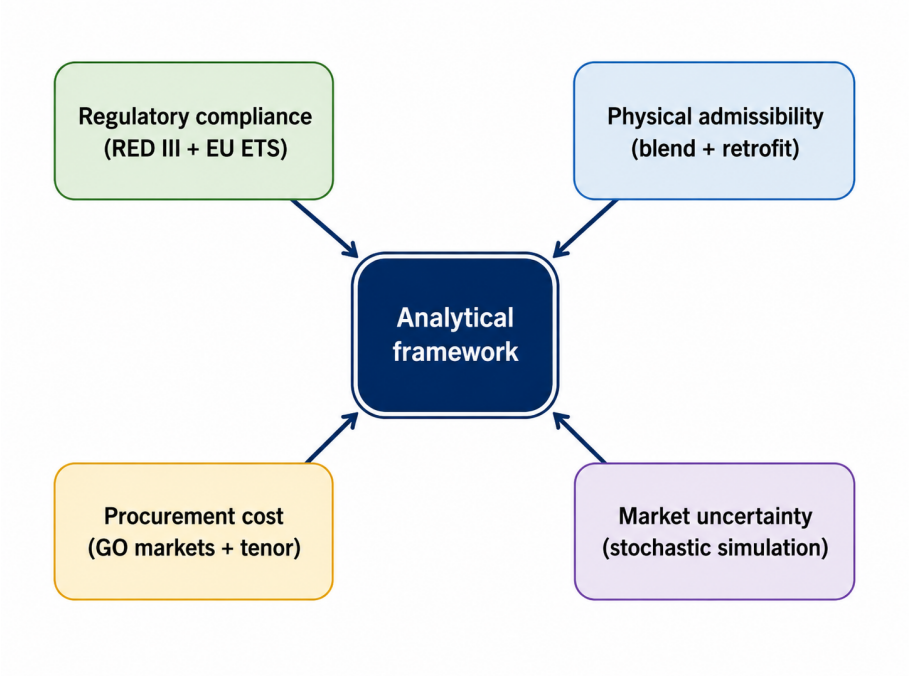


Figure 3.1: Main drivers of the analytical framework. Source: own elaboration.

The computational framework was implemented and organised into three sequential models, followed by a stochastic extension, as illustrated in Figure 3.2.

Model 1 characterises the thermophysical and combustion properties of the gas blend delivered during each network phase. It then evaluates the applicable interchangeability criteria and determines whether the resulting composition can be accommodated by the existing equipment or requires retrofit investment.

Using the physical outputs from Model 1, Model 2 calculates the annual operating expenditure associated with each configuration. Finally, Model 3 aggregates these annual results over the full planning horizon and calculates the principal economic and environmental indicators. These include net present value, the levelised cost of decarbonised energy, carbon abatement cost, and cumulative avoided emissions relative to a baseline.

Carbon-price uncertainty is introduced through a Monte Carlo extension. Repeated EU ETS price simulations are propagated through the integrated framework, producing distributions of economic outcomes rather than a single deterministic estimate.

A time index t identifies each year of the planning horizon and governs the evolution of network phases, procurement costs, renewable attribute coverage, emissions, and economic performance.

Two independent dimensions are evaluated in each year. The network phases,

$$k \in \{0, 1, 2, 3\}, \tag{3.1}$$

defines the physical gas composition delivered to the installation. It therefore determines the thermophysical behaviour of the blend, its compatibility with the existing equipment, and any associated retrofit requirement.

The biomethane procurement scenario,

$$S \in \{\mathrm{S1}, \mathrm{S2}, \mathrm{S3}\}, \tag{3.2}$$

defines the contract-price trajectory for certified biomethane and the corresponding incremental procurement premium. Unlike the network phase, S does not alter the physical composition of the gas supplied to the installation. Its influence is confined to renewable attribute procurement, compliance expenditure, and the resulting economic performance.

Keeping k and S separate prevents physical blend admissibility from being conflated with contractual renewable attribution. **Their annual effects are combined only after the technical and procurement calculations have been completed, allowing Model 3 to evaluate the overall economic and environmental performance of each pathway over the planning horizon.**

3.1. Motivation and Analytical Framework

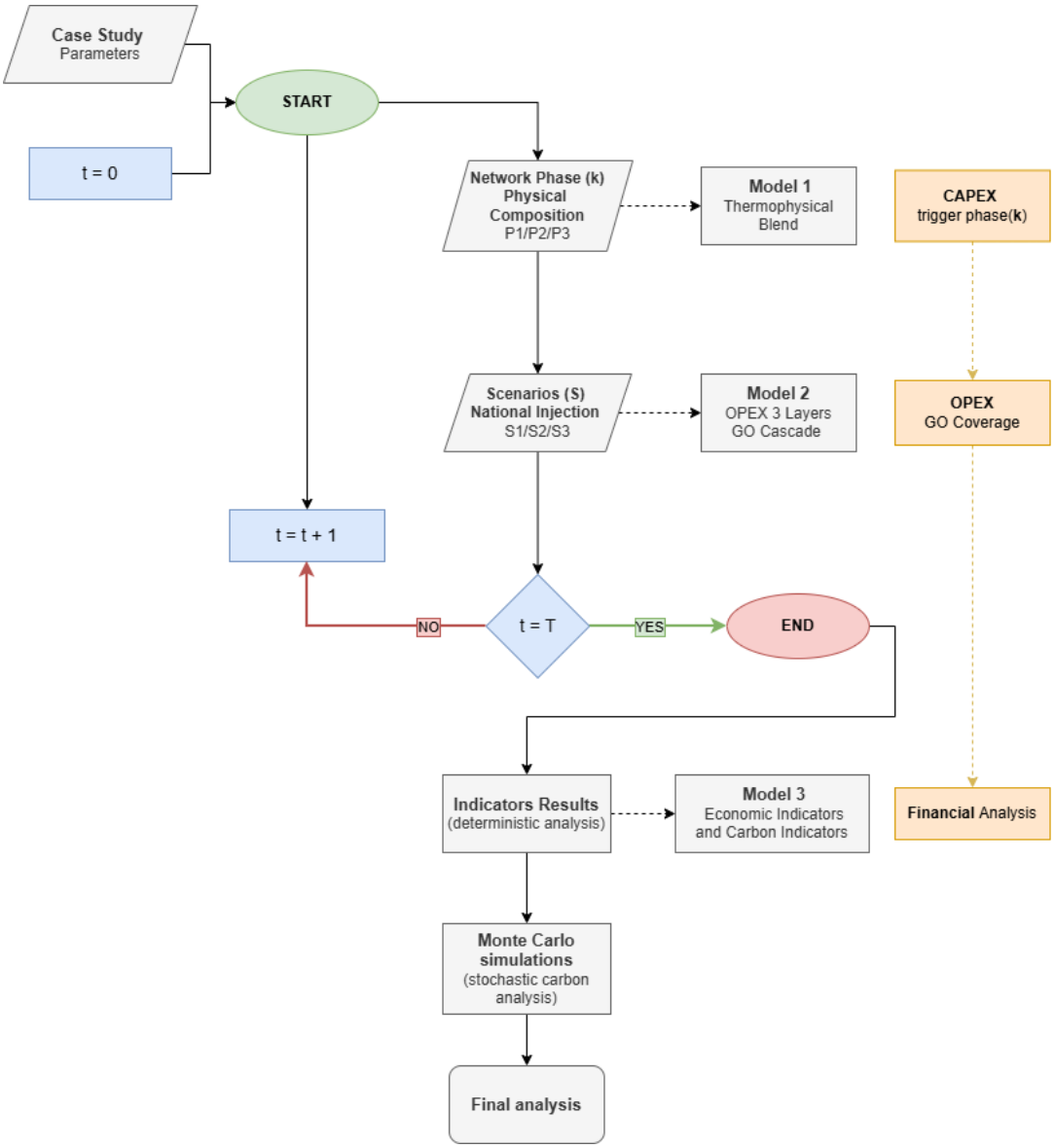


Figure 3.2: Model architecture and sequential execution pipeline.

Building on the modelling principles established above, the framework adopts the following structural assumptions:

- Physical and contractual layers are evaluated separately, although both remain active throughout the analysis
- Industrial installations considered are assumed to be connected to an existing natural gas distribution network, not included the capital cost of establishing an initial network connection.
- Network transition is represented through four discrete phases, P_0 to P_3, with progressively increasing shares of hydrogen and biomethane. The timing and composition of each phase are defined exogenously and applied consistently to the industrial installations supplied by the modelled network segment.
- Renewable attribute procurement determines the contractual share of energy recognised as

renewable, subject to the applicable certification, chain-of-custody, and regulatory rules. It does not alter the physical composition of the gas, the local combustion process, or specifically in the direct stack emissions generated at the installation.

- Procurement decisions are governed by relative energy costs, renewable attribute prices, carbon exposure, and the applicable regulatory obligations. For now, no specific investment grant, operating subsidy, or other public support instrument is assumed unless explicitly introduced in the case-study parameterisation.
- Network gas price is represented on a lower-heating-value (LHV) energy basis, in EUR/MWh. Changes in volumetric flow resulting from hydrogen or biomethane injection therefore do not modify the procurement cost within the scope of the present model. Although the regulated tariff structure includes both energy- and capacity-based components, the capacity-related effect is neglected, and the gas price is treated as a single all-in cost escalating at a fixed nominal rate.
- Biomethane and renewable hydrogen attribute availability is assumed to be domestically sourced, allowing the installation to satisfy at least the mandatory RED III compliance threshold through certificates under the national deployment trajectory. The conditions under which domestic availability may fall short of compliance requirements, and the implications for industrial consumers connected to the REN–Portgás network, are identified as a priority for future work and discussed qualitatively in Section 3.9.

3.2 Physical Baseline

A single reference baseline is adopted in the present model to evaluate the economic and carbon performance of renewable gas integration. This baseline, denoted as the Physical Baseline $B0$, represents the counterfactual situation in which the industrial installation remains exposed to the physical evolution of the gas network but does not procure renewable attributes through Guarantees of Origin.

Under $B0$, the installation consumes the gas physically delivered by the distribution network, undertakes any retrofit physically required by the network blend composition, procures no Guarantees of Origin, and therefore remains fully exposed to EU ETS carbon costs associated with emissions not covered by renewable attribution. $B0$ therefore constitutes an analytical reference used to measure the incremental cost, emissions reduction, and carbon-abatement value of renewable gas procurement relative to continued fossil exposure, rather than a regulatory-compliance strategy.

This distinction is important because retrofit requirements are triggered by the physical composition of the gas delivered at the meter, rather than by the contractual procurement strategy selected by the industrial consumer. Whenever a given network phase exceeds the admissible operating limits of the existing equipment, the corresponding retrofit requirement is applied to all pathways evaluated under the same physical conditions. Retrofit CAPEX is therefore treated as a mandatory adaptation cost associated with the network transition, rather than as a voluntary decarbonisation expenditure arising solely from renewable attribute procurement.

The baseline used for this comparison should, however, be interpreted as a hypothetical counterfactual rather than as a realistic long-term operating strategy. Once RED III obligations are transposed into binding national requirements, together with the corresponding compliance costs and penalties, continued operation without any form of decarbonisation response becomes increas-

ingly implausible. Industrial installations would therefore be expected to adopt either physical measures, contractual renewable procurement, or a combination of both

Consequently, the same $B0$ reference is used for Net Present Value, Carbon Abatement Cost (CAC), Levelised Cost of Decarbonised Energy, and cumulative avoided emissions. For CAC, B0 provides the fossil-exposure reference against which avoided emissions are measured, consistent with the interpretation of CAC as the incremental cost per tonne of CO_2 avoided relative to a counterfactual without renewable procurement [63]. For investment and cost indicators, B0 provides the common reference against which the incremental economic value of renewable attribute procurement and carbon-cost reduction is assessed.

3.3 Network Physical Phase Composition

The gas composition delivered at the industrial meter is treated as an exogenous input determined by the renewable gas injection schedule of the distribution network. It is not selected by the industrial consumer. Instead, the installation receives the blend available at its connection point and must adapt its technical and economic response to the resulting operating conditions.

The network transition is represented through four discrete phases, P_0–P_3. Each phase defines the physical blend composition used to assess gas properties, equipment compatibility, and potential retrofit requirements.

Two temporal indices are used throughout the model. The phase index k, also the year index,

$$t \in \{1, \ldots, T\}, \tag{3.3}$$

that identifies each year of the planning horizon, over which market prices, costs, emissions, and economic indicators evolve. The indices are therefore related but not interchangeable. The value of k establishes the physical boundary condition applicable in year t, while t governs the broader temporal evolution of the all model analysis.

Phase P_0 represents the reference gas supplied before the introduction of renewable gases. It provides the baseline composition for the thermophysical and interchangeability comparisons performed in Model 1, and its properties correspond to the Portuguese natural gas reference described in Table A.1.

Phases P_1, P_2, and P_3 describe progressively more advanced stages of renewable gas integration. Phase P_1 introduces relatively low hydrogen and biomethane fractions, with limited deviation from the reference gas. Phase P_2 represents an intermediate composition, for which changes in gas properties may become increasingly relevant to combustion equipment. Phase P_3 describes the most advanced blend considered in the model and may approach or exceed the operating limits of conventional industrial systems. Whether a retrofit is required is not assumed in advance, but determined through the interchangeability assessment conducted in Model 1.

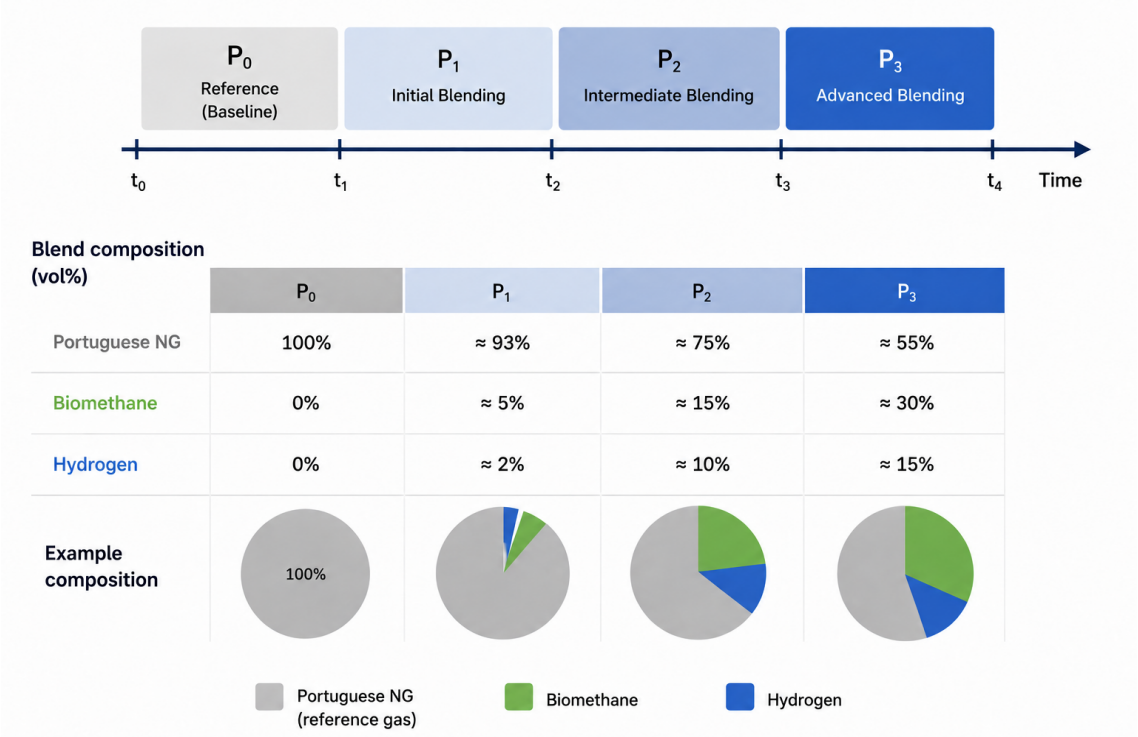


Figure 3.3: Illustrative evolution of hydrogen and biomethane volume fractions across network phases P_0–P_3.

Figure 3.3 illustrates an example of a renewable gas transition pathway at an industrial consumer connection point. Phase compositions shown are illustrative and do not represent a forecast of Portuguese gas network evolution. Instead, they demonstrate how the proposed framework models progressive changes in delivered gas composition.

Phase composition and duration are user-defined inputs, allowing different network-transition pathways to be represented while respecting applicable gas-quality limits and equipment constraints. In the case study presented in the following chapter, these phases are parameterised according to DSO expectations for network transition.

Remembering that network phases describe physical evolution of gas supplied to the installation and should not be confused with market scenarios introduced later, which represent alternative renewable gas procurement and pricing conditions. Each phase composition is evaluated in Model 1, and resulting technical outputs are subsequently transferred to Model 2.

3.4 Model 1 - Thermophysical Blend Characterisation

Model 1 receives the physical gas composition assigned to each network phase and converts it into the properties required to assess blend interchangeability and equipment compatibility. For phases P_0–P_3, the model calculates the mixture molecular weight, M_{mix}, density, ρ_{mix}, volumetric lower and higher heating values, LHV_{mix} and HHV_{mix}, specific gravity, SG_{mix}, and Wobbe Index, WI_{mix}. The calculations follow the molar mixing rules established in Section 2.1.

Because the network injection schedule determines the blend composition, Model 1 does not optimise the fuel received by the industrial consumer. Instead, it evaluates the technical consequences of the physical conditions imposed at the installation connection point.

3.4. Model 1 - Thermophysical Blend Characterisation

Biomethane is treated as a near drop-in substitute for natural gas when the applicable gas-quality requirements are satisfied, and therefore introduces comparatively limited deviations from the reference composition. Hydrogen has a more pronounced influence, particularly on volumetric energy density, specific gravity, Wobbe Index, and combustion behaviour. When both renewable gases are present, their combined effects must be assessed for each phase rather than inferred from either component in isolation.

The computational sequence of Model 1 is presented in Figure 3.4. The corresponding pseudocode is provided in Appendix B, Algorithm **B.4** .

Model 1 produces both technical and economic outputs. The technical outputs comprise the calculated blend properties and the interchangeability indicators J_H, J_A, and J_{HT}, assessed against the criteria defined in Section 3.4.2. The resulting admissibility assessment is then translated into the combustion retrofit expenditure, $CAPEX_{\text{comb}}$, according to the retrofit level defined in Section 3.4.3.

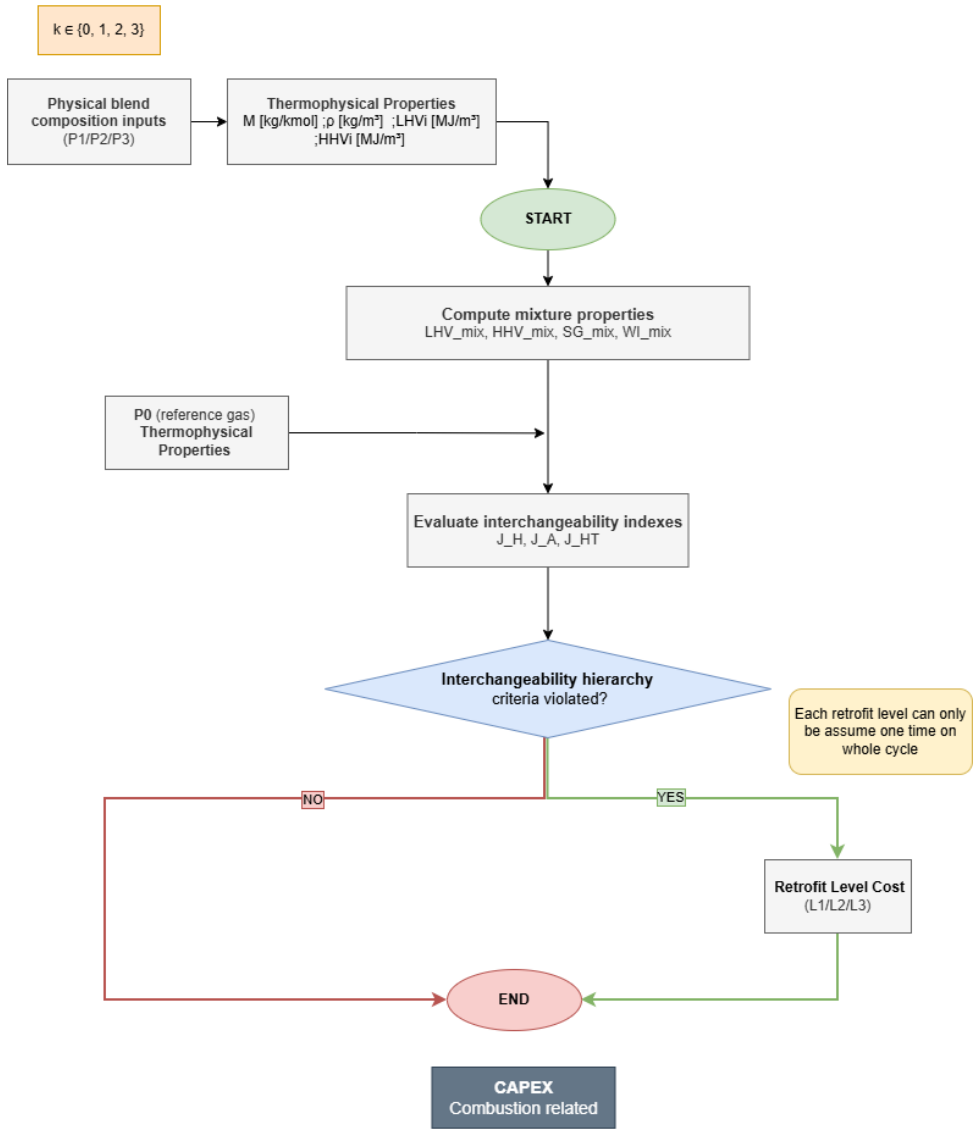


Figure 3.4: Model 1 Flowchart

3.4.1 Gas Mixture Properties

The thermophysical characterisation is performed relative to the reference composition assigned to phase P_0. This phase provides the baseline against which changes in energy density, specific gravity, Wobbe Index, and gas interchangeability are evaluated throughout the network transition. It represents the gas supplied to the industrial installation before renewable gas injection and is characterised using the reference properties established in Section 2.1.

Within the physical layer, biomethane is represented as a methane-equivalent component, provided that the applicable upgrading and grid-quality requirements are satisfied and its properties are therefore approximated by those of pure methane, as reported in Table A.1. This simplification allows the model to isolate the influence of renewable methane substitution from the more pronounced effects introduced by hydrogen.

The property table reports the Wobbe Index on an HHV basis. For consistency with the energy calculations used in the industrial model, the interchangeability assessment is instead performed on an LHV basis. Also the corresponding reference value and admissible band must therefore be calculated using the same energy basis throughout the analysis.

The physical blend is represented as a ternary mixture comprising the reference natural gas, methane-equivalent biomethane, and hydrogen. Their molar fractions satisfy

$$x_{\mathrm{NG}} + x_{\mathrm{CH_4}} + x_{\mathrm{H_2}} = 1, \qquad [-] \tag{3.4}$$

with

$$x_{\mathrm{NG}},\, x_{\mathrm{CH_4}},\, x_{\mathrm{H_2}} \in [0, 1]. \qquad [-] \tag{3.5}$$

Gas composition is expressed in molar fractions throughout Model 1. Under the ideal-gas approximation adopted for distribution-network conditions, molar and volumetric fractions are treated as numerically equivalent. Blend compositions reported in vol.% may therefore be introduced directly into the mixture-property calculations.

For instance, the volumetric lower heating value of the blend is calculated as

$$LHV_{\mathrm{mix}} = x_{\mathrm{NG}} LHV_{\mathrm{NG}} + x_{\mathrm{CH_4}} LHV_{\mathrm{CH_4}} + x_{\mathrm{H_2}} LHV_{\mathrm{H_2}}, \qquad [\mathrm{MJ/m^3}]. \tag{3.6}$$

All remaining properties are obtained using the molar mixing rules established in Section 2.1. The Wobbe Index is then calculated from the blend heating value and specific gravity using the LHV-based formulation adopted consistently in the interchangeability assessment.

Thus for each network phase P_0-P_3, Model 1 produces the property vector

$$\mathbf{\Phi}_k = \{M_{\mathrm{mix},k}, \rho_{\mathrm{mix},k}, SG_{\mathrm{mix},k}, LHV_{\mathrm{mix},k}, HHV_{\mathrm{mix},k}, WI_{\mathrm{mix},k}\}\,. \tag{3.7}$$

These phase-specific properties provide the main inputs to the interchangeability assessment presented in Section 3.4.2. The corresponding computational procedure is documented in Appendix B, Algorithm **B.1**.

3.4.2 Interchangeability Criteria

The interchangeability assessment converts the criteria introduced in Section 2.4.1 into a conservative screening procedure for industrial combustion equipment. Its purpose is not to certify burner compatibility, but to identify the network phase at which the delivered blend may move beyond the operating range associated with the reference gas P_0.

Three criteria are retained in the model: the heat-input index, J_H, the primary-air index, J_A, and the hydrogen-content threshold, J_{HT}. The first two are calculated from the mixture properties obtained in Section 3.4.1, while J_{HT} is evaluated directly against the hydrogen fraction of the blend.

Heat-input index, J_H, represents the change in thermal input at the burner under fixed supply pressure and burner geometry. A deviation from the admissible band indicates that the delivered heat rate may no longer remain consistent with the reference operating condition.

Primary-air index, J_A, captures the change in the air requirement associated with the new gas composition. Variations in this index may affect excess-air control, combustion stability, carbon monoxide formation, and NO_x emissions.

Finally, the hydrogen-content threshold, J_{HT}, introduces an additional compatibility constraint that cannot be captured through Wobbe Index compliance alone. Once the hydrogen fraction exceeds the prescribed limit, the model assumes that more extensive intervention is required because of the increased risk of flashback, altered flame behaviour, and material incompatibility.

Together, these criteria provide, characterized before in 2.4.1 a compact representation of the main burner-level consequences of hydrogen-containing gas blends. At low hydrogen fractions, existing equipment may remain within the admissible operating range, although site-specific testing and manufacturer confirmation would still be required. At intermediate fractions, burner adjustment, gas-quality monitoring, or improved air-to-fuel control may become necessary. Beyond the J_{HT} threshold, the model activates the highest retrofit level as a conservative representation of full combustion-system adaptation [7].

For each network phase, the three criteria are evaluated relative to P_0, using the admissibility bands summarised in Table 2.2. A retrofit flag is activated whenever one of the corresponding limits is exceeded. The resulting combination of flags determines the retrofit level introduced in Section 3.4.3.

The screening logic is also formalized in Appendix B, Algorithm **B.2**. Since the procedure is deliberately conservative, a modelled violation should be interpreted as an indication that further engineering assessment is required, rather than as a substitute for site-specific combustion testing or manufacturer validation.

3.4.3 Retrofit Capital Expenditure

Within Model 1, the retrofit capital expenditure module converts the interchangeability assessment into an installation-level investment requirement. Retrofit expenditure is represented through a combustion-adaptation component normalised by the installed thermal capacity of the industrial installation. The applicable unit cost is selected according to the retrofit level activated by the criteria introduced in Section 3.4.2.

The purpose of this module is to approximate the investment required to maintain safe and stable combustion as the delivered gas composition departs from the reference condition. The corresponding decision logic is detailed in Appendix B, Algorithm **B.3**.

Retrofit requirements may arise from changes in heat input, primary-air demand, flame behaviour, hydrogen tolerance, and the compatibility of the existing combustion equipment [7, 9]. To distinguish retrofit severity from the network phase itself, the phase index remains k, while the retrofit level assigned to that phase is denoted by

$$L_k \in \{L_0, L_1, L_2, L_3\}, \tag{3.8}$$

where L_0 represents operation without retrofit and L_1-L_3 represent progressively more extensive combustion-system adaptation. Their unit cost coefficients satisfy

$$0 = \alpha_{L_0} < \alpha_{L_1} < \alpha_{L_2} < \alpha_{L_3}, \tag{3.9}$$

where α_{L_k} is expressed in EUR/kW.

For a retrofit level L_k activated during network phase k, the corresponding screening-level capital requirement is calculated as

$$CAPEX_{\text{comb},k} = \alpha_{L_k} E_{\text{th}}, \qquad [\text{EUR}], \tag{3.10}$$

where E_{th} is the installed thermal capacity of the industrial installation, expressed in kW.

The installed thermal capacity is estimated from annual metered gas consumption and the operating capacity factor:

$$E_{\text{th}} = \frac{E_{\text{annual}} \times 1000}{CF \times 8760}, \qquad [\text{kW}], \tag{3.11}$$

where E_{annual} is the annual metered gas consumption in MWh/yr, and $CF \in [0, 1]$ represents the ratio between average annual thermal demand and installed thermal capacity.

Plant-specific costs associated with piping, gas trains, controls, material qualification, downtime, maintenance, commissioning, and process-quality effects are excluded unless explicitly incorporated into the retrofit coefficients used in the case-study parameterisation. Resulting $CAPEX_{\text{comb},k}$ should therefore be interpreted as a screening-level investment estimate.

3.5 Model 2 - Operational Expenditure and Renewable Attribute Coverage

Model 2 converts the physical outputs of Model 1 into annual operating expenditure. Three cost components are considered: **physical energy procurement, renewable attribute procurement, and carbon compliance.**

For each year t, the model combines the gas composition and technical conditions inherited from Model 1 with the applicable energy prices, certificate costs, emission factors, and regulatory parameters. The result is an annual cost structure that distinguishes the energy physically supplied to the installation from the contractual instruments used to support renewable energy claims and regulatory compliance.

Annual operating expenditure is decomposed into three layers. Layer C_1 represents the cost of purchasing the gas energy required to satisfy the installation's annual demand. Layer C_2 captures the additional expenditure associated with certified biomethane attributes and RFNBO-compliant hydrogen. Layer C_3 represents the remaining EU ETS compliance cost after accounting for the emissions treatment recognised under the applicable regulatory and certification rules.

Total annual operating expenditure is therefore given by

$$OPEX_t = C_{1,t} + C_{2,t} + C_{3,t}, \qquad \text{[EUR/yr]}. \tag{3.12}$$

The three-layer structure preserves the distinction between physical supply, contractual renewable procurement, and carbon exposure. Changes in certificate coverage affect the renewable procurement cost in C_2 and, where recognised by the applicable accounting framework, the carbon-compliance cost in C_3. They do not alter the physical energy procurement represented by C_1.

As illustrated in Figure 3.5, Model 2 applies this decomposition sequentially for each year of the planning horizon. The full computational procedure and decision logic are outlined in Appendix C.

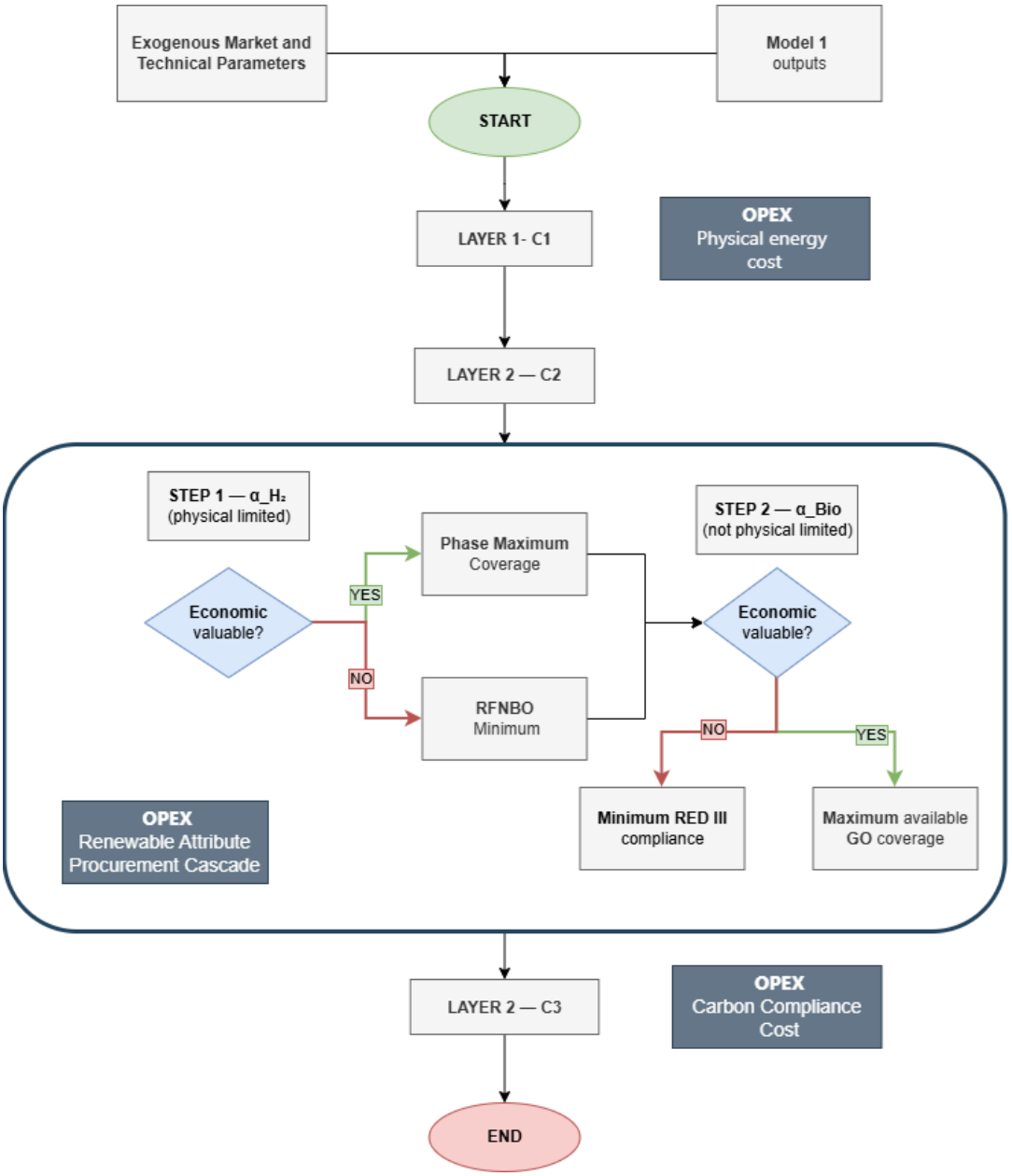


Figure 3.5: Model 2 Flowchart

3.5.1 Physical Energy Cost

The physical energy cost represents the expenditure associated with the gas energy supplied to the installation before renewable attribute procurement and carbon-compliance costs are considered.

Within the model, the physical energy supplied through the distribution network is valued at a common base gas price, independently of the renewable composition of the delivered blend. This assumption reflects an energy-based billing structure and isolates the additional cost of certified renewable gases within Layer C_2.

The annual physical energy cost is calculated as

$$C_{1,t} = E_{\text{annual}}\, p_{\text{Gas},t}, \qquad [\text{EUR/yr}], \tag{3.13}$$

where E_{annual} is the annual metered gas-energy consumption, expressed in MWh/yr, and $p_{\text{Gas},t}$ is the base network gas price in year t, expressed in EUR/MWh.

The value of E_{annual} represents the gross fuel energy supplied to the installation and therefore already incorporates the energy required to compensate for combustion and process-conversion losses. It should not be interpreted as net useful heat demand.

Because billing is represented on an energy basis, changes in volumetric flow arising from variations in blend composition do not enter the calculation of $C_{1,t}$. This treatment assumes, an important factor, that the annual metered energy requirement remains fixed across the pathways evaluated.

Any additional expenditure associated with certified biomethane or RFNBO-compliant hydrogen is excluded from C_1 and represented separately in Layer C_2.

3.5.2 Renewable Attribute Procurement Cascade

Renewable attribute procurement cascade determines the share of the installation's annual gas consumption that is assigned eligible renewable attributes. The resulting coverage is governed by the compliance pathway adopted in the model, the availability of certified renewable gases, and the economic comparison between renewable procurement and residual carbon exposure. The sequence is illustrated in Figure 3.6 and formalised in Appendix C, Algorithm **C.2**.

The cascade first evaluates the contribution of certified renewable hydrogen. Physical hydrogen availability is constrained by the hydrogen fraction delivered during the applicable network phase. Regulatory recognition, however, requires the corresponding quantity to satisfy the certification and sustainability criteria applicable to RFNBOs. The model therefore distinguishes between the hydrogen physically present in the blend and the share that can be contractually recognised as RFNBO consumption.

The RED III RFNBO requirement is applied to the relevant industrial hydrogen demand, in accordance with the compliance assumptions summarised in Table 1.1. Within the present framework, the physical hydrogen fraction establishes an upper bound on the RFNBO quantity that can be associated with the installation through the network pathway. It does not, by itself, demonstrate RFNBO eligibility.

The minimum RFNBO coverage fraction is computed on a volumetric blend basis rather than on the energy-content basis consistent with the statutory language of RED III (Art. 22a) [3]. Since hydrogen has a substantially lower heating value than natural gas, the volumetric convention overstates the RFNBO obligation relative to the energy-share interpretation.

After the eligible RFNBO contribution has been determined, the model calculates the additional renewable coverage required to satisfy the remaining industrial renewable energy pathway. This residual requirement is assigned to certified biomethane attributes, subject to their availability under the applicable chain-of-custody and certification arrangements.

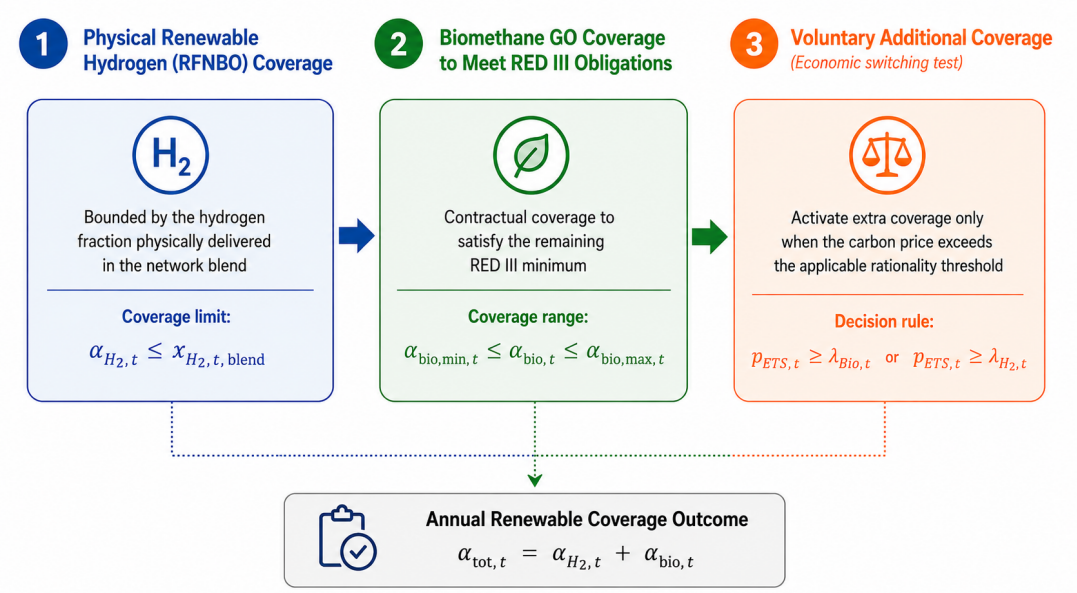


Figure 3.6: Sequential renewable attribute procurement cascade combining eligible RFNBO coverage, mandatory biomethane procurement, and additional economically justified renewable coverage.

Biomethane coverage is represented as a contractual procurement decision and is not required to coincide with the biomethane fraction physically present at the industrial meter. This treatment is consistent with the physical-contractual distinction introduced in Section 1.1.2, provided that the corresponding certificates are available, valid, and eligible under the accounting framework adopted in the model.

Once the minimum compliance coverage has been established, the model evaluates whether additional renewable procurement is economically justified. For each year t, the incremental cost of extending certified renewable coverage is compared with the carbon-compliance expenditure that would be avoided under the emissions-accounting rules assumed in the analysis. Additional coverage is selected only when the recognised reduction in carbon expenditure exceeds the associated renewable procurement premium.

Each year is evaluated using the applicable carbon price, biomethane procurement premium, renewable hydrogen cost, and regulatory parameters. This annual formulation allows procurement levels to respond to changing market conditions without imposing a binding multi-year purchasing commitment.

The resulting approach should be interpreted as a flexible annual procurement formulation rather than as a detailed representation of a specific spot or long-term contracting strategy. Multi-year supply agreements, take-or-pay provisions, indexation mechanisms, and contract-renewal constraints would require an intertemporal optimisation structure and are therefore outside the scope of the present model.

GO and RFNBO Procurement Cost

Layer 2 prices the renewable attribute independently of the physical gas delivered. The cost represents the contractual premium required to secure Guarantees of Origin for biomethane and RFNBO certification for renewable hydrogen above the fossil gas reference price. The annual procurement cost is expressed as:

$$C_{2,t} = \alpha_{\text{Bio},t} \cdot E_{\text{util}} \cdot p_{\text{GO,Bio}}(t) + \alpha_{\text{H}_2,t} \cdot E_{\text{util}} \cdot p_{\text{GO,H}_2}(t) \quad [\text{EUR/year}] \tag{3.14}$$

where E_{util} [MWh/year] is the annual useful energy demand delivered to the industrial process:

$$E_{\text{util}} = E_{\text{annual}} \cdot \eta \quad [\text{MWh/year}] \tag{3.15}$$

with $\eta \in [0, 1]$ representing the burner thermal efficiency, of the processes consider. The coverage fractions $\alpha_{\text{Bio},t}$ and $\alpha_{\text{H}_2,t}$ represent the shares of annual useful energy contractually attributed to biomethane GOs and hydrogen RFNBOs, respectively, while $p_{\text{GO,Bio}}(t)$ and $p_{\text{GO,H}_2}(t)$ [EUR/MWh] are the corresponding procurement premiums above the fossil gas reference price.

These premiums represent the incremental cost of the renewable attributes relative to the fossil gas energy already accounted for in Layer 1, thereby avoiding double counting between the physical and contractual layers.

The coverage fractions $\alpha_{\text{Bio},t}$ and $\alpha_{\text{H}_2,t}$ are determined through the sequential procurement cascade established in Section 3.5.2. The corresponding bounds are also defined in that section.

EU ETS Carbon Compliance Cost

Layer 3 converts residual emissions recognised under EU ETS combustion accounting into an annual carbon-compliance cost. It is therefore not a lifecycle greenhouse-gas assessment.

For fossil natural gas, the combustion emission factor is set at $EF_{\text{NG}} = 0.202\ \text{tCO}_2\,\text{MWh}^{-1}$, consistent with the IPCC default value for natural gas combustion [80]. For certified sustainable biomethane and RFNBO hydrogen, (Directive 2003/87/EC), as amended by (Directive 2023/959/EU), allows the attributed renewable energy fraction to be exempt from allowance surrender, provided that the applicable sustainability, traceability, certification, and monitoring requirements are satisfied [28]. Under a strict EU ETS allowance-surrender treatment, this would justify assigning $EF_{\text{Bio}} = EF_{\text{H}_2} = 0$ in the carbon-compliance layer.

A conservative departure from this zero-rated treatment is adopted in the model. Instead of assigning zero emissions to eligible renewable gases, the RED III lifecycle intensities are retained as modelling approximations: $EF_{\text{Bio}} = 0.020\ \text{tCO}_2\,\text{MWh}^{-1}$ for biomethane and $EF_{\text{H}_2} = 0.003\ \text{tCO}_2\,\text{MWh}^{-1}$ for renewable hydrogen [3]. This choice reduces the modelled avoided-emission benefit from EF_{NG} to $(EF_{\text{NG}} - EF_{\text{Bio}}) = 0.182\ \text{tCO}_2\,\text{MWh}^{-1}$ for biomethane and $(EF_{\text{NG}} - EF_{\text{H}_2}) = 0.199\ \text{tCO}_2\,\text{MWh}^{-1}$ for hydrogen.

This convention is conservative because it understates the EU ETS cost saving attributable to renewable coverage relative to a zero-surrender treatment. For biomethane, it would increases the rationality threshold formalised later. Results are therefore biased against voluntary procurement, which strengthens the robustness of conclusions that remain favourable to network-based compliance.

After renewable attribution, the effective emission factor used in the carbon-compliance layer is:

$$EF_{\text{eff},t} = f_{\text{uncov},t} \cdot EF_{\text{NG}} + \alpha_{\text{Bio},t} \cdot EF_{\text{Bio}} + \alpha_{\text{H}_2,t} \cdot EF_{\text{H}_2} \quad [\text{tCO}_2\text{eq/MWh}] \tag{3.16}$$

By construction, the coverage fractions satisfy:

$$f_{\text{uncov},t} + \alpha_{\text{Bio},t} + \alpha_{\text{H}_2,t} = 1 \tag{3.17}$$

The net emissions subject to EU ETS compliance in year t are calculated as:

$$Em_{\text{ETS},t} = E_{\text{util}} \cdot EF_{\text{eff},t} - FA_t \quad [\text{tCO}_2\text{eq/year}] \tag{3.18}$$

where E_{util} is the annual useful energy demand defined previously and is consistent with the energy basis adopted in Layer 2, $EF_{\text{eff},t}$ is the effective emission factor in year t, and FA_t [tCO_2] denotes the free allowances allocated in that year. The free-allocation trajectory follows the EU ETS phase-out schedule illustrated in Figure 1.4 and parameterised in Table 3.1.

To operationalise this trajectory, the free allowances in year t are represented as:

$$FA_t = \phi_t \cdot FA_{\text{ref}} \quad [\text{tCO}_2\text{eq/year}] \tag{3.19}$$

where ϕ_t is the fraction of free allowances retained in year t, and $FA_{\text{ref}} = E_{\text{util}} \cdot EF_{\text{NG}}$ is the reference free-allocation level, consistent with the physical baseline defined in Section 3.2. It represents the full fossil-emission load of the installation before any phase-out reduction is applied. After 2034, $\phi_t = 0$, meaning that all remaining emissions are fully exposed to EU ETS compliance costs.

This formulation introduces a conservative assumption because hard-to-abate and energy-intensive industrial sectors are not necessarily subject to identical free-allocation conditions. Actual allocation depends on type of industry, benchmark values, historical activity levels, sector-specific rules, carbon-leakage exposure, and potential adjustments over time [81, 82].

Nevertheless, the adopted formulation is appropriate for the present techno-economic model, since it intentionally provides a general way to represent the progressive phase-out of free allowances and the resulting increase in carbon-cost exposure across hard-to-abate industrial sectors.

Table 3.1: EU ETS free-allocation phase-out trajectory [82].

Year	**Free allocation retained, ϕ_t [%]**
2026	97.5
2027	95.0
2028	90.0
2029	77.5
2030	51.5
2031	39.0
2032	26.5
2033	14.0
2034	0.0
2035 onwards	0.0

Finally, the annual carbon-compliance cost is then calculated as:

$$C_{3,t} = \max\left(Em_{\text{ETS},t}, 0\right) \cdot p_{\text{ETS},t} \quad [\text{EUR/year}] \tag{3.20}$$

The $\max(0, \cdot)$ operator ensures that no revenue is generated from surplus allowances. Free allocations can be acumulated and reduce carbon expenditure but do not generate trading income, consistent with the conservative cost-avoidance approach adopted for the contractual layer.

GO Procurement Rationality Thresholds

The procurement cascade defined in Section 3.5.2 determines renewable gas coverage by comparing the marginal cost of renewable attribute procurement with the corresponding avoided carbon-compliance expenditure. Two rationality thresholds, one for biomethane and one for renewable hydrogen, identify the carbon price above which voluntary coverage beyond the regulatory minimum becomes economically justified, subject to attribute availability in each year.

These thresholds are formalised in Appendix C, Algorithm **C.1**, and constitute the economic decision criteria that activate the switching logic of the procurement cascade. Their evolution over time, driven by changes in renewable attribute premiums, determines when voluntary procurement becomes economically preferable to residual EU ETS exposure.

For biomethane, the threshold corresponds to the carbon price at which the incremental cost of procuring a biomethane GO equals the avoided EU ETS expenditure:

$$\lambda_{\text{Bio},t} = \frac{p_{\text{GO,Bio}}(t)}{EF_{\text{NG}} - EF_{\text{Bio}}} \quad [\text{EUR/tCO}_2\text{eq}] \tag{3.21}$$

where $p_{\text{GO,Bio}}(t)$ [EUR/MWh] is the biomethane GO premium in year t, EF_{NG} [tCO_2eq/MWh] is the emission factor of fossil natural gas, and EF_{Bio} [tCO_2eq/MWh] is the effective emission factor of certified biomethane.

For renewable hydrogen, the analogous threshold is:

$$\lambda_{\text{H}_2,t} = \frac{p_{\text{GO,H}_2}(t)}{EF_{\text{NG}} - EF_{\text{H}_2}} \quad [\text{EUR/tCO}_2\text{eq}] \tag{3.22}$$

where $p_{\text{GO,H}_2}(t)$ [EUR/MWh] is the RFNBO procurement premium and EF_{H_2} [tCO_2eq/MWh] is the effective emission factor of certified renewable hydrogen. Since $EF_{\text{H}_2} < EF_{\text{Bio}}$, the denominator of $\lambda_{\text{H}_2,t}$ exceeds that of $\lambda_{\text{Bio},t}$ for equal procurement premiums, implying that a lower carbon price is required to justify voluntary RFNBO procurement relative to biomethane.

As renewable hydrogen procurement costs decline over time, the corresponding rationality threshold $\lambda_{\text{H}_2,t}$ also decreases. Voluntary RFNBO coverage beyond the regulatory minimum is activated whenever $p_{\text{ETS},t} \geq \lambda_{\text{H}_2,t}$, following the same decision logic applied to biomethane.

3.6 Model 3 - Economic and Carbon Performance Indicators

Model 3, illustrated in Figure 3.7, converts the annual technical and operational outputs generated by Models 1 and 2 into economic and carbon-performance indicators over the full 20-year planning horizon. Its computational sequence and indicator calculations are formalised in the pseudocode provided in Appendix D.

Planning-horizon outputs are aggregated into four indicators: NPV, LCDE, CAC, and avoided emissions. Together, these metrics characterise the economic viability and carbon performance of each decarbonisation pathway relative to its baseline.

These indicators capture complementary dimensions of the techno-economic consequences of progressive renewable gas integration through the distribution network. NPV evaluates economic performance relative to Baseline $B0$, while LCDE expresses the associated cost on a consistent energy basis. CAC measures the incremental cost per tonne of CO_2 avoided, and cumulative avoided emissions quantify the total carbon reduction achieved over the planning horizon. Together, these indicators provide a structured basis for evaluating investment viability, cost efficiency, and environmental performance across the scenarios considered.

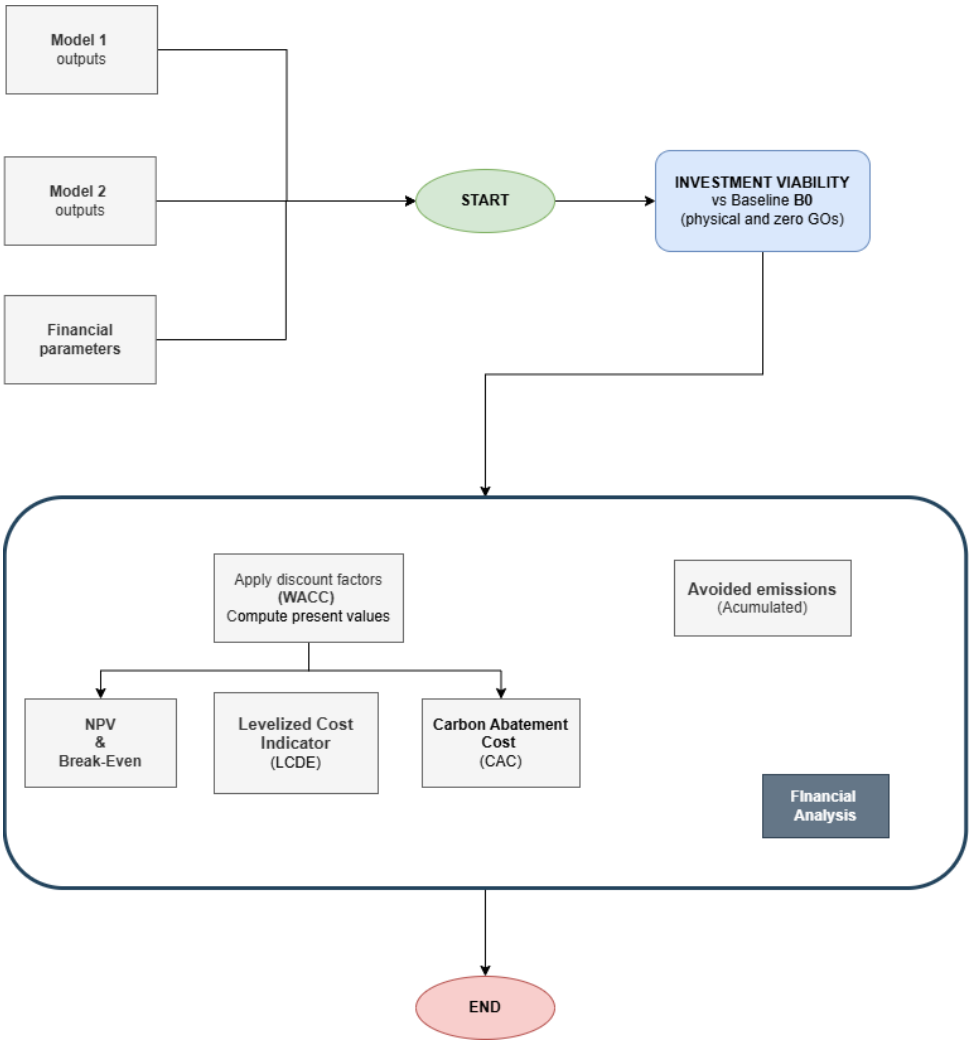


Figure 3.7: Model 3 Flowchart

3.6.1 Discounted Cash-Flow Structure

Costs and benefits arise at different points over the planning horizon and are converted into present values through a discounted cash-flow approach. The discount factor applied in year t is defined as:

$$DF_t = \frac{1}{(1+r)^t} \quad [-] \tag{3.23}$$

where r is the nominal discount rate and t denotes the year index relative to the 2026 base year. A common discount rate is applied to capital expenditure, operational expenditure, and carbon-compliance costs, ensuring the consistent temporal aggregation of all cash flows included in the analysis.

For concision, total expenditure (TOTEX) denotes the present value of the capital and operational costs incurred over the planning horizon:

$$\text{TOTEX} = \sum_{k} CAPEX_{\text{comb},k}\, DF_{t_k} + \sum_{t=1}^{T} OPEX_t\, DF_t \quad [\text{EUR}] \tag{3.24}$$

where $CAPEX_{\text{comb},k}$ is the combustion retrofit expenditure triggered by the interchangeability assessment in network phase k, assumed to occur in the first year of that phase, t_k. Annual operational expenditure $OPEX_t$ is obtained from Model 2 and comprises the physical energy cost $C_{1,t}$, renewable attribute procurement cost $C_{2,t}$, and carbon-compliance cost $C_{3,t}$, as defined in Section 3.5.

When the same physical blend composition imposes an identical retrofit obligation on both the evaluated strategy and Baseline $B0$, the corresponding $CAPEX$ terms cancel from the incremental comparison. TOTEX is therefore retained as an absolute cost measure for the LCDE computation, whereas incremental indicators consider only the cost differences between the evaluated pathway and the baseline.

The discount factor structure and annual present-value calculations are outlined in Appendix D, Algorithm **D.1**.

3.6.2 Levelised Cost of Decarbonised Energy

The Levelised Cost of Decarbonised Energy **(LCDE)** expresses the total discounted cost of the evaluated pathway per unit of useful energy delivered over the planning horizon:

$$LCDE = \frac{\text{TOTEX}}{\sum_{t=1}^{T} E_{\text{util},t}} \quad [\text{EUR/MWh}] \tag{3.25}$$

where TOTEX represents the present value of all capital and operational costs defined in Equation 3.24, and $E_{\text{util},t}$ denotes the useful energy delivered in year t. Useful energy demand is assumed constant throughout the planning horizon.

Unlike net present value, which measures the incremental economic performance of renewable procurement relative to Baseline $B0$, LCDE is an absolute cost indicator. It combines physical energy expenditure, renewable attribute procurement, combustion retrofit CAPEX, and carbon-compliance costs into a single discounted cost per unit of useful energy. The indicator therefore

represents the overall cost intensity of the evaluated decarbonisation pathway, enabling comparison between alternative strategies on a common energy basis. The computation is detailed in Appendix D, Algorithm **D.3**.

3.6.3 Avoided Emissions

Avoided emissions are treated as a dynamic indicator of environmental performance, rather than as a fixed annual value. Their evolution depends on the renewable gas pathway adopted over time, the availability of biomethane, the corresponding GO premium, and the level of renewable attribute procurement.

This relationship creates a direct causal chain within the model: biomethane market conditions determine the GO premium $p_{\mathrm{GO,Bio}}(t)$, which governs the rationality threshold $\lambda_{\mathrm{Bio},t}$, which in turn determines the procurement level and the resulting avoided emissions ΔEm_t, explicited in 3.26.

This formulation distinguishes between latent and realised decarbonisation potential. Latent potential corresponds to the renewable gas coverage that could be supported by the applicable regulatory and availability constraints, whereas realised potential corresponds to the coverage effectively procured under the contractual and economic decision rules of Model 2. Avoided emissions therefore provide the environmental expression of the central finding that decarbonisation value depends not only on the physical network trajectory but also on the economic conditions that determine whether available renewable potential is converted into measurable emission reductions.

3.6.4 Carbon Abatement Cost

The carbon abatement cost (CAC) quantifies the net incremental expenditure per tonne of CO_2 avoided relative to Baseline $B0$ under full fossil exposure, providing a welfare-consistent metric for evaluating renewable gas procurement strategies independently of their absolute cost level [63]. The full algorithmic implementation is documented in Appendix D, Algorithm **D.4**.

Anual avoided emissions relative to $B0$ in year t are calculated as:

$$\Delta Em_t = Em_{0,t} - Em_t \quad [\mathrm{tCO_2eq/year}] \tag{3.26}$$

where $Em_{0,t}$ represents the emissions associated with full fossil exposure under Baseline $B0$, calculated as:

$$Em_{0,t} = EF_{\mathrm{NG}} \cdot E_{\mathrm{util}} \quad [\mathrm{tCO_2eq/year}] \tag{3.27}$$

and the strategy inventory reflects the energy-weighted combination of fossil and renewable fuel-cycle intensities:

$$Em_t = \left(f_{\mathrm{uncov},t}\, EF_{\mathrm{NG}} + \alpha_{\mathrm{bio},t}\, EF_{\mathrm{bio}} + \alpha_{\mathrm{H_2},t}\, EF_{\mathrm{H_2}}\right) E_{\mathrm{util}} \quad [\mathrm{tCO_2eq/year}] \tag{3.28}$$

where $f_{\mathrm{uncov},t}$, $\alpha_{\mathrm{bio},t}$, and $\alpha_{\mathrm{H_2},t}$ denote the uncovered, biomethane-attributed, and hydrogen-attributed energy fractions,

The annual emission-factor reduction normalised to useful energy demand is:

$$\Delta EF_t = \frac{\Delta Em_t}{E_{\text{util}}} = \alpha_{\text{bio},t}(EF_{\text{NG}} - EF_{\text{bio}}) + \alpha_{\text{H}_2,t}(EF_{\text{NG}} - EF_{\text{H}_2}) \quad [\text{tCO}_2\text{eq/MWh}] \tag{3.29}$$

ensuring that the avoided-emission indicator and the carbon-cost saving term in the NPV, formalised later, share an identical abatement basis. Eventually, the Carbon Abatement Cost over the planning horizon is calculated as:

$$CAC = \frac{\sum_{t=0}^{T} (C_t - C_{0,t})\, DF_t}{\sum_{t=0}^{T} \Delta Em_t} \quad [\text{EUR/tCO}_2] \tag{3.30}$$

where $C_t = C_{1,t} + C_{2,t} + C_{3,t}$ represents the total annual cost of the renewable gas strategy, including physical energy procurement, renewable attribute procurement, and carbon compliance. $C_{0,t}$ represents the total annual cost under Baseline $B0$, comprising physical energy procurement and full EU ETS exposure without GO or RFNBO coverage. The differential $(C_t - C_{0,t})$ therefore isolates the incremental cost of implementing the renewable gas strategy.

Discounting is applied to annual cost differences using the factor DF_t defined in Equation 3.23, while physical emission reductions are aggregated in undiscounted tonnes over the planning horizon. This convention, commonly adopted in carbon-abatement cost analysis [63], avoids implicitly assigning lower weight to future emission reductions.

A positive CAC indicates that the renewable gas strategy incurs a net cost per tonne of CO_2 avoided relative to $B0$, whereas a negative CAC indicates that the strategy produces net savings while simultaneously reducing emissions, which may occur under sufficiently high carbon prices.

The physical energy cost $C_{1,t}$ and the corresponding carbon-compliance cost are included in $C_{0,t}$, since the installation bears both costs under $B0$ in the absence of any renewable coverage. This ensures that CAC measures only the incremental economic impact of the renewable gas strategy relative to the physical baseline $B0$.

3.6.5 Investment Viability Metrics

Since Baseline $B0$ and the investment scenario share identical retrofit capital expenditure, CAPEX cancels in the incremental NPV calculation. This formulation isolates the net economic value of GO procurement relative to unmitigated EU ETS exposure, independently of the physical adaptation cost.

The net present value over the full planning horizon is therefore defined as:

$$NPV = \sum_{t=0}^{T} [\Delta EF_t \cdot E_{\text{util}} \cdot P_{\text{CO}_2,t} - C_{2,\text{Bio},t} - C_{2,\text{H}_2,t}] \cdot DF_t \quad [\text{EUR}] \tag{3.31}$$

where E_{util} [MWh/year] is the annual useful energy demand, $P_{\text{CO}_2,t}$ [EUR/tCO$_2$] is the EU ETS carbon allowance price, and $C_{2,\text{Bio},t}$ and $C_{2,\text{H}_2,t}$ [EUR/year] are the annual biomethane GO and hydrogen RFNBO procurement premiums, respectively. The product $\Delta EF_t \cdot E_{\text{util}}$ gives the annual avoided emissions attributable to renewable attribute coverage, expressed in tCO$_2$/year.

A positive NPV indicates that the EU ETS cost savings generated by renewable attribute procurement exceed the associated GO and RFNBO procurement costs over the planning horizon. A negative NPV indicates that the avoided carbon-compliance costs are insufficient to compensate for the additional renewable attribute expenditure.

The discounted break-even year is defined as the first year in which the cumulative discounted net value of renewable attribute procurement relative to Baseline $B0$ becomes non-negative:

$$BE = \min \left\{ t \in \mathbb{N}_0 : \sum_{\tau=0}^{t} [\Delta EF_\tau \cdot E_{\text{util}} \cdot P_{\text{CO}_2,\tau} - C_{2,\text{Bio},\tau} - C_{2,\text{H}_2,\tau}] \cdot DF_\tau \geq 0 \right\} \tag{3.32}$$

A lower break-even year indicates faster recovery of the incremental GO and RFNBO procurement costs through avoided EU ETS expenditure, while the absence of a break-even year within the planning horizon indicates that the renewable attribute strategy does not recover its additional procurement costs relative to $B0$. The break-even computation is presented in Appendix D, Algorithm **D.6**.

Both NPV and BE are also computed for each Monte Carlo iteration as discussed below in 3.8, generating distributions of investment outcomes rather than single deterministic estimates.

3.7 Market Scenarios Architecture

Three scenarios define alternative total contract-price levels for certified biomethane over the planning horizon, using the Portuguese procurement mechanism established under Portaria n.º 15/2023 as the principal national reference [83]. The outcome of the corresponding procurement procedure revealed the limited ability of the Portuguese market to supply biomethane at the established ceiling price. Although the mechanism allowed for the procurement of up to 150 GWh/yr, only one biomethane bid was submitted, resulting in the award of 1.99 GWh/yr at 62 EUR/MWh, equivalent to approximately 1.3% of the available volume [84].

The extremely limited uptake indicates that the maximum procurement price of 62 EUR/MWh was insufficient to mobilise a meaningful volume of biomethane supply under the prevailing Portuguese market conditions. Rather than revealing a representative market-clearing price, the auction outcome suggests that the reference value remained below the cost level required by most potential producers to develop, finance, and commit eligible projects. The 62 EUR/MWh value is therefore not adopted as a realistic current-market benchmark, but as a lower-bound scenario associated with a substantially more mature and deployment-effective biomethane market. The three scenarios consequently represent distinct stages of national market development, ranging from nascent conditions, in which viable production and contracting costs remain significantly above the procurement ceiling, to a mature market in which the national reference price becomes attainable.

The total contract price, p_{total,S_i}, represents the all-in cost of certified biomethane, combining the physical gas-energy value and the GO premium. The corresponding GO premium is derived as

$$p_{\text{GO,Bio},t} = \max\left(p_{\text{total},S_i} - p_{\text{Gas},t},\, 0\right), \qquad [\text{EUR/MWh}], \tag{3.33}$$

where $p_{\text{Gas},t}$ is the physical network gas price in year t, as defined in Section 4.2.3. This formulation operationalises the physical–contractual dissociation adopted in the model. As $p_{\text{Gas},t}$

increases, the GO premium declines even when the total biomethane contract price remains fixed, reflecting the gradual narrowing of the cost differential between fossil and renewable gas. When $p_{\text{total},S_i} \leq p_{\text{Gas},t}$, the incremental GO premium reaches zero and certified biomethane becomes cost-competitive with fossil gas. Under the economic assumptions of the model, additional renewable procurement then becomes rational independently of avoided EU ETS expenditure.

Scenario S_1 represents nascent market conditions and adopts a total contract price of 90 EUR/MWh. This value is consistent with European biomethane production-cost estimates for anaerobic digestion under emerging-market conditions [70, 85, 86] and is further motivated by the limited uptake observed in the Portuguese procurement procedure at the reference price of 62 EUR/MWh [83].

Scenario S_2 represents an intermediate stage of market development, with $p_{\text{total}} = 75$ EUR/MWh, reflecting the partial achievement of the national deployment targets and the associated development of scale economies [79, 85].

Scenario S_3 adopts the 62 EUR/MWh reference price as the lower-bound scenario, representing the cost level that may become attainable under successful market maturation.

The contrasting auction outcomes further support the differentiated treatment of biomethane and renewable hydrogen in the scenario architecture. While the biomethane lot attracted only one bid, corresponding to approximately 1.3% of the available volume, the renewable hydrogen lots awarded almost the entire quantity offered. This suggests that the maximum price of 127 EUR/MWh was sufficiently attractive to mobilise some hydrogen projects, whereas the 62 EUR/MWh ceiling failed to elicit a meaningful biomethane supply response. Nevertheless, the concentration of hydrogen bids at the maximum admissible price indicates limited downward price competition and suggests that the procurement ceiling remained close to the minimum level required by participating projects [87].

Renewable hydrogen procurement costs are therefore not differentiated across the three scenarios. Within the adopted framework, the RFNBO contribution associated with the RED III pathway is constrained by the hydrogen fraction physically delivered at the industrial meter [24]. Over the planning horizon considered, hydrogen cost uncertainty is consequently treated as secondary to the greater uncertainty surrounding biomethane procurement prices. A single deterministic central trajectory, anchored to the 127 EUR/MWh reference value, is therefore adopted [83].

3.8 Monte Carlo Simulations

Fixed-point estimates alone do not capture the uncertainty associated with future EU ETS carbon allowance prices, which directly affect the economic value of GO and RFNBO procurement through avoided carbon-compliance costs. Since the procurement cascade defined in Section 3.5.2 depends on the comparison between renewable attribute premiums and avoided EU ETS expenditure, carbon-price uncertainty may materially affect the timing, frequency, and economic value of voluntary renewable attribute coverage.

In the Monte Carlo extension, EU ETS carbon allowance prices are treated as the sole stochastic variable and modelled through a Geometric Brownian Motion process calibrated against market data, as established in Section 3.8. As discussed before, the uncertainty in $p_{\text{GO,Bio}}(t)$ is instead represented through deterministic scenario contrast rather than stochastic sampling, reflecting its structural dependence on policy implementation and national market development rather than short-term market volatility.

No modification is made to the model structure introduced in the preceding sections. Instead,

the same computational pipeline comprising Model 1, Model 2, and Model 3 is repeatedly evaluated under sampled EU ETS carbon-price trajectories. In each iteration, the simulated carbon-price path is propagated through the procurement cascade, annual operational expenditure calculation, emissions-accounting layer, and economic indicator module. This procedure generates distributions of NPV, LCDE, CAC, avoided emissions, and break-even year, together with the probability that each indicator exceeds or falls below economically relevant thresholds. These include the probability of a positive NPV relative to Baseline $B0$ and the probability that CAC falls below the prevailing carbon allowance price.

The computational logic of a single Monte Carlo iteration, including the annual procurement decision loop and the aggregation of discounted indicators, is illustrated schematically in Appendix E, Algorithms **E.1** to **E.3**.

Stochastic Carbon Price and Monte Carlo Simulation

EU ETS allowance prices constitute the dominant stochastic driver because they simultaneously determine the operating cost associated with unabated fossil gas consumption and the avoided-carbon-cost value of renewable gas procurement. Following Abadie and Chamorro [67], who demonstrate that carbon price volatility can materially affect investment timing under carbon-constrained operating decisions, allowance prices are modelled through a Geometric Brownian Motion (GBM) process. This formulation ensures strictly positive simulated price trajectories and results in a lognormal marginal distribution of the price level, properties commonly adopted in the modelling of commodity and emissions allowance markets [15, 67].

In continuous time, the allowance price evolves according to:

$$dP_{\mathrm{CO}_2,t} = \mu P_{\mathrm{CO}_2,t}\, dt + \sigma P_{\mathrm{CO}_2,t}\, dW_t, \tag{3.34}$$

where $P_{\mathrm{CO}_2,t}$ [EUR/tCO$_2$] is the EU ETS carbon allowance price, μ is the annual drift parameter, σ is the annual volatility parameter, and dW_t is the increment of a standard Wiener process.[1]

For an annual simulation step, with $\Delta t = 1$ year, the exact discrete-time solution is obtained by applying Itô's lemma to $f(P,t) = \ln P$ and integrating over the interval $[t, t+\Delta t]$:[2]

$$P_{\mathrm{CO}_2,t+\Delta t} = P_{\mathrm{CO}_2,t} \exp\left[\left(\mu - \frac{\sigma^2}{2}\right)\Delta t + \sigma\sqrt{\Delta t}\,\varepsilon_t\right], \tag{3.35}$$

where $\varepsilon_t \sim \mathcal{N}(0,1)$ is an independent standard normal shock drawn at each annual time step. Reflecting barriers are imposed at a lower price bound and an upper structural bound.

Alternative mean-reverting specifications, such as the Ornstein–Uhlenbeck and Cox-Ingersoll-Ross processes, define a long-run equilibrium level towards which allowance prices tend to converge.

[1] A standard Wiener process W_t satisfies $W_0 = 0$; its increments follow $W_t - W_s \sim \mathcal{N}(0, t-s)$ for $t > s$; increments over non-overlapping intervals are independent; and its sample paths are continuous but nowhere differentiable. It provides the mathematical foundation for Brownian motion in financial and energy-price processes [67].

[2] Itô's lemma is the stochastic-calculus analogue of the deterministic chain rule. When applied to $f(P,t) = \ln P$ for a GBM process, it yields

$$d(\ln P) = \left(\mu - \frac{\sigma^2}{2}\right) dt + \sigma\, dW_t.$$

Integrating this expression over one time step produces Equation (3.35). The correction term $-\sigma^2/2$, commonly referred to as the Itô correction, arises from the non-negligible quadratic variation of Brownian sample paths and ensures that the expected value of $P_{t+\Delta t}$ is equal to $P_t e^{\mu \Delta t}$, consistently with the continuous-time formulation.

This behaviour is theoretically plausible in a cap-and-trade system, since sustained increases in carbon prices encourage abatement, reduce allowance demand, and may consequently exert downward pressure on the market [88]. Their implementation, however, requires the estimation of both a stable long-run price and a mean-reversion speed. These parameters are difficult to identify robustly for the EU ETS, whose historical development has been affected by successive regulatory reforms, changes in allowance supply, energy-market disruptions, and broader macroeconomic regime shifts. A GBM specification is therefore retained as a more parsimonious and transparent representation of long-term carbon-price uncertainty. Its principal limitation, the potentially excessive dispersion of simulated prices over long horizons, is controlled through model-imposed lower and upper bounds, which constrain extreme trajectories without being interpreted as regulatory EU ETS price limits [67, 88].

This representation of EUA procurement introduces an additional simplification. Any annual allowance deficit is valued at the prevailing spot-equivalent price in the corresponding year, without explicitly modelling the banking of allowances acquired or allocated in earlier periods, derivative-based hedging, or the optimisation of purchase timing. In practice, industrial operators may accumulate EUAs in their Union Registry accounts and use them to fulfil future compliance obligations, thereby separating the year in which emissions occur from the year in which the associated procurement expenditure is incurred [89]. In a spot-based analysis such as the one adopted here, these effects are not modelled explicitly in order to keep the scenario presentation transparent and tractable, consistent with the conservative treatment already adopted for free allowances [89].

3.9 Model Limitations

The following limitations define the scope of the model and should be considered when interpreting its results.

From a physical modelling perspective, biomethane is represented as a pure methane equivalent, consistent with grid-quality requirements.

Interchangeability criteria are applied as conservative screening filters rather than validated operational boundaries for site-specific industrial equipment, reflecting the absence of harmonised standards for industrial combustion systems above 300 kW discussed in Section 2.4.1. The resulting flags do not explicitly represent detailed burner phenomena such as flame recirculation, detachment, flashback dynamics, local temperature gradients, or combustion instabilities. Consequently, retrofit expenditure is represented through the normalised coefficients α_{L1}, α_{L2}, and α_{L3}, which serve as screening-level approximations in the absence of standardised supplier pricing and site-specific engineering data.

From an economic and regulatory perspective, the natural gas price follows a deterministic trajectory, while network tariffs are assumed constant. Consequently, short-term price volatility, tariff revisions, capacity-based charges, and changes in contracted capacity are not represented. RED III non-compliance penalties are also excluded because the Portuguese transposition mechanism and its associated penalty structure were not fully operationalised within the model scope [18]. The phase-out of EU ETS free allocation is treated as a fixed input throughout the analysis. The only source of uncertainty introduced in the Monte Carlo simulation is the carbon allowance price, $P_{\mathrm{CO}_2,t}$.

The stochastic extension includes only the EU ETS carbon allowance price as a sampled variable. Biomethane GO premiums remain deterministic within scenarios $S1$, $S2$, and $S3$, while renewable hydrogen procurement costs follow a central deterministic trajectory. Uncertainty in biomethane market development is therefore represented through scenario contrast rather than probabilistic sampling. Renewable attribute procurement follows an annual binary switching rule between the regulatory minimum and the maximum modelled voluntary coverage whenever $P_{\mathrm{CO}_2,t}$ exceeds the relevant rationality threshold. Intermediate procurement positions, risk-averse partial coverage, hedging strategies, and gradual portfolio adjustment are not represented.

A further limitation concerns biomethane availability. Present formulation assumes that sufficient certified national biomethane supply, is accessible in each year to satisfy the mandatory RED III coverage, an assumption that isolates the economic effect of alternative GO premium trajectories but does not represent the possibility that marketable supply may lag behind theoretical or technical resource potential.

In an emerging market, effective availability depends on the mobilisation, quality, and cost of feedstocks, collection and transport logistics, plant commissioning, upgrading capacity, network connection, and the issuance and transferability of the corresponding sustainability attributes and GOs [76, 90, 91]. Supply constraints may therefore affect both the volume accessible to industrial consumers and the formation of GO premiums, particularly while the market remains characterised by limited liquidity and relatively inflexible short-term supply [91].

Altough, a separate trajectory of continuously increasing GO premiums is not modelled, persistent demand-led price pressure and insufficient supply growth are represented by the binding conditions associated with scenario $S3$. Factors that could produce this outcome, including competition from the transport sector, feedstock scarcity, and delays in network-connection cost allocation, are

discussed qualitatively in Section 4.4.

Lastly, planning horizon is limited to the 20-year period adopted in the case study. Post-horizon behaviour and alternative long-term configurations are also outside the central formulation scope.

Finally and already introducing some of the **future work and policy implication** that will be formalised later, we should endogenise an annual certified biomethane availability variable and jointly represent quantity and price constraints. Such an extension could link maximum feasible coverage to the operational project pipeline, feedstock mobilisation, injection capacity, and certificate availability, thereby capturing supply shortfalls, involuntary non-compliance risk, and the relationship between scarcity and GO premiums. Moreover long-term bilateral agreements like BPAs, take-or-pay provisions, counterparty risk, and supply-assurance mechanisms would require a separate contracting structure and remain outside the present formulation.

Chapter 4

Case Study

4.1 Case Study Overview

A continuous container-glass production facility operates through a sequence of interconnected stages, from raw-material handling and batch preparation to melting, forming, annealing, quality control, and final packaging. Each stage has distinct thermal and operational requirements, but the melting furnace remains the dominant energy-consuming unit and the main focus for fuel-related decarbonisation.

Natural gas is typically used as the primary fuel for high-temperature melting, feeders, and annealing lehrs. Melting furnaces operate continuously at temperatures of approximately 1400 °C or higher and are commonly equipped with regenerative air systems or oxy-fuel burners. These combustion systems are sensitive to changes in fuel composition, particularly Wobbe Index, calorific value, flame speed, heat input, and air-to-fuel ratio. Hydrogen blending may therefore affect flame stability, NO_x formation, heat transfer, and local furnace atmosphere, with potential implications for both energy performance and glass quality [34–36, 48].

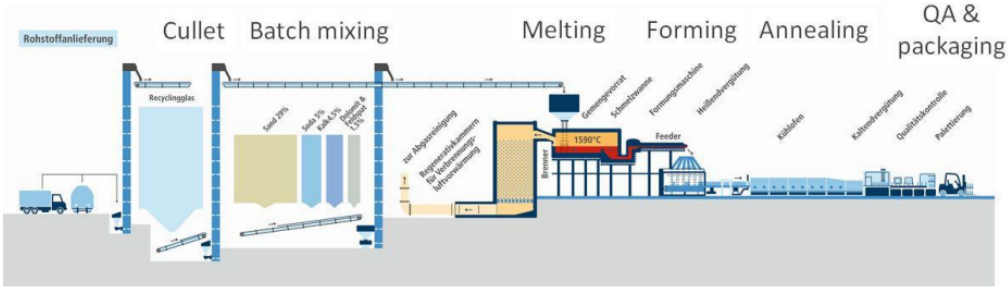


Figure 4.1: Typical process chain in container-glass manufacturing [35].

Feeders and annealing lehrs are less energy-intensive than melting furnaces, but remain important for process stability. Feeders maintain melt homogeneity before forming, while lehrs control the cooling profile required to reduce thermal stress in the final product. Their lower energy share does not make them irrelevant, since both stages require precise thermal control and may also be affected by fuel-quality variations [36].

These operational characteristics support the phased approach adopted in the case study. In glass manufacturing, a large share of direct emissions is associated with fossil-fuel combustion, while furnace investment and rebuild cycles typically extend over long periods [92]. Deep technological changes therefore cannot always be implemented immediately and may need to **coincide with refurbishment or furnace-rebuild windows.** Progressive integration of biomethane and renewable hydrogen through the gas distribution network is consequently analysed as an intermediate pathway that can reduce combustion-related emissions while preserving operational continuity.

Evidence from HyGlass and related studies further indicates that hydrogen blending requires careful adjustment of combustion control and monitoring systems to avoid changes in local oxidising or reducing conditions, which may affect glass colour, defects, and product quality [36]. This evidence motivates the conservative retrofit-screening approach adopted in Model 1. Rather than assuming that all hydrogen blending requires complete equipment replacement, the model links increasing deviations in fuel properties to staged intervention levels, ranging from monitoring and burner adjustment to more extensive combustion-system adaptation.

The following sections present the specific network conditions, installation parameters, and market scenarios adopted for this case study, together with the resulting techno-economic and carbon performance outcomes.

4.1.1 Network Node Characterisation

Treating the network phase composition as an exogenous deterministic input allows each phase to represent a projected distribution-network blend. These blends are subsequently used to calculate core mixture properties, such as the lower heating value, higher heating value, specific gravity, Wobbe Index, and hydrogen volume fraction. Methodologically, this aligns with the approach developed in Section 3.4.1, where the physical gas mixture dictates both the energy content of the supplied fuel and the corresponding interchangeability indicators. Consequently, the phase-specific composition constitutes a central independent parameter in this framework rather than a secondary sensitivity.

Historical gas composition data at a specific network node would not constitute an appropriate basis for this analysis, since the objective is not to reproduce past natural gas operating conditions, but to evaluate prospective blend compositions associated with the physical integration of renewable gases in the distribution network. The network phases adopted in this case study therefore represent forward-looking concession-level operating states, aligned with the expected evolution of renewable gas injection and circulation within the REN-Portgás distribution area over the coming years. Rather than being derived from historical natural gas quality data, phases $P1$, $P2$, and $P3$ are formulated as projected blend-composition conditions that reflect how hydrogen and biomethane may progressively enter and circulate in the modelled network segment. This allows the model to assess the resulting implications for gas quality, interchangeability, retrofit triggering, and techno-economic performance from the perspective of an industrial consumer connected to the concession network.

Defining the projected gas blend composition for each phase of renewable gas injection establishes the necessary exogenous inputs for the model. Each phase $k \in \{P1, P2, P3\}$ corresponds to a specific planning interval, outlining target hydrogen and biomethane volumetric fractions:

- **P1 (2026–2031)**: $x_{H_2} = 3\%$, $x_{bio} = 15\%$
- **P2 (2032–2036)**: $x_{H_2} = 8\%$, $x_{bio} = 25\%$
- **P3 (2037–2046)**: $x_{H_2} = 18\%$, $x_{bio} = 40\%$

Deriving these values from the distribution system operator's planned network-development projections ensures that the adopted assumptions remain aligned with the expected renewable gas injection pathways for northern Portugal. Since these projections were provided specifically to support the present modelling exercise, **the resulting phase structure should be interpreted as a regionally grounded reference scenario for an industrial installation located in the north of the country, rather than as a fixed or universally applicable forecast.** The model remains flexible, and the phase compositions can be updated if revised network-planning information or alternative deployment assumptions become available.

For the calculation of mixture properties consider, the network composition is treated as a predefined input within the mathematical framework. The adopted phase configurations and their corresponding gas compositions are summarised in Table 4.1.

Table 4.1: Projected network phase composition for renewable gas injection.

Phase	x_{H_2} [vol.%]	x_{bio} [vol.%]	Natural gas [vol.%]
P1	3	15	82
P2	8	25	67
P3	18	40	42

Acting as direct inputs to the thermophysical and interchangeability assessments of Model 1, these phase compositions directly influence both the physical energy layer and the subsequent retrofit CAPEX that can be consider. This computational architecture remains fully adaptable, allowing the model to be readily updated to reflect alternative renewable gas deployment pathways, new operational monitoring data, or higher future injection levels.

The thermophysical characterisation of the delivered gas blend for each network phase relies on the mixture property formulations presented in Section 2.1. For each phase $k \in \{P_1, P_2, P_3\}$, the ternary composition $(x_{H_2}, x_{bio}, x_{NG})$ defined in Section 3.3 is substituted into Equations 2.11, 2.4–2.12 to calculate the volumetric lower heating value (LHV_{mix}), specific gravity (SG_{mix}), and net Wobbe Index (WI_{mix}) at the industrial meter, respectively. All of these calculated properties across the network phases are exposed in Figure 4.2.

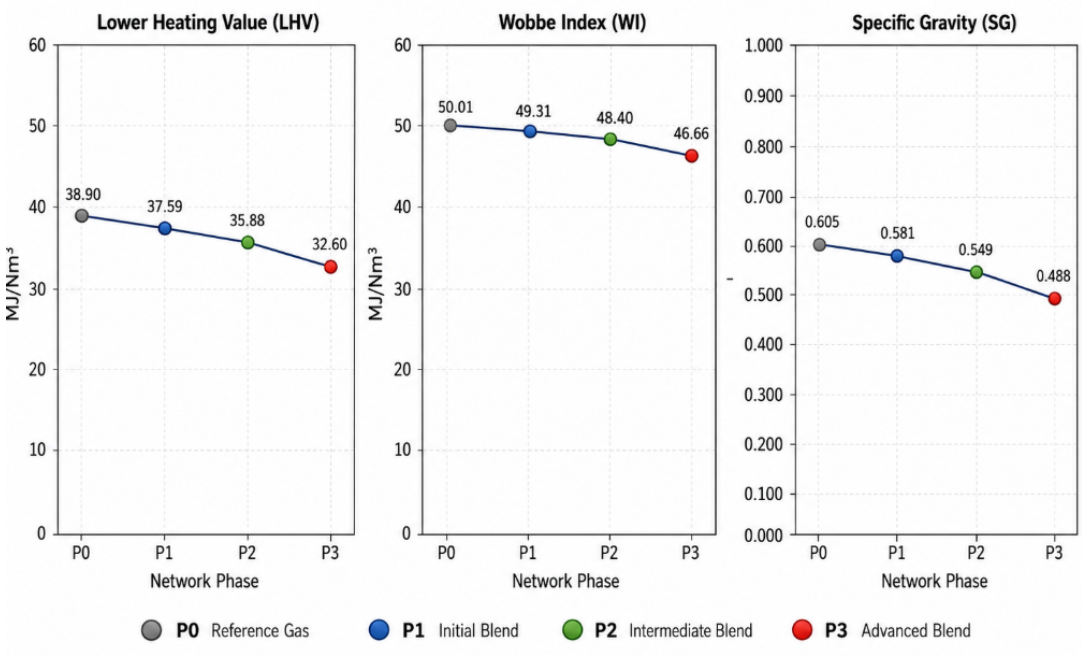


Figure 4.2: Evolution of thermophysical properties across network phases.

As the hydrogen fraction increases, the lower heating value decreases from 38.90 to 32.60 MJ/Nm^3, reflecting the lower volumetric energy density of hydrogen relative to methane-rich gases. The net Wobbe Index also declines, although less sharply, from 50.01 to 46.66 MJ/Nm^3. This indicates a progressive deviation from the Phase P_0 reference condition and, in Phase P_3, places the blend below the model-derived lower screening bound adopted for J_H. In parallel, the specific gravity decreases from 0.605 to 0.488, confirming the increasing influence of the low-density hydrogen fraction in the delivered blend. These trends are consistent with the literature reviewed in the State of the Art and show that renewable gas penetration must be assessed not only through energy-content variation, but also through independent interchangeability criteria, including heat input, primary-air requirement, and hydrogen-specific compatibility limits.

4.1.2 Installation Characterisation

In a continuous container glass melting facility in the Porto metropolitan area, connected to the Portgás medium-pressure distribution network, that operates three air-regenerative glass melting furnaces in continuous service, producing container and packaging glass for the food and beverage sector. Each furnace operates at high temperatures (1400 °C) using natural gas as the primary energy source, with a design capacity enabling 24 h/day and 365 days/year operation. Table 4.2 summarises the principal factors and parameters that characterise this installation.

Table 4.2: Industrial installation specifications used for model parameterisation.

Parameter	Value
Number of furnaces	Three air-regenerative glass melting furnaces
Annual total metered gas consumption, E_{annual}	448,000 MWh/yr
Capacity factor, CF	0.872
Operating temperature	Approximately 1400 °C
Process type	Continuous container-glass melting

The annual metered gas consumption, $E_{\text{annual}} = 448{,}000$ MWh/yr, constitutes the main energy input used to calibrate the case study. This value was provided internally for the present modelling exercise and is therefore treated as the most reliable basis for representing the scale of the industrial installation. More detailed plant-level information, including furnace configuration, burner layout, internal fuel distribution, operating profiles, and retrofit-specific engineering data, was not available with sufficient resolution, constituing an extra limitation for these parametrization.

Modelling this facility within a Monte Carlo framework allows assessment of exposure to carbon prices, renewable gas availability, and GO optimized procurement strategies. By simulating both deterministic and stochastic carbon trajectories, the model provides realistic projections of cost-effective compliance pathways and identifies short- to medium-term technical and economic solutions for a viable decarbonisation alternative, while respecting the operational and essencial constraints of high-temperature, continuous glass production.

4.2 Model Parameterisation

This section defines the inputs used to apply the techno-economic model to the selected industrial case study. Rather than repeating the modelling structure developed in Chapter 3, it identifies the case-specific assumptions required to represent the network transition, retrofit cost levels, market conditions, and regulatory framework considered in the analysis.

Retrofit cost coefficients are applied according to the staged structure defined in Section 3.4.3, with the numerical values calibrated specifically for this case study. In line with the phase-based logic of the model, these coefficients are used as screening-level inputs, allowing different degrees of combustion adaptation to be represented without assuming complete equipment replacement at every hydrogen blending level.

Economic and regulatory assumptions are introduced in the following subsections. These include the network gas price, biomethane procurement scenarios, renewable hydrogen cost trajectory, EU ETS exposure, RED III-based renewable coverage, and the annual procurement strategy adopted in the model. The carbon allowance price is the only variable treated stochastically, while renewable gas procurement costs follow the scenario structure already defined in Section 3.7.

Together, these inputs establish the case-study baseline against which the techno-economic and carbon performance of renewable gas integration is evaluated.

4.2.1 Combustion Retrofit Parameterisation

The retrofit capital expenditure adopted in the case study follows the single-component formulation of Section 3.4.3, comprising combustion-system adaptation only. On-site hydrogen separation is excluded from the central formulation on regulatory grounds, as established in Section 3.4.3.

The required operational thermal power, representing the baseline thermal demand of the burners, is estimated from the annual metered gas consumption and the operating capacity factor defined in Section 4.2:

$$\dot{E}_{\text{th}} = \frac{E_{\text{annual}} \cdot 10^3}{CF \cdot 8760} = \frac{448{,}000 \cdot 10^3}{0.872 \cdot 8760} \approx 58{,}649 \text{ kW} \tag{4.1}$$

where $E_{\text{annual}} = 448{,}000$ MWh/yr is the annual metered gas consumption, $CF = 0.872$ is the operating capacity factor, and 8760 h/yr is the number of hours in a standard calendar year. The resulting thermal power of approximately 58.6 MW_{th} is consistent with a large industrial installation operating under continuous high-load conditions.

All combustion-retrofit coefficients were defined from the order of magnitude reported in the HyNet Industrial Fuel Switching demonstration. In that project, hydrogen firing was tested in an existing glass furnace, and the cost of switching comparable sites was estimated at approximately 500,000 GBP in plant and equipment costs for a furnace with an installed firing capacity of around 50 MW [93]. This value corresponds to an indicative retrofit intensity close to 10 EUR/kW, which is used as the basis for the combustion-retrofit CAPEX formulation in Equation 3.10.

In the present case study, this value is assigned to the upper retrofit level L_3, while lower coefficients are adopted for less intrusive adaptation levels.

Table 4.3: Specific combustion retrofit costs adopted in the case study.

Level	Technical interpretation	Specific CAPEX
L_1	Limited burner adaptation, recalibration, additional monitoring, and control adjustment.	2 EUR/kW
L_2	Partial combustion-system retrofit, including burner adaptation, fuel-train adjustment, valve and instrumentation upgrades, and safety validation.	5 EUR/kW
L_3	More extensive hydrogen-compatible burner conversion or equivalent combustion-system redesign, potentially including additional safety and control systems.	10 EUR/kW

Using the operational thermal power calculated in Equation 4.1, the resulting combustion-system retrofit costs are

$$CAPEX_{\text{comb},L1} = 2 \cdot 58{,}649 \approx 117 \text{ kEUR} \tag{4.2}$$

$$CAPEX_{\text{comb},L2} = 5 \cdot 58{,}649 \approx 293 \text{ kEUR} \tag{4.3}$$

$$CAPEX_{\text{comb},L3} = 10 \cdot 58{,}649 \approx 586 \text{ kEUR} \tag{4.4}$$

Under the central formulation, only Level 1 combustion retrofit is activated, triggered by the Wobbe Index violation at Phase P_3.

The resulting CAPEX of approximately 117 kEUR is modest relative to the annual operational expenditure of the installation and cancels in the incremental NPV, as both the investment pathway and Baseline $B0$ incur this obligation. Although retrofit CAPEX is a critical parameter for any future real-world application of the integrated model, it is not the main uncertainty explored in this thesis. Its contribution is therefore included in the broader economic assessment, while a dedicated retrofit-cost sensitivity analysis is left as a possible extension of the framework.

4.2.2 Economic and Regulatory Parameters

Table 4.4 summarises the main financial assumptions adopted and provides the baseline inputs used in the model.

Table 4.4: Financial parameters adopted in the case study.

Parameter	Value
Planning horizon, T	2026–2045
Discount rate, r	8%
Base year	2026

The 2026–2045 horizon covers the full network-transition pathway considered in the case study and captures the long-term effects of renewable gas procurement, retrofit activation, and EU ETS exposure. Future incremental cash flows are discounted at 8%, following the net present value formulation presented in Section 3.6.1.

Figure 4.3 translates the RED III provisions into the compliance pathway used for case-study calibration. Industrial renewable energy use is represented by a linear increase of 1.6 percentage points per year from the 2021 baseline. RFNBO requirements apply specifically to eligible industrial hydrogen consumption, reaching 42% in 2030 and 60% in 2035. Both trajectories are included for modelling clarity and should not be interpreted as equivalent. They represent EU-level targets that, at the time of writing, had not yet been transposed into Portuguese law.

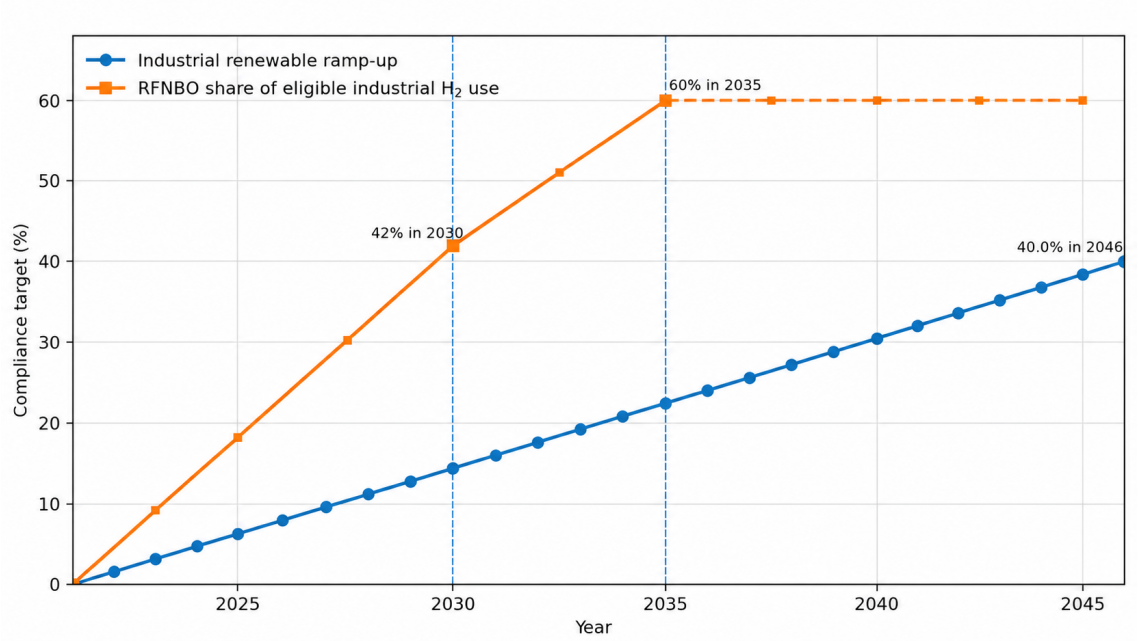


Figure 4.3: RED III compliance trajectories adopted in the case study, with the dashed extension beyond 2035 indicating uncertainty in future RFNBO targets [3].

In operational terms, the RED III industrial pathway results in a minimum renewable attribute coverage of approximately 5% of useful energy in 2026. This share increases by 1.6 percentage points per year until 2030 and by 1.9 percentage points per year thereafter, reaching 40% of final energy use by the end of the planning horizon. Compliance may be achieved through the combined contribution of biomethane GOs and RFNBO-certified hydrogen.

RFNBO sub-targets apply specifically to the hydrogen fraction physically delivered at the meter. Under the adopted modelling assumption, 42% of eligible hydrogen consumption must be certified as RFNBO from 2028 to 2034, increasing to 60% from 2035 onwards. Since the hydrogen volume fraction available at the meter is determined by the network-phase schedule rather than by the installation's procurement decisions, the corresponding RFNBO contribution is constrained by the DSO injection pathway [24].

Certified renewable attributes are assumed to be procured annually through the spot market, with coverage determined by the procurement cascade introduced in Section 3.5.2. Carbon compliance costs are determined by residual fossil emissions, the prevailing allowance price, and the progressive reduction in free allocation, applied according to the phase-out trajectory defined in Section 1.1.3.

Table 4.5 summarises the regulatory assumptions adopted in this case study.

Table 4.5: Regulatory and carbon-market parameters adopted in the case study.

Parameter	Value / treatment
EU ETS exposure	Active throughout 2026–2045
Free-allocation phase-out	2026–2034 trajectory
Annual industrial renewable ramp-up	+1.6 pp/year / +1.9 pp/year
RFNBO hydrogen sub-target	42% by 2030; 60% by 2035
Carbon price, $P_{\mathrm{CO}_2,t}$	Stochastic trajectory
Renewable gas certification	GO-based procurement

At the time of writing, RED III defined RFNBO targets for industrial hydrogen use only for 2030 and 2035, with no subsequent target specified for the post-2035 period [3]. The 60% requirement is therefore maintained over the remainder of the planning horizon as a conservative modelling assumption, consistently with the regulatory uncertainty declared in Section 3.9. The free-allocation phase-out is incorporated in parallel according to the methodology defined above.

4.2.3 Market Assumptions

Market assumptions define the price trajectories adopted in the analysis and play a central role in the interpretation of the results. The key relationship in the contractual layer is the derivation of the biomethane GO premium from the spread between the total certified biomethane contract price and the prevailing network gas price, as established in Equation 3.33. Accordingly, $p_{\mathrm{Gas},t}$ and p_{total,S_i} jointly determine the evolution of $p_{\mathrm{GO,Bio},t}$ and, consequently, the rationality threshold $\lambda_{\mathrm{Bio},t}$ over the planning horizon.

This relationship is particularly important because renewable gas markets in Portugal remain at an early stage, with limited empirical data available to support a robust price forecast. The scenario structure is therefore not intended to predict precise market prices, but to explore how different levels of biomethane market development may change the economic rationale for renewable procurement. In this sense, the price assumptions provide a structured way to assess which

market conditions could make biomethane adoption more attractive, and what this implies for the development of a future renewable gas market in Portugal.

The individual trajectories of each price input are defined in the following subsections and are later used to interpret the rationality thresholds and economic outcomes presented in the results discussion.

Network Gas Price

Physical network gas price, $p_{\text{gas},t}$, represents the non-carbon industrial procurement cost at the network connection point. Carbon-compliance costs are deliberately excluded from this layer and are modelled separately in Layer 3 as a function of the EU ETS allowance price. This separation avoids **double counting of carbon costs**. Accordingly, $p_{\text{gas},t}$ is interpreted as a reduced-form price that captures the main non-carbon components of industrial gas procurement, including the wholesale molecule cost, regulated network-access tariffs, and applicable fiscal components.

The adopted initial value of 45 EUR/MWh is consistent with recent Portuguese market evidence. The wholesale molecule component is referenced to the MIBGAS Iberian benchmark, reported at approximately 38.5 EUR/MWh in 2026 [94]. The final industrial procurement price also includes regulated network-access tariffs set annually by ERSE for transmission, distribution, and system-management activities, as well as fiscal components. Eurostat reports a Portuguese non-household gas price of approximately 48.1 EUR/MWh in the second half of 2025 [95]. Since this reported value includes carbon-related surcharges that are not included in $p_{\text{gas},t}$, it is used only as an upper reference for the adopted 45 EUR/MWh non-carbon modelling value, rather than as a direct input. The value should therefore be read as a transparent reduced-form assumption, not as a detailed bottom-up tariff and fiscal build-up.

Future gas-price evolution remains uncertain. Progressive renewable gas integration could reduce exposure to the fossil wholesale molecule component, but the final non-carbon procurement price is not determined by wholesale dynamics alone. As total gas volumes decline, regulated network-access costs may increase because fixed infrastructure costs are recovered over a smaller consumption base, partially offsetting any wholesale-price reductions [96]. For this reason, the model adopts a constant escalation rate of 3%/yr for $p_{\text{gas},t}$. This rate should not be interpreted as a forecast, but as a moderate long-term assumption for non-carbon industrial gas procurement costs. It is broadly consistent with the EU Reference Scenario approach [97] and remains within the 3.3–3.6%/yr range reported in Enerdata's long-term European gas-market scenarios [98]. Against this background, the adopted 3% trajectory represents a comparatively moderate and transparent long-term assumption.

The resulting trajectory at selected reference years is shown in Table 4.6.

Table 4.6: Reference values for the deterministic network gas price trajectory.

Year	$p_{\text{gas},t}$ **[EUR/MWh]**
2026	45.00
2030	50.65
2035	58.72
2040	68.07
2045	78.90

This trajectory applies to the metered gas energy physically delivered at the network connection point, forming the basis for the Layer 1 physical energy cost.

Biomethane and H2 GOs Scenarios

Biomethane GO premium is derived from the spread between the total certified biomethane contract price and the prevailing network gas price, following Equation 3.33. The three scenarios should therefore be interpreted not as point forecasts, but as alternative policy-market conditions under which certified biomethane could become available in Portugal. Each scenario reflects a different level of market maturity, policy effectiveness, and project-financing feasibility.

A declining total contract-price trajectory is not imposed in any scenario. This choice is both methodological and conservative, since the Portuguese biomethane market does not yet provide sufficient empirical evidence to calibrate a robust cost-reduction curve. The market remains at an early stage, no liquid biomethane GO market exists, and the main national reference, the 2024 procurement procedure, failed to attract meaningful producer uptake. Direct extrapolation from more established European markets would therefore risk imposing a maturity profile that does not yet reflect Portuguese market conditions.

Instead, the three fixed price levels are used as a structured sensitivity framework rather than as forecasts of future biomethane prices. This does not imply that the biomethane GO premium remains constant over time. Because $p_{\text{gas},t}$ increases at 3% per year, a declining premium emerges endogenously under each fixed total contract price, as the spread between fossil gas and certified biomethane progressively narrows.

This formulation makes the scenario interpretation clearer. Rather than attempting to forecast an immature and uncertain market, the model isolates how different policy-market price levels affect biomethane adoption, rationality thresholds, and economic performance. The fixed-price structure also improves the readability of the results, since changes in $\lambda_{\text{Bio},t}$ can be directly linked to the interaction between $p_{\text{gas},t}$ and p_{total,S_i}. This is particularly useful for discussing what type of renewable gas market may need to develop in Portugal for biomethane procurement to become economically attractive.

Table 4.7 reports the resulting $p_{\text{GO,Bio},t}$ trajectories at selected reference years.

Table 4.7: Biomethane GO premium and rationality threshold by scenario and reference year.

Year	p_{gas}	S_1		S_2		S_3	
	[EUR/MWh]	p_{GO} **[EUR/MWh]**	λ_{Bio} **[EUR/tCO$_2$]**	p_{GO} **[EUR/MWh]**	λ_{Bio} **[EUR/tCO$_2$]**	p_{GO} **[EUR/MWh]**	λ_{Bio} **[EUR/tCO$_2$]**
2026	45.0	45.0	247	30.0	165	17.0	93
2030	50.6	39.4	216	24.4	134	11.4	63
2035	58.7	31.3	172	16.3	90	3.3	18
2040	68.1	21.9	120	6.9	38	0.0	0
2045	78.9	11.1	61	0.0	0	0.0	0

The progressive decline in $p_{\text{GO,Bio},t}$ across all scenarios reflects the dissociation between the fixed total contract price and the rising fossil gas reference. As $p_{\text{gas},t}$ increases, the GO premium is compressed even without assuming any market-driven reduction in biomethane production costs. Under S_3, the GO premium reaches zero from 2040 onwards, meaning that certified biomethane becomes cost-competitive with fossil gas under the assumptions of the model. The implications of this result are discussed in greater detail in the results section.

Hydrogen cost uncertainty is therefore treated as secondary to biomethane procurement-price uncertainty over the planning horizon considered. This does not imply that renewable hydrogen costs are unimportant, but rather that the central analysis focuses on the market variable

(biomethane) with greater relevance for the procurement scenarios developed in the consider temporal horizon.

Table 4.8 reports the resulting $p_{\mathrm{GO},\mathrm{H}_2,t}$ and $\lambda_{\mathrm{H}_2,t}$ at selected reference years.

Table 4.8: Hydrogen GO premium and rationality threshold by reference year.

Year	p_{gas} **[EUR/MWh]**	$p_{\mathrm{GO},\mathrm{H}_2}$ **[EUR/MWh]**	λ_{H_2} **[EUR/tCO$_2$]**
2026	45.0	82.0	412
2030	50.6	76.4	384
2035	58.7	68.3	343
2040	68.1	58.9	296
2045	78.9	48.1	242

A multi-scenario hydrogen cost analysis is retained as a possible extension of the framework, particularly for post-2035 conditions, when electrolyser cost trajectories, RFNBO regulation, and hydrogen market liquidity may become more uncertain. A different approach is adopted in the extended scenario and is justified in the corresponding results section.

4.2.4 Monte Carlo´s Parameterisation

The simulation stage combines the deterministic scenario structure defined above with the stochastic carbon-price process 3.8. Rather than redefining the full set of model inputs, this section specifies how the calibrated trajectories are used to generate deterministic and probabilistic outputs for the case study.

While the deterministic evaluation provides a clear baseline for cost and compliance assessment, it does not capture the full range of potential futures for market-driven variables, particularly those with structural uncertainty. In response, a stochastic extension was implemented through Monte Carlo simulations. The stochastic framework focuses on the dominant source of market uncertainty, such as the EU ETS carbon allowance price $P_{CO_2,t}$, which determines both the operating cost of fossil gas consumption and the avoided-cost value of GO procurement. The carbon price trajectory is assigned a probability distribution and sampled across 10,000 iterations, enabling exploration of variability in carbon market conditions and their effect on the economic attractiveness of renewable gas procurement.

Following the exact discrete-time solution introduced in Equation 3.35, the process is initialised at $P_{\mathrm{CO}_2,0} = 75.36$ EUR/tCO$_2$, corresponding to the 2026 base-year anchor calibrated against the EEX annual average auction settlement price [99].

The annual drift parameter, $\mu = 5\%$ yr^{-1}, reflects the expected upward price pressure arising from the progressive tightening of the EU ETS emissions cap reviewed in 1.1.3.

The annual volatility parameter, $\sigma = 35\%$, is calibrated using EU ETS auction settlement prices published by the European Energy Exchange, covering approximately 1,737 inter-auction log-return observations between January 2018 and December 2025 [87]. All dataset was processed and analysed in Excel, and the resulting volatility estimates and supporting graphical analysis are presented in Appendix F

Annualised realised volatility is estimated as:

$$\hat{\sigma} = \text{std}\left[\ln\left(\frac{P_t}{P_{t-1}}\right)\right]\sqrt{252} \tag{4.5}$$

From deep analysis, explicit in Appendix F, was concluded, for example that post-crisis calibration window from 2023 to 2025 yields $\hat{\sigma} = 32.5\%$ over only 654 observations, consistent with the and Markets Authority (ESMA) annualised daily volatility calculator, a estimate of 34.9% for 2024 [100].

To prevent economically implausible trajectories over the 2026–2045 planning horizon, reflecting barriers, are applied at a lower bound of $P_{\min} = 30$ EUR/tCO$_2$ and an upper bound of $P_{\max} = 200$ EUR/tCO$_2$.

In one hand, the lower bound reflects the structural price support provided by the MSR implications analysed before in 1.1.3. In the other hand, the upper bound has no explicit regulatory basis and is introduced solely as a methodological simplification to truncate the lognormal right tail at a level broadly consistent with long-run marginal abatement cost projections.

It becomes binding only in the far-right tail of high-volatility trajectories and therefore does not materially affect central or median estimates. The resulting distribution of simulated carbon-price paths is presented in Figure 4.4.

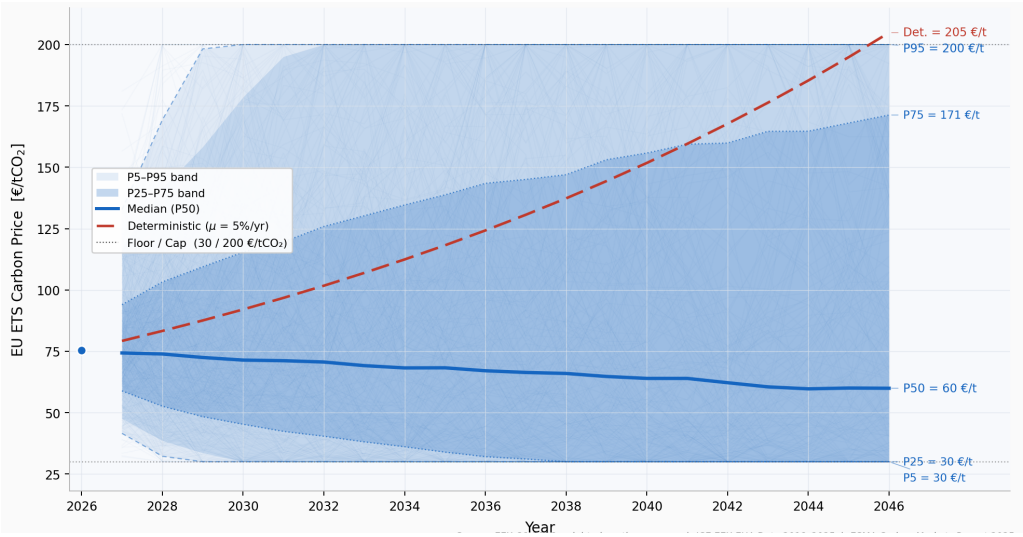


Figure 4.4: Simulated EU ETS carbon-price trajectories under the GBM parameterisation.

The deterministic EUA price trajectory is defined as

$$P_{\text{CO}_2}(t) = P_0 e^{\mu t}. \tag{4.6}$$

Within the GBM framework, this expression represents the expected value of thesimulated price distribution rather than its median trajectory. Since the GBM generates a positively skewed lognormal distribution, a comparatively small number of high-price outcomes exerts a disproportionate influence on the arithmetic mean. As a result, the expected-value trajectory lies above the median, and more than half of the simulated price outcomes remain below it at each point in time.

The median price instead evolves according to the drift of the logarithmic price process, given by $\mu - \sigma^2/2$. The drift parameter μ is not derived mechanically from the EU ETS Linear Reduction Factor. The Linear Reduction Factor defines the annual reduction in the emissions cap, whereas allowance prices also depend on **fuel prices, industrial activity, banking behaviour, policy credibility, hedging demand, and expectations regarding future scarcity**. Therefore, $\mu = 5\%$ is adopted as a long-term scenario assumption representing progressive tightening of the EU ETS market, rather than as a direct conversion of the cap-reduction rate into price growth.

For the adopted parameters, $\mu = 5\%$ and $\sigma = 35\%$, the corresponding annual median growth rate is:

$$\mu - \frac{\sigma^2}{2} = 0.05 - \frac{0.35^2}{2} = -0.01125 \approx -1.1\% \text{ yr}^{-1}. \tag{4.7}$$

A declining median trajectory is therefore not indicative of a modelling inconsistency. It arises because the volatility correction, $\sigma^2/2$, exceeds the assumed drift, causing the typical simulated outcome to decrease even though the expected price continues to rise. Accordingly, $P_0 e^{\mu t}$ is interpreted as the mean price implied by the stochastic process and is used only as a deterministic reference for comparison with the economic thresholds discussed later in the model results.

Under these assumptions, the deterministic reference also has a high-carbon interpretation. Although the median simulated trajectory decreases because of the volatility correction, the expected trajectory reaches values close to 200 EUR/tCO$_2$ by the end of the planning horizon. Such values are above more moderate long-term reference projections, including European energy-system scenarios in which carbon prices remain closer to 150 EUR/tCO$_2$ over comparable horizons [97]. For that reason, the deterministic benchmark should not be read as a neutral forecast, but as a transparent mean-price reference and the robustness of the economic conclusions is therefore assessed through the Monte Carlo distributions, rather than through the deterministic mean trajectory alone.

4.3 Model Results

4.3.1 Deterministic Results

The deterministic analysis establishes the central technical and economic outcomes for each biomethane GO premium scenario under the expected EU ETS carbon-price trajectory. These results are not intended to provide a definitive forecast. Instead, they define a transparent reference case that supports the interpretation of the stochastic analysis and of the extended scenario developed later in the chapter.

Detailed annual outputs for all three scenarios, including the full decomposition of operational expenditure, GO coverage fractions, carbon compliance costs, and cumulative NPV, are compiled in Appendix G and are intended to support verification and replication of the analytical reasoning underlying the model.

Physical Layer and Retrofit Activation

Model 1 indicates that Phase P_3 is the only network transition phase requiring retrofit intervention. At this stage, the net Wobbe Index of the delivered blend decreases from 50.01 MJ/Nm^3 in the Phase P_0 reference composition to 46.66 MJ/Nm^3. This value falls below the model-derived

lower screening bound of 47.51 MJ/Nm^3, corresponding to a 5% reduction relative to the Phase P_0 net Wobbe Index. A Level 1 combustion retrofit is therefore activated in 2037.

Associated CAPEX is approximately 117 kEUR. Since this obligation is driven by the physical gas blend, it is identical across all biomethane price scenarios. It also cancels in the incremental NPV calculation, because Baseline $B0$ is exposed to the same physical blend conditions and therefore incurs the same retrofit obligation. No retrofit is activated in Phases P_1 or P_2, where the net Wobbe Index remains within the adopted $\pm 5\%$ screening band around Phase P_0.

This result should be interpreted as a conservative screening outcome rather than as a detailed engineering retrofit specification. The purpose of the criterion is to link retrofit activation to gas-quality deviation under a consistent screening rule, not to define the exact equipment-level intervention required. Site-specific burner testing, manufacturer validation, and combustion-control assessment would still be required before implementation.

GO Premium Trajectories and Rationality Thresholds

Figure 4.5 compares the biomethane rationality thresholds obtained under scenarios S_1, S_2, and S_3 with the deterministic mean EU ETS carbon-price trajectory defined in Equation 4.6. The markers identify the first year in which the expected carbon price, $\bar{P}_{\mathrm{CO}_2,t} = P_0 e^{\mu t}$, exceeds the biomethane rationality threshold. These years are therefore interpreted as mean-price crossing points, rather than as typical outcomes of the stochastic carbon-price process.

Renewable hydrogen procurement is still included in the model calculations, as shown in the annual summary tables presented in Appendix G. However, since the hydrogen procurement cost is treated as a fixed central input and is not varied across scenarios, it is not the focus of the threshold comparison shown in Figure 4.5.

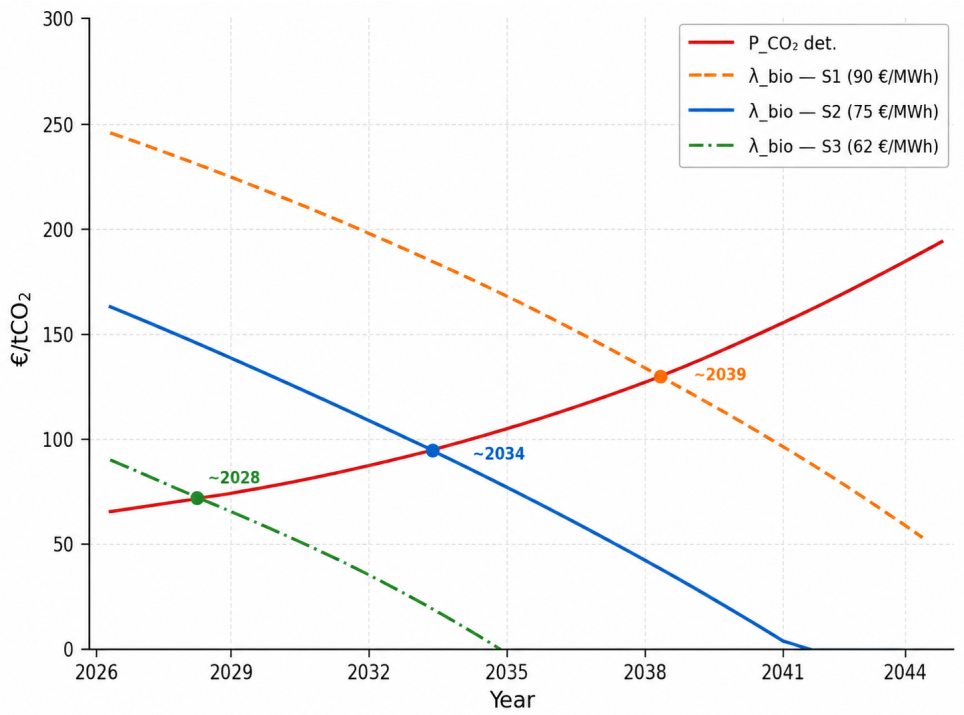


Figure 4.5: Biomethane rationality thresholds under three scenarios compared with the mean EU ETS carbon-price trajectory.

The threshold trajectories follow directly from the GO premium formulation defined in Equation 3.33. Since the total certified biomethane contract price is fixed within each scenario, the GO premium decreases as the network gas price increases at 3%/yr. The decline in $\lambda_{\text{Bio},t}$ therefore reflects the compression of the spread between fossil gas and certified biomethane, rather than an assumed reduction in biomethane production cost.

On the deterministic mean carbon-price trajectory, voluntary biomethane procurement becomes economically rational around 2039 in S_1, 2034 in S_2, and 2028 in S_3. These crossing years are useful as deterministic benchmarks because they indicate when the expected EU ETS price becomes high enough to offset the biomethane GO premium. However, they should not be interpreted as robust switching dates. Under the GBM parameterisation adopted in the Monte Carlo analysis, with $\mu = 5\%$ and $\sigma = 35\%$, the log-drift is negative. As a result, the median carbon-price trajectory declines over time, while the expected trajectory increases because of the right tail of the lognormal distribution.

This distinction is important for interpreting the economic results. The deterministic crossing years show when biomethane procurement becomes rational under the mean EU ETS trajectory, but the robustness of that decision is assessed only through the Monte Carlo distributions presented in Section 4.3.2.

4.3.2 Monte Carlo Simulation Results

The Monte Carlo analysis introduces uncertainty in the EU ETS carbon price and propagates it through the full model. For each biomethane GO premium scenario, the simulation generates a distribution of economic and carbon-performance outcomes, rather than a single deterministic result. This makes it possible to assess not only the expected outcome of each scenario, but also the probability that renewable gas procurement becomes economically favourable under alternative carbon-price trajectories.

NPV Distribution

Figure 4.6 presents the cumulative NPV distribution relative to Baseline $B0$ across the 10,000 Monte Carlo iterations. The vertical line at zero separates outcomes in which biomethane procurement creates a positive net return from those where additional GO procurement costs remain higher than the avoided EU ETS expenditure.

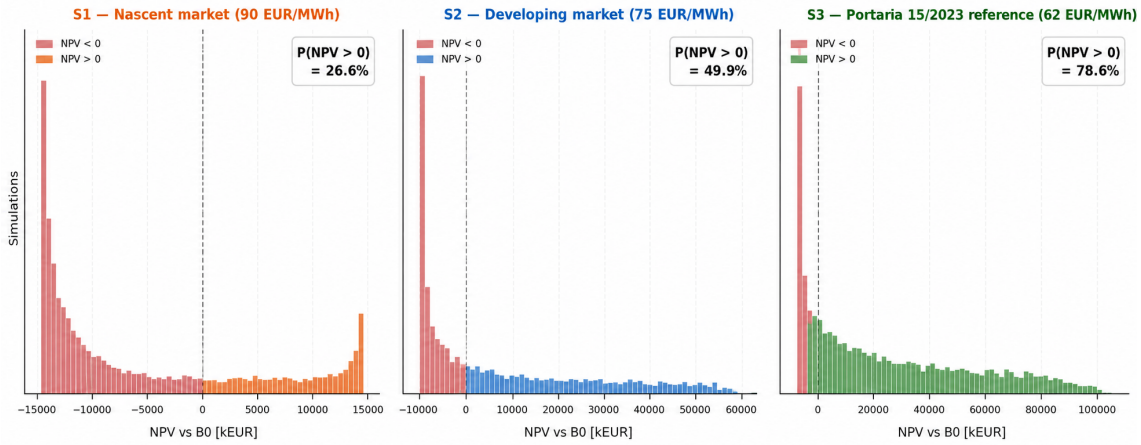


Figure 4.6: Monte Carlo NPV distribution relative to Baseline $B0$ under scenarios S_1, S_2, and S_3.

4.3. Model Results

The main information extracted from Figure 4.6 is the probability of obtaining a positive NPV, rather than the absolute value of each simulated outcome. This probability changes markedly across scenarios. In S_1, only 26.6% of the simulations generate a positive result. The share increases to 49.9% in S_2 and reaches 78.6% in S_3. This progression is consistent with the rationality-threshold analysis presented above that lower biomethane contract prices reduce the carbon-price level required for voluntary procurement to become economically attractive.

In S_1, the higher biomethane price keeps the rationality threshold above most simulated carbon-price paths, so positive outcomes remain limited. In S_3, lower procurement costs move the distribution towards favourable results, with most iterations supporting biomethane procurement beyond the mandatory minimum. Scenario S_2 sits close to the breakeven region, representing a transitional market condition in which the economic case depends strongly on the realised EU ETS price path.

Carbon Abatement Cost and Avoided Emissions

Carbon abatement cost and avoided emissions are analysed separately because they answer different questions. The CAC indicates the economic cost, or saving, associated with each tonne of CO_2 avoided. It therefore provides a direct measure of whether biomethane procurement acts as a costly compliance option or as an economically favourable decarbonisation strategy. Avoided emissions, by contrast, quantify the environmental scale of the procurement decision over the planning horizon.

Figure 4.7 presents the Monte Carlo distribution of CAC across the three biomethane scenarios.

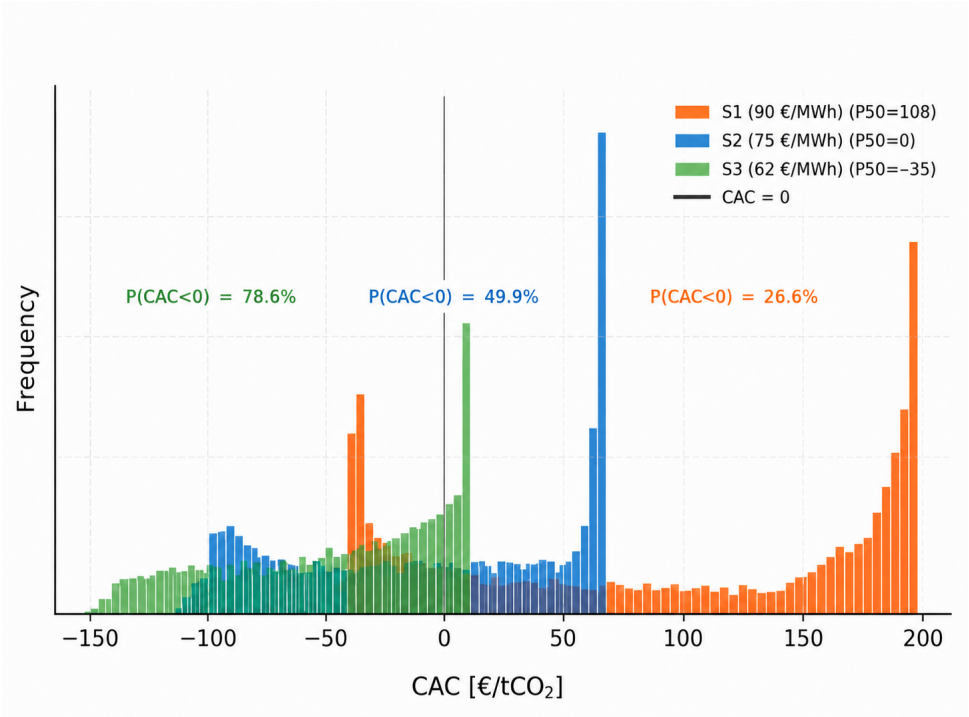


Figure 4.7: Monte Carlo distribution of carbon abatement cost across biomethane scenarios.

The CAC distribution reinforces the economic interpretation of the scenario results. Under S_1, the median CAC remains positive, indicating that avoided EU ETS expenditure is generally

insufficient to offset the higher biomethane procurement cost. In this case, biomethane adoption still delivers emissions reductions, but these reductions come at an additional net cost to the industrial consumer.

Under S_3, the median CAC becomes negative. This means that, in the median Monte Carlo outcome, biomethane procurement not only reduces emissions but also generates net savings relative to Baseline $B0$. The result follows directly from the lower GO premium. Once certified biomethane becomes sufficiently close to fossil gas in cost, avoided carbon expenditure can exceed the additional procurement cost. Scenario S_2 lies between these two cases, with a median value close to zero, suggesting a transitional market condition in which biomethane procurement is near the economic breakeven point.

This indicator is important because it links climate performance to industrial competitiveness. A lower or negative CAC means that emissions reductions are achieved without imposing a persistent additional cost burden. In the context of this thesis, the CAC therefore helps identify the market conditions under which renewable gas procurement moves from being a compliance-driven expense to becoming an economically defensible decarbonisation pathway.

Figure 4.8 presents the corresponding distribution of cumulative avoided emissions over the 20-year planning horizon.

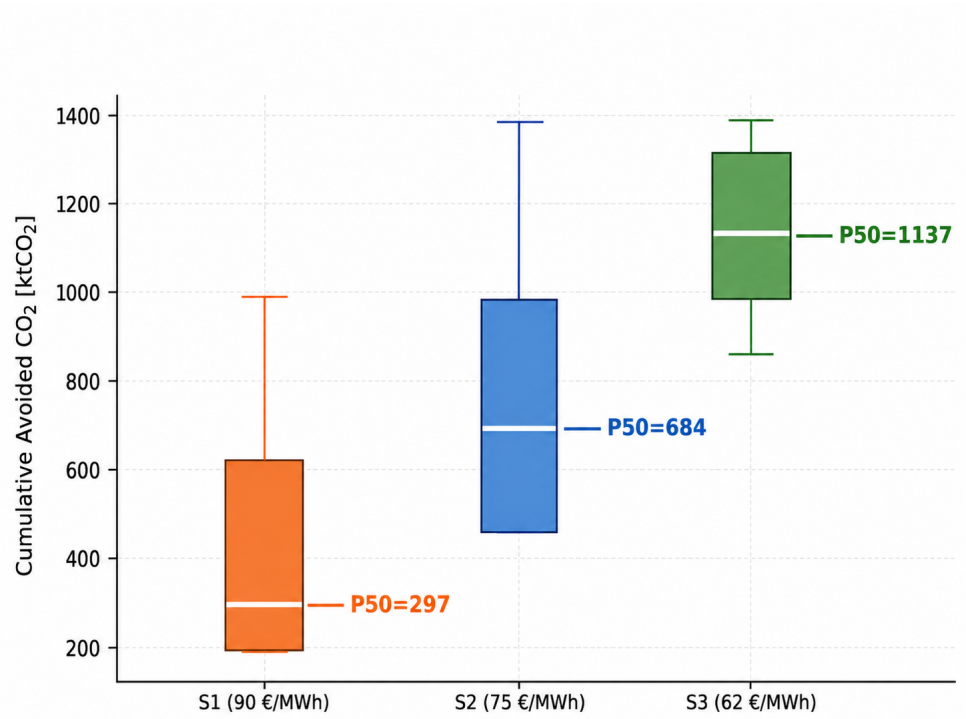


Figure 4.8: Monte Carlo distribution of cumulative avoided emissions over the 2026–2045 planning horizon.

The avoided-emissions results show a clear increase in carbon benefit as the biomethane market becomes more favourable. Median cumulative avoided emissions reach approximately 297 $ktCO_2$ in S_1, 684 $ktCO_2eq$ in S_2, and 1,137 $ktCO_2eq$ in S_3.

For a single connected industrial installation, this variation is substantial. Moving from a nascent-market condition to a mature-market price level increases both the economic attractiveness and the environmental impact of renewable gas procurement.

The combined reading of Figures 4.7 and 4.8 therefore shows that biomethane market development affects not only the cost of abatement, but also the scale of emissions reductions that can be achieved through voluntary procurement of these GOs.

4.3.3 Extended Scenario

Central model assumes that renewable hydrogen is supplied through the blended gas network and accounted for through RFNBO certification. However, the practical implementation of RFNBO certification for hydrogen blended in distribution grids remains uncertain in Portugal, as discussed in Section 3.9. This uncertainty motivates an additional question: **if network-based certification is not available in time, or proves difficult to operationalise, could on-site hydrogen production through electrolysis offer a viable alternative for the industrial consumer?**

The extended scenario addresses this question through a simplified screening assessment over the 2026–2045 planning horizon. It compares the central network-based pathway with an alternative in-situ pathway, in which the industrial consumer produces hydrogen locally. The objective is not to optimise an electrolyser system or to represent all engineering requirements associated with on-site hydrogen production. Instead, a basic comparison assesses whether local electrolysis could plausibly compete with network-based renewable gas supply under conservative assumptions, while also identifying the additional capital commitment and investment-risk allocation implied by this option.

In the **network pathway**, the installation follows the deterministic S_2 case. It receives the progressively hydrogen-enriched gas blend across Phases P_1, P_2, and P_3, procures biomethane GOs to comply with the RED III renewable energy trajectory, and includes the Level 1 combustion retrofit activated in the central model. The resulting annual outputs correspond to the deterministic S_2 case presented in Table G.

In the **in-situ pathway**, the modelled network segment supplies biomethane only, with no hydrogen injection. Hydrogen is instead produced locally through a PEM electrolyser commissioned in 2037 and sized to match the Phase P_3 hydrogen energy equivalent. A Level 3 combustion retrofit is also assigned in the same year, since local production requires the installation to handle a dedicated hydrogen stream.

From 2037 onwards, local hydrogen production is treated consistently with network-delivered RFNBO hydrogen in the EU ETS accounting, so that the in-situ pathway receives the emission-reduction benefit associated with the hydrogen it produces. Before 2037, no local RFNBO hydrogen production is modelled; consequently, the pathway relies only on biomethane attribution and faces higher residual EU ETS exposure during the earlier phases.

Technical and economic assumptions adopted in this comparison are summarised in Appendix H, including the electrolyser sizing calculations, the incremental cost structure, and the sensitivity analysis pseudocode.

The clearest difference between the two pathways is the level of upfront investment required. The network pathway requires only a Level 1 combustion retrofit in 2037, with a cost of approximately 117 kEUR. By contrast, the in-situ pathway requires both a 6.00 MEUR (millions of euros) electrolyser and a Level 3 combustion retrofit of 586 kEUR, resulting in a total capital requirement of approximately 6.58 MEUR.

One possible **objection** is that the two pathways do not assume the same retrofit level. This difference is intentional and reflects a conservative methodological choice. In the network pathway,

hydrogen is introduced gradually through the blended gas supply, and retrofit activation follows the gas-quality deviations identified in Model 1. In the in-situ pathway, however, the installation would invest in local green hydrogen production and would need to be technically prepared to receive and use a dedicated hydrogen stream at the site level. For this reason, a Level 3 retrofit is assigned to the in-situ case, even though the hydrogen share blending with natural gas is considered in the central network model does not itself activate this level.

This **assumption** avoids understating the engineering implications of local hydrogen production. An industrial consumer choosing in-situ electrolysis would not only purchase an electrolyser, but would also need to adapt the combustion system, safety procedures, fuel handling, and control infrastructure to a hydrogen-specific configuration. The resulting comparison is therefore conservative, but, more consistent with the technical nature of the in-situ pathway.

All of this can represents around 56 times the retrofit cost of the network pathway. Even if a Level 3 retrofit were assumed in both pathways, the in-situ option would still require a substantially higher capital commitment because of the initial electrolyser investment. Before operational costs are even considered, this difference implies much greater capital exposure for the industrial consumer.

It also changes the nature of the investment decision: **the network pathway relies mainly on upstream infrastructure and distributed certification, while the in-situ pathway transfers a large share of the decarbonisation investment directly to the individual installation.**

Sensitivity Analysis

The operational comparison is more sensitive to the assumed trajectory of renewable hydrogen costs. Under the central parameterisation, based on a fixed 127 EUR/MWh total hydrogen reference value, in-situ production can appear favourable at the individual installation level. This occurs because the network RFNBO premium in 2037 remains higher than the estimated cost of PPA-based hydrogen production.

Figure 4.9 shows how the LCDE differential responds to **different annual decline rates in the total hydrogen contract price**. The indicator is defined as

$$\Delta LCDE = LCDE_{\text{in-situ}} - LCDE_{\text{network}}.$$

As we can analyse, negative values indicate an in-situ advantage, while positive values indicate a network advantage.

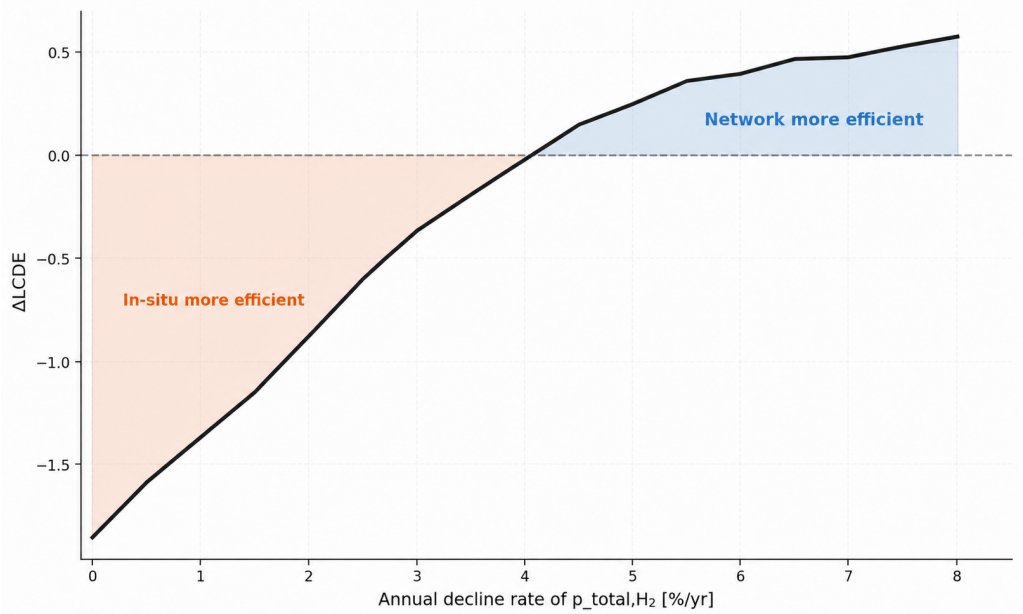


Figure 4.9: Sensitivity of $\Delta LCDE$ to the annual decline rate of the total hydrogen contract price.

The network pathway becomes more favourable when the total hydrogen contract price declines by more than approximately 4.1%/yr, corresponding to a value close to 80 EUR/MWh in 2037. Under slower cost reductions, or under a fixed-price assumption, in-situ production may be competitive from the perspective of a single installation.

Also in the extended scenario , the **Art. 22 hydrogen requirement** is applied on a **volumetric blend basis** rather than on its lower energy-content equivalent, which is the basis used consistently in the main modelling framework. **This is a deliberately conservative modelling choice**: by inflating the compliance cost of the network pathway, the comparison is biased **in favour of the in-situ alternative.** This choice is adopted to make the comparison between the two pathways more demanding and analytically useful, therefore creating a more conservative test of network competitiveness, as discussed later in the results interpretation.

However, this result should be interpreted with caution. It depends strongly on the assumed **electricity price, electrolyser CAPEX, utilisation level, and future hydrogen procurement cost**, all of which remain uncertain and sensitive. Therefore, this scenario is not intended to provide a definitive alternative pathway. Rather, it offers a complementary comparison that helps identify the conditions under which in-situ hydrogen production could become competitive with the network continuity pathway. It also indicates how the network-based renewable gas pathway would need to evolve in order to remain economically attractive relative to a decentralised production option.

These parameters are kept explicit in the model so that **alternative assumptions can be tested in future applications** and adapted to different industrial or market conditions.

Should be consider, that centralised production and injection can serve multiple consumers through shared infrastructure, spreading production, certification, storage, and network-integration costs across a broader demand base. This logic is consistent with the Hydrogen Valley approach, which promotes geographically integrated hydrogen ecosystems linking production, infrastructure, and multiple end-use sectors [101].

Finally, in-situ electrolysis, by contrast, replicates production assets at each industrial site and

concentrates investment, operational, and integration risk at installation level. It does not quantify the additional system benefits that network-based renewable gas deployment could provide through shared infrastructure, coordinated demand aggregation, and regional economies of scale.

4.4 Discussion and Validation

Results for the case-study installation show that physical adaptation to progressive renewable gas injection is not the main constraint. Over the 20-year planning horizon, only one retrofit intervention is activated by network blend evolution, with an estimated Level 1 cost of 117 kEUR. Even a higher Level 3 intervention, used as an upper-bound comparison in the pure-hydrogen extended scenario, would reach 586 kEUR. For this installation, the relevant challenge is therefore not mainly the cost of adapting combustion equipment, but will be the availability and price of certified renewable gas.

Network-level data from the Portgás concession area help place the case-study installation in context. In 2025, the concession served 410,521 active connection points and supplied 5,172,249 MWh/yr of gas [102]. Consumption, however, is far from evenly distributed. Only 1,776 CUIs, around 0.4% of all supply points, consumed more than 10,000 m^3/yr, yet this group accounted for approximately 78% of total concession-area demand. The case-study installation alone consumes 448,000 MWh/yr, equivalent to 8.7% of total demand in the concession and 11.1% of the large-consumer segment.

This concentration is important. A single industrial facility of this scale is not marginal within the regional gas system. Its decarbonisation pathway can therefore affect more than its own emissions balance. If large consumers remain connected and decarbonise through certified renewable gas, they help preserve network utilisation during the transition. If they move instead towards decentralised options, such as in-situ hydrogen production, demand supporting the shared distribution infrastructure may gradually decline, while investment requirements shift to each individual site.

Local biomethane potential is also relevant, but limited. Within the same concession area, maximum technically registered biomethane potential from agricultural, livestock, and wastewater-treatment feedstocks is estimated at approximately 2.0 TWh/yr [102]. This corresponds to 38.7% of total concession-area consumption and roughly half of large-consumer demand. At the scale of the case-study installation, it would supply about 4.5 comparable facilities. Therefore, biomethane could clearly contribute to regional industrial decarbonisation, but only if certified supply is mobilised at sufficient scale and at prices compatible with industrial procurement rationality.

Under the **annual spot procurement** assumption adopted, the installation procures certificates at the prevailing market price in each year of the planning horizon. Long-term offtake contracts analysis, represented here as biomethane purchase agreements (BPAs), are not modelled as a distinct procurement strategy for three reasons:

- A preliminary sensitivity analysis was conducted using the methodology described above, but assuming a fixed biomethane procurement price over a ten-year period (BPA10). The results showed that the $LCDE$ difference between Spot and BPA10 procurement remains below 0.1 EUR/MWh across all scenarios, mainly because the mandatory renewable quota represents a small share of total energy consumption.
- The three $p_{\mathrm{GO,bio},t}$ trajectories defined in Section 3.7 already capture the price uncertainty that a BPA would otherwise fix contractually. Including contract tenor would therefore add limited analytical value and make the scenario structure unnecessarily complex.
- Absence of a mature biomethane injection market in Portugal in 2026 makes long-term bilateral contracting operationally implausible within the near-term planning horizon.

Whether renewable gas procurement represents an economic opportunity or a net regulatory

cost depends strongly on the relationship between biomethane GO premiums and EU ETS carbon prices. Under the price assumptions considered, the biomethane rationality threshold remains above the initial carbon price in all scenarios. In 2026, this threshold ranges from 247 EUR/tCO_2 in S_1 to 93 EUR/tCO_2 in S_3, while the initial EU ETS price is 75.36 EUR/tCO_2. As a result, the initial gap between carbon price and procurement threshold varies from 172 EUR/tCO_2 in the nascent-market scenario(or so we call S_1) to only 18 EUR/tCO_2 under reference-price scenario(or so wee call S_3) [83].

On a **national level**, under the C^0 mandate trajectory, the phased industrial incorporation obligations announced under the PAB, namely 1.5% in 2027, 3.0% in 2028, 6.0% in 2029, and 9.0% in 2030, generate approximately 2.0 TWh/yr of certified biomethane availability by 2030 under central demand projections specified in Appendix I. Even so, this volume remains insufficient to close the RED III minimum compliance gap, estimated at 0.72 to 0.77 TWh/yr in 2030 under C^0. Assuming full transposition of RED III into Portuguese law, part of industrial compliance would therefore still depend on imported GOs from more mature European markets rather than on domestic certified supply.

If domestic certified supply is not sufficient to cover voluntary procurement beyond the mandatory minimum, the installation cannot fully convert the economic signal created by the crossing of $\lambda_{\mathrm{Bio},t}$ into actual procurement. In this sense, the 2034 threshold crossing under S_2 is a necessary but not sufficient condition for voluntary procurement. It identifies when procurement becomes economically rational, but not whether **enough domestic biomethane is available** to meet the resulting demand.

This scaling exercise highlights a simple but important limitation: **even if biomethane becomes economically attractive, there may not be enough domestic supply to meet industrial demand.**

Measuring an annual increase of 1.6 percentage points from the 2021 reference year, reaching approximately 14.4 percentage points by 2030 [3]. Applied to the RMSA-G 2025 industrial gas consumption benchmark of 18.7 TWh/yr, this corresponds to about 2.69 TWh/yr, close to the 2.7 TWh/yr PAB reference value [76].

Plausibility of the case-study emissions profile can be checked against publicly reported data for container glass plants in the United States. According to the US EPA Greenhouse Gas Reporting Program, 41 large container glass plants reported total annual direct emissions of 2.92 $MtCO_2e$ in 2019, corresponding to an average of approximately 71,100 tCO_2/yr per installation [103]. Baseline fossil ($B0$) emissions for the case-study installation under, equal to 76,922 tCO_2/yr, are within about 8% of this independent sectoral benchmark. Such proximity supports the plausibility of the installation's scale and emissions profile relative to comparable international container glass facilities.

Under S_3, median avoided emissions reach approximately 56,850 tCO_2/yr when annualised over the 20-year horizon. For comparison, this represents around 80% of the annual emissions of a typical container glass plant of similar scale. Such a result illustrates the material decarbonisation potential that favourable biomethane market conditions could unlock for a single hard-to-abate industrial facility.

However, meeting minimum compliance is not the same as satisfying potential voluntary demand. Once biomethane prices become attractive, the main constraint may no longer be economic rationality at installation level, but the physical availability of certified domestic biomethane. In that sense, Portugal may face two different gaps: **a compliance gap, related to meeting min-**

imum renewable gas obligations, and a market-scale gap, related to whether domestic supply can satisfy voluntary industrial demand once procurement becomes economically rational.

Closing this second gap is both a supply-side policy objective and a demand-side enabler. Without sufficient domestic certified availability, the market self-reinforcement mechanism identified in the threshold analysis cannot fully materialise, regardless of how favourable the carbon-price trajectory becomes.

Biomethane certificate prices appear to depend more on short-to-medium-term supply–demand balance than on a predictable technology learning curve. Recent European evidence supports this view, with prices increasing sharply in some market segments due to FuelEU Maritime compliance demand and tighter national blending mandates [104]. Fixed-price scenarios are therefore not only a response to limited Portuguese data, but also a reasonable way to represent an emerging commodity-like market where prices may rise or fall non-uniformly with scarcity conditions.

Scenario S_2 is particularly informative because it lies close to the breakeven region. Under this intermediate market condition, the installation faces an almost even probability of obtaining a positive NPV, meaning that the economic case for voluntary biomethane procurement depends strongly on the realised EU ETS price path. As shown below, this result suggests that biomethane market development and long-term carbon-price signalling should be viewed as **complementary policy levers**.

Although biomethane prices available to industrial consumers are not determined by market forces alone, they depend strongly on the support architecture available to producers and on whether that framework can make projects bankable.

In this context, the technical report associated with the PAB public consultation provides the reference for the lower biomethane scenario adopted in this thesis. For reconversion of existing biogas units, it estimates a final biomethane price of approximately 62 EUR/MWh, indicating that this pathway may be close to economic competitiveness under favourable market conditions [105].

For new anaerobic digestion units with upgrading, estimated costs are substantially higher. The final price reaches approximately 125 EUR/MWh without CAPEX support and decreases to approximately 93 EUR/MWh with 40% CAPEX support [105]. By **linear interpolation** of these two reference values, reaching a price close to the S_1 scenario adopted in this thesis, 90 EUR/MWh, would require a CAPEX support level of approximately 44%, a comparison that reinforces the interpretation of S_1 as a high-cost but still policy-accessible market condition, rather than as an arbitrary price assumption.

Considering this case, if total biomethane contract price is fixed at 125 EUR/MWh, while procurement is limited to the RED III mandatory minimum throughout the planning horizon [105]. Under these conditions, the rationality threshold starts at 440 EUR/tCO_2 in 2026 and is never crossed by the deterministic EU ETS trajectory, which reaches only 195 EUR/tCO_2 by 2045. The result is a negative NPV of $-14{,}488$ kEUR relative to $B0$, combined with only 196.4 ktCO_2 of cumulative avoided emissions over 20 years. This represents a **worst-case benchmark** and the weakest environmental outcome among the cases considered. Mandatory RED compliance alone, when paired with a high and rigid biomethane price, therefore produces limited decarbonisation value and a poor economic result, reinforcing the need for support mechanisms capable of reducing certified biomethane costs.

In 2024, the net value of Portuguese national gas transportation network assets exceeded almost 900 MEUR [106]. If fossil natural gas consumption declines, the fixed costs associated with main-

taining and amortising this infrastructure may have to be recovered from a smaller consumption base, creating upward pressure on network tariffs. This effect is particularly relevant for hard-to-abate industrial consumers, which may remain dependent on gaseous fuels for high-temperature processes for longer than other sectors [4].

Extended scenario results are strongest on upfront capital exposure. Network-based RFNBO compliance requires only a 117 kEUR Level 1 retrofit, whereas in-situ electrolysis requires approximately 6.58 MEUR in combined electrolyser and retrofit investment. Decentralised production therefore implies a capital commitment around 56 times higher, making CAPEX exposure the most robust indicator of the economic advantage of remaining connected to the network.

Break-even hydrogen contract-price decline should be interpreted only as an illustrative proxy. It refers to the reduction in renewable hydrogen contract price required for network-based compliance to retain its cost advantage, not directly to electrolyser CAPEX. Under **the volumetric basis** adopted and explicited before, network-based compliance remains favourable if the hydrogen contract price declines by more than 4.16%/yr. Under an energy-content basis, more consistent with the final-energy logic of RED III, this threshold falls to 0.95%/yr. Since an 18% volumetric hydrogen fraction corresponds to only about 6% of delivered energy in Phase P_3, the volumetric convention overstates network GO procurement by approximately a factor of three. Reported break-even results are therefore conservative, and network advantage becomes larger under the energy-content interpretation.

Using the European PEM learning curve estimated by Holst et al. [107], a decline rate of this order would correspond to approximately 2.6 GW of cumulative European electrolyser capacity by 2037. Such calculation assumes favourable pass-through from electrolyser CAPEX reductions to hydrogen contract prices and should be read as a first-order consistency check, not as a deployment forecast. Across both accounting bases, and under deliberately conservative assumptions, the central conclusion remains unchanged: network-based compliance retains a decisive capital-efficiency advantage, anchored in the 56× CAPEX differential rather than in any specific assumption about future hydrogen price trajectories.

Lastly, progressive renewable gas injection offers a partial response to this risk. By replacing fossil molecules with certified biomethane and hydrogen while continuing to use existing network assets, renewable gas deployment can help preserve infrastructure fixed costs across a broader low-carbon supply base. For a specific installation, this means that the Layer 1 network cost is not only a transport charge, but also part of the wider economic framework that enables renewable procurement**(through GOs)** with the pipeline.

Ultimately, this infrastructure effect is outside the scope of the model, it reinforces the systemic argument for network-based decarbonisation. Compared with isolated in-situ solutions, investment in renewable gas injection at network level can support a positive **feedback between supply-side deployment, tariff sustainability, infrastructure value preservation, and industrial decarbonisation.**

Chapter 5

Conclusions

This dissertation developed an integrated techno-economic framework to assess how hard-to-abate industrial consumers connected to gas distribution networks can decarbonise under progressive renewable gas integration. Rather than treating renewable gas supply as a single physical and economic variable, the framework separates two layers: the gas blend delivered at the industrial meter and the renewable content attributed through Guarantees of Origin. This distinction is central to RED III compliance, yet it is rarely represented explicitly in techno-economic assessments at an industrial level.

The framework combines gas-quality analysis, retrofit activation, renewable attribute procurement, EU ETS exposure, and stochastic carbon-price simulation. In doing so, it provides a proof-of-concept decision-support tool for industrial consumers and specially distribution system operators. With more detailed site-specific data, the same structure could be adapted to other gas-connected industrial installations facing similar compliance and decarbonisation challenges.

Also at this stage of the project, a basic version of the decision-support interface can be presented. A interface would **package the all model into a simple tool** developed in Streamlit on Python, allowing users to enter the main inputs and obtain the key results automatically.

Results are based on real annual gas consumption data, however, detailed as said, information on combustion equipment, burner configuration, control systems, and hydraulic conditions was not available within the scope of this work.

Beyond the case-study results, the thesis also highlights a wider strategic issue. Network-based decarbonisation can help preserve the role of existing gas infrastructure by maintaining industrial demand for renewable gaseous fuels. In-situ solutions, such as local hydrogen production, may reduce exposure to certification uncertainty, but they also shift investment risk to the industrial consumer and may weaken the demand base needed to sustain renewable gas injection at network level. For this reason, the comparison between network-based and decentralised pathways is not only a cost question, but also an infrastructure and policy question.

Following sections summarise the main findings, policy implications, limitations, and directions for future work.

Dissertation Main Conclusions

- **A physical–contractual modelling framework was developed.**

  This dissertation proposes a replicable framework for assessing renewable gas compliance pathways at the level of an individual hard-to-abate industrial installation. Its main methodological contribution is the explicit separation between the gas blend physically delivered to the installation and the renewable content contractually attributed through GO procurement. This distinction makes it possible to capture interactions that conventional cost comparisons would miss, particularly the difference between combustion behaviour, regulatory emissions attribution, carbon-price exposure, and voluntary procurement rationality.

- **Physical compatibility is not the main constraint in the case study.**

  Across the network phases considered, the case-study installation remains technically compatible with progressive renewable gas injection until Phase P_3. At that stage, the Wobbe Index decreases to 46.66 MJ/Nm^3, below the admissibility limit of 47.51 MJ/Nm^3, activating a Level 1 combustion retrofit in 2037. For this installation, the physical layer is therefore manageable and does not represent the binding decarbonisation constraint.

- **Biomethane market maturity determines the procurement window.**

  The rationality threshold for voluntary biomethane procurement declines over time in all scenarios, mainly because the network gas price increases throughout the planning horizon. Crossing this threshold marks the point at which biomethane procurement becomes economically justified beyond mandatory compliance. This occurs around 2028 in S_3, 2034 in S_2, and 2039 in S_1. The resulting 11-year difference shows how strongly industrial procurement timing depends on biomethane market development and on the ability of policy to reduce certified biomethane costs.

- **EU ETS uncertainty dominates economic variability.**

  Monte Carlo simulation results show that carbon-price uncertainty is the main source of economic variability across scenarios. Biomethane market development and long-term EU ETS price signalling are therefore complementary: lower GO premiums reduce the carbon-price threshold, but a credible carbon-price trajectory is still needed for renewable gas procurement to become a robust industrial investment.

- **Market development has a large environmental value.**

  Cumulative avoided emissions vary substantially across scenarios. At the P50 level, avoided emissions increase from approximately 297 ktCO$_2$ in S_1 to 1,137 ktCO$_2$ in S_3, a difference of about 840 ktCO$_2$ over the 20-year planning horizon. This difference reflects the additional voluntary procurement enabled by lower biomethane costs. Under S_3, median carbon abatement cost becomes negative, meaning that emissions reductions are achieved with net savings in the central Monte Carlo outcome.

- **Network-based decarbonisation is more capital-efficient than in-situ hydrogen production.**

  The extended scenario shows that local hydrogen production through electrolysis would require a capital commitment of approximately 6.58 MEUR in 2037, around 56 times higher than the network-compliance retrofit. Operating-cost competitiveness depends on future green hydrogen prices, with the network pathway recovering its advantage if hydrogen pro-

curement costs decline by more than approximately 4.1%/yr from the adopted reference [83]. Even so, the systemic advantage of the network pathway is clearer: centralised renewable gas injection spreads production, certification, and infrastructure costs across multiple connected consumers, while isolated in-situ strategies concentrate investment risk at installation level.

- **Supply-side policy is the binding condition.**

  Economic outcomes depend less on the installation's technical configuration than on the availability of certified biomethane at prices compatible with industrial procurement rationality. The framework also helps identify which decarbonisation pathway is most suitable for each industrial consumer and what conditions are required for that pathway to become feasible. This supports a more targeted policy discussion, developed later in the thesis. Portugal must not only define renewable gas targets, but also create the supply-side instruments, bankable production capacity, and procurement conditions needed to make those targets operational for gas-connected industries.

- **The framework supports DSO-led prioritisation rather than only single-site assessment.**

  Although applied to a single industrial installation, this model framework can support portfolio-level planning by the DSO. Large industrial consumers are not marginal loads within the gas distribution system, since their decisions affect network utilisation, renewable gas demand, and the value of shared infrastructure. By combining retrofit timing, GO costs, EU ETS exposure, NPV, CAC, and avoided emissions, the model helps identify which consumers should be prioritised and when renewable gas pathways become credible. In this way, the framework moves beyond site-level feasibility and becomes a decision-support tool for coordinating industrial decarbonisation across the distribution network.

Framework Industrial Implementation

A practical use of the framework would be to support direct discussions between DSOs and connected industrial consumers. Instead of treating renewable gas integration only as a network-planning issue, the model can translate it into installation-level decisions:

- when a possible retrofit may be required;
- how much renewable gas procurement may cost;
- how much EU ETS exposure can be reduced depending on current situation;
- what emissions can be avoided with certain scenarios;
- whether remaining connected to the network is more attractive than investing in other alternatives.

Implementation could follow five practical steps:

- **Installation characterisation** → A DSO would first collect the minimum data needed to run the model for a specific consumer: annual metered gas consumption, capacity factor, combustion equipment type, connection point, and expected network phase schedule.
- **Physical admissibility screening** → Model 1 would then be applied to the consumer's specific network conditions to identify whether any gas-quality limit is exceeded and whether retrofit is required. In the case study, this step showed that only a Level 1 retrofit would be needed in Phase P_3, allowing the intervention to be planned several years in advance.

- **Procurement scenario assessment** → Biomethane scenarios S_1, S_2, and S_3 would be used to compare how different market conditions affect GO costs, EU ETS exposure, NPV, carbon abatement cost, and avoided emissions. These scenarios should be interpreted as decision windows, not as forecasts.
- **Risk assessment** → The Monte Carlo module would provide probabilistic results instead of a single deterministic value. This allows the consumer to understand how EU ETS carbon-price uncertainty affects the likelihood of obtaining a positive NPV or achieving low-cost emissions reductions.
- **Alternative pathway benchmarking** → Where uncertainty around RFNBO certification or GO availability is relevant, the extended scenario can compare network-based supply with in-situ hydrogen production. This gives the consumer a screening-level view of the capital and operating-cost implications of decentralised electrolysis.

In practical terms, this framework could allow a DSO like REN-Portgás to act not only as a network operator, but also as a technical and economic partner in industrial decarbonisation planning. **For industrial consumers, it converts a complex regulatory and energy-market problem into a clearer investment decision based on their own consumption profile, retrofit needs, procurement options, and carbon-price exposure.**

5.1 Policy Implications

Results from this dissertation lead to **policy implications** across several questions and areas:

Targets alone do not mobilise bankable supply.

PAB incorporation obligations create demand-side pressure, but do not by themselves provide the revenue certainty required for new biomethane projects. If certified domestic biomethane is to become available at prices compatible with industrial procurement rationality, support instruments must reduce project risk, stabilise revenues, and convert technical potential into bankable production capacity.

Large consumers should be prioritised in targeted decarbonisation policy.

As shown in Section 4.4, data from the case-study concession area indicate that a very small group of large consumers accounts for most gas demand. This suggests that renewable gas support instruments and DSO-led decarbonisation programmes should prioritise high-consumption industrial users, rather than applying uniform intervention across all connection points. Focusing on these high consumers locations, would create stronger leverage for network decarbonisation, since a limited number of installations can drive a large share of emissions reductions and renewable gas demand.

Required support levels are quantifiable and currently unmet.

Portuguese CfD assessments indicate that reconversion of existing biogas units may already be close to economic competitiveness, while new anaerobic digestion capacity still requires support in the range of 27 to 59 EUR/MWh, depending on CAPEX subsidy levels [105]. Limited uptake in the 2024 auction at 62 EUR/MWh is consistent with this evidence: the reference price was not sufficient to provide the revenue certainty required to mobilise new supply at scale [84].

5.1. Policy Implications

Voluntary procurement potential structurally exceeds compliance-calibrated supply targets.

Under S_3 ,the most optimistic scenario, the case-study installation rationally **seeks** biomethane GO coverage of 98.7% of useful energy by 2030, corresponding to 376 GWh/yr. Scaling to the 42 installations implied by the 18.7 TWh/yr national industrial gas consumption benchmark [76] yields **aggregate voluntary demand** of approximately 15.8 TWh/yr, a figure that full C^+ materialisation (2.72 TWh/yr) covers at 17%. Since C^+ already presupposes a price support instrument that does not yet exist, national deployment targets calibrated to the RED III minimum are structurally misaligned with the procurement volumes that a **functioning carbon price and competitive GO market would jointly generate**. An **extrapolation that assumes uniform installation scale** and should be read as an order-of-magnitude bound rather than a sectoral forecast.

Timing is a binding constraint.

Given realistic project development lead times, like wee see 2.6 the 2030 compliance window is effectively closed for new policy instruments introduced today. The 2035 window remains more relevant, but is already narrowing. A support mechanism activated no later than 2027 would be needed for domestic supply to contribute meaningfully before 2035.

RFNBO certification clarity is essential for preserving network-based economies of scale.

Clear RFNBO certification for hydrogen blended in gas networks is essential to avoid shifting compliance from shared infrastructure to fragmented site-level investment. If network-delivered hydrogen cannot be certified in time, industrial consumers may be pushed towards in-situ electrolysis, replicating production assets across multiple consumption nodes and transferring cost, operational risk, and investment responsibility from the network to individual installations. Results from the extended scenario show that network-based compliance remains economically robust if green hydrogen contract prices decline by more than approximately 4.1%/yr, a rate compatible with plausible electrolyser deployment levels. Regulatory uncertainty around RFNBO certification therefore represents a more critical risk to network-based hydrogen procurement than insufficient technology learning alone.

Carbon-price credibility complements biomethane market development.

EU ETS uncertainty is the dominant source of economic variability in the model. Even under the most favourable biomethane scenario, S_3, positive NPV probability reaches 78.6%, compared with 49.9% in S_2 and 26.6% in S_1. Lower GO premiums therefore improve the economic case for renewable gas procurement, but do not remove carbon-price risk. Long-term EU ETS credibility remains necessary alongside biomethane support policy, rather than as a substitute for it.

Iberian Book-and-Claim could turn renewable gas certification into a strategic export channel.

Portuguese renewable gas gaps reflect unmobilised potential more than primary resource scarcity. Portugal and Spain have favourable renewable electricity conditions, particularly for solar and onshore wind, which can support competitive renewable electricity PPAs and create a comparative advantage in electrolytic hydrogen production [108]. However, this physical advantage only becomes relevant if it is converted into bankable, certified, and tradeable renewable gas supply. From

this perspective, an Iberian Book-and-Claim framework under RED III could allow renewable gas value to be exported through Guarantees of Origin, even when the renewable molecule is not physically consumed by the final industrial user. This opportunity is especially relevant for RFNBO hydrogen, since biomethane remains constrained by sustainable feedstock availability, while renewable hydrogen can scale with renewable electricity deployment, electrolyser capacity, and certification infrastructure. Still, Book-and-Claim should not become a form of paper compliance disconnected from physical decarbonisation. Its credibility depends on additionality, traceability, transparent GO cancellation, and robust cross-border accounting. For Portugal, the policy priority is therefore twofold: closing the domestic industrial compliance gap already identified and creating the institutional conditions for certified renewable gas production to become an Iberian strategic asset capable of supporting wider European industrial decarbonisation through exportable GO value.

5.2 Future Works

The following future works are proposed:

- **Carbon capture and alternative process solutions should be integrated in future model extensions.**

  Future work could extend the framework beyond fuel substitution by including CCS and process-efficiency measures as additional decarbonisation pathways. Adding capture costs, capture-rate-dependent OPEX, and process interventions such as waste-heat recovery, batch preheating, or furnace redesign would allow network-based procurement, CCS, and efficiency measures to be compared within the same NPV, LCDE, and CAC structure.

- **Site-specific calibration with real industrial data should also replace the screening-level retrofit coefficients used in this thesis with site-specific engineering data.**

  Although the case study uses real annual gas consumption, detailed information on burners, control systems, combustion equipment, and hydraulic conditions was not available. Applying this calibration across several industrial consumers would also strengthen the framework as a transferable planning tool rather than a single-installation case study.

- **From screening model to forecasting-aware consulting tool.**

  The model could be extended into a more forecasting-aware decision-support tool. In this dissertation, only the EU ETS carbon price is modelled stochastically. This choice is transparent, but reflects limited Portuguese market data. As more data become available, future versions of the model could extend the Monte Carlo framework to, gas prices, biomethane GO premiums, green hydrogen costs, and renewable electricity PPA prices.

- **Operational deployment via an interactive decision-support interface.**

  A browser-based implementation of the framework has been developed as a proof-of-concept using the Streamlitn library, allowing a consulting practitionerto parameterise the full model. Future development should extend this interfaceto incorporate the full Weaver interchangeability hierarchy of Model 1, multi-installation portfolio aggregation, and scenario comparison across simultaneously loaded parameterisations, enabling its deployment as an operational DSO advisory instrument rather than a single-installation screening tool.

- **Multi-installation and concession-level aggregation should extend the model from a single-installation case study to a concession-level portfolio tool.**

Instead of applying the framework only to one industrial consumer, Models 1, 2 and 3 could be run individually for each large consumer in the concession, using installation-specific consumption, combustion technology, and network-node composition. Results could then be aggregated into concession-wide NPV, CAC, and avoided-emissions distributions. This would allow a DSO like REN-Portgás to identify which consumers offer the greatest decarbonisation impact per unit of support required, prioritise engagement with high-impact installations, and provide a stronger basis for estimating the domestic biomethane volumes needed for industrial decarbonisation at regional or national scale.

- **Real-options valuation of network connectivity.**

  Future work could also extend the Monte Carlo framework to treat the network versus in-situ hydrogen choice as a flexible investment decision. A connected industrial consumer can defer the electrolysis investment until future potencial and costs become clearer. This flexibility could be formalised as a **Network Decarbonisation Option Value (NDOV)**, by modelling $p_{\text{total},\text{H}_2}$ as a stochastic variable alongside $P_{\text{CO}_2,t}$ and applying least-squares Monte Carlo to value, on an annual basis, the option of remaining connected while preserving the possibility of switching to in-situ production. This would give the DSO a quantitative measure of the economic benefit associated with keeping industrial consumers on-grid.

Appendix A– Fundamental Thermophysical and Combustion Properties

Table A.1: Fundamental thermophysical and combustion properties adopted for hydrogen, pure methane, and Portuguese natural gas.

Property	**Portuguese NG**	**Pure CH_4**	**Pure H_2**
LHV volumetric [MJ/Nm^3]	37.5–40.3	35.88	10.80
Density [kg/Nm^3]	0.78–0.85	0.717	0.090
Specific gravity, SG	0.57–0.64	0.554	0.070
Gross Wobbe Index [MJ/Nm^3]	48.2–53.2	53.5	48.3
Laminar flame speed [cm/s]	35–40	37.6	229.2
Flammability range [% vol. in air]	5–15	5–15	4–75
Adiabatic flame temperature [°C]	1950–2000	$\approx$ 1950	$\approx$ 2100

Note: Volumetric heating values and densities are reported on the normal cubic metre basis used in the model property database. Values are therefore kept internally consistent with the mixture calculations in Model 1. The EN 437 G20 gross Wobbe value is not used as a numerical input to the model-derived net Wobbe screening threshold.

Appendix B– Model 1 Computational Implementation

This appendix presents the core computational logic of Model 1, implemented in `model1.py`. The model receives the ternary blend composition $(x_{\mathrm{H_2}}, x_{\mathrm{bio}}, x_{\mathrm{NG}})$ for each network phase as an exogenous input and returns thermophysical properties, interchangeability flags, and retrofit capital expenditure obligations. The methodology is formalised in Section 3.4.

B.1 Mixture Property Calculation

`Function: calcular_propriedades(comp)`

$x_{\mathrm{NG}} \leftarrow \max(0,\ 1 - x_{\mathrm{H_2}} - x_{\mathrm{bio}})$
$LHV_{\mathrm{mix}} \leftarrow x_{\mathrm{NG}} \cdot LHV_{\mathrm{NG}} + x_{\mathrm{bio}} \cdot LHV_{\mathrm{CH_4}} + x_{\mathrm{H_2}} \cdot LHV_{\mathrm{H_2}}$
$HHV_{\mathrm{mix}} \leftarrow x_{\mathrm{NG}} \cdot HHV_{\mathrm{NG}} + x_{\mathrm{bio}} \cdot HHV_{\mathrm{CH_4}} + x_{\mathrm{H_2}} \cdot HHV_{\mathrm{H_2}}$
$SG_{\mathrm{mix}} \leftarrow x_{\mathrm{NG}} \cdot SG_{\mathrm{NG}} + x_{\mathrm{bio}} \cdot SG_{\mathrm{CH_4}} + x_{\mathrm{H_2}} \cdot SG_{\mathrm{H_2}}$
$WI_{\mathrm{mix}} \leftarrow LHV_{\mathrm{mix}} / \sqrt{SG_{\mathrm{mix}}}$
$V_{\mathrm{air}} \leftarrow \sum_i x_i \cdot V_{\mathrm{air},i}$
return $\{LHV_{\mathrm{mix}}, HHV_{\mathrm{mix}}, SG_{\mathrm{mix}}, WI_{\mathrm{mix}}, V_{\mathrm{air}}\}$

B.2 Interchangeability Screening

`Function: filtro_interchangeabilidade`

$WI_{\mathrm{lower}} \leftarrow 47.51$ MJ/m^3
$WI_{\mathrm{upper}} \leftarrow 52.51$ MJ/m^3
if $WI_{\mathrm{mix}} < WI_{\mathrm{lower}}$ **or** $WI_{\mathrm{mix}} > WI_{\mathrm{upper}}$ **then**
    J_H-flag $\leftarrow$ `TRUE`
else
    J_H-flag $\leftarrow$ `FALSE`
end if
if $x_{\mathrm{H_2}} > 0.20$ **then**
    J_{HT}-flag $\leftarrow$ `TRUE`
else
    J_{HT}-flag $\leftarrow$ `FALSE`
end if
$J_A \leftarrow (V_{ts}/V_{ta}) \cdot \sqrt{SG_a/SG_s}$
if $J_A < 0.95$ **or** $J_A > 1.05$ **then**
    J_A-flag $\leftarrow$ `TRUE`
else

17: J_A-flag ← `FALSE`
18: **end if**
19: CAPEX-flag ← J_H-flag **or** J_{HT}-flag **or** J_A-flag
20: **return** flags and violation reasons

B.3 Retrofit CAPEX Assignment

`Function: calculate_capex(filter)`

1: **if** J_H-flag **and not** J_{HT}-flag **and not** J_A-flag **then**
2: $Level \leftarrow L_1$
3: $\alpha \leftarrow 2$ €/kW
4: **else if** J_H-flag **and** J_A-flag **then**
5: $Level \leftarrow L_2$
6: $\alpha \leftarrow 5$ €/kW
7: **else if** J_{HT}-flag **then**
8: $Level \leftarrow L_3$
9: $\alpha \leftarrow 10$ €/kW
10: **else**
11: $Level \leftarrow L_0$
12: $\alpha \leftarrow 0$ €/kW
13: **end if**
14: $CAPEX_{\text{comb}} \leftarrow \alpha \cdot \dot{E}_{\text{th}}$
15: **return** $CAPEX_{\text{comb}}$, $Level$

B.4 Main Entry Point

1: **for** each network phase $k \in \{P_0, P_1, P_2, P_3\}$ **do**
2: $props_k \leftarrow$ `calcular_propriedades`$(comp_k)$
3: $flags_k \leftarrow$ `filtro_interchangeabilidade`$(props_k,\ props_{\text{ref}},\ x_{\text{H}_2,k})$
4: $capex_k \leftarrow$ `calcular_capex`$(flags_k)$
5: Store $\{props_k,\ flags_k,\ capex_k\}$ for phase k
6: **end for**
7: **return** results dictionary indexed by phase

Key outputs passed to subsequent models:

- $WI_{\text{mix},k}$, $LHV_{\text{mix},k}$, and $SG_{\text{mix},k}$, corresponding to thermophysical inputs used in Model 2.

Appendix C– Model 2 Computational Implementation

This appendix presents the core computational logic of Model 2, implemented in `model2.py`. The model translates the thermophysical outputs of Model 1 into annual operational expenditure across three cost layers, and determines the GO procurement strategy through a sequential decision cascade. The methodology is formalised in Section 3.5.

C.1 Rationality Thresholds

$\lambda_{\text{bio}} \leftarrow p_{\text{GO,bio},t}/(EF_{\text{GN}} - EF_{\text{bio}})$
$\lambda_{\text{H}_2} \leftarrow p_{\text{GO,H}_2,t}/(EF_{\text{GN}} - EF_{\text{H}_2})$
return λ_{bio}, λ_{H_2} $\quad [€/\text{tCO}_2]$

C.2 GO Procurement Decision Cascade

Require: $P_{\text{CO}_2,t}$, $p_{\text{GN},t}$, $p_{\text{GO,bio},t}$, $p_{\text{GO,H}_2,t}$, x_{H_2}
Ensure: $\alpha_{\text{bio},t}$, $\alpha_{\text{H}_2,t}$
$\alpha_{\text{H}_2,\min} \leftarrow$ `quota_min_rfnbo_h2`$(t,\ x_{\text{H}_2})$
$\alpha_{\text{H}_2,\max} \leftarrow x_{\text{H}_2}$
if $P_{\text{CO}_2,t} \geq \lambda_{\text{H}_2}$ **or** $p_{\text{GO,H}_2,t} \leq 0$ **then**
    $\alpha_{\text{H}_2} \leftarrow \alpha_{\text{H}_2,\max}$
else
    $\alpha_{\text{H}_2} \leftarrow \alpha_{\text{H}_2,\min}$
end if
$\alpha_{\text{bio},\min} \leftarrow \max(0,\ $ `quota_min_art22`$(t) - \alpha_{\text{H}_2})$
$\alpha_{\text{bio},\max} \leftarrow \min(1 - \alpha_{\text{H}_2},\ 1.0)$
if $P_{\text{CO}_2,t} \geq \lambda_{\text{bio}}$ **then**
    $\alpha_{\text{bio}} \leftarrow \alpha_{\text{bio},\max}$
else
    $\alpha_{\text{bio}} \leftarrow \alpha_{\text{bio},\min}$
end if
return α_{bio}, α_{H_2}

C.3 Three-Layer OPEX Computation

for each year $t \in \{2026, \ldots, 2045\}$ **do**
    $C_{1,t} \leftarrow E_{\text{annual}} \cdot p_{\text{GN},t}$
    $C_{2,\text{bio},t} \leftarrow \alpha_{\text{bio},t} \cdot E_{\text{util}} \cdot p_{\text{GO,bio},t}$
    $C_{2,\text{H}_2,t} \leftarrow \alpha_{\text{H}_2,t} \cdot E_{\text{util}} \cdot p_{\text{GO,H}_2,t}$

$C_{2,t} \leftarrow C_{2,\text{bio},t} + C_{2,\text{H}_2,t}$

$EF_{\text{legal},t} \leftarrow f_{\text{uncov}} \cdot EF_{\text{GN}} + \alpha_{\text{bio}} \cdot EF_{\text{bio}} + \alpha_{\text{H}_2} \cdot EF_{\text{H}_2}$

$E_{\text{legal},t} \leftarrow E_{\text{util}} \cdot EF_{\text{legal},t}$

$A_{\text{free},t} \leftarrow E_{\text{util}} \cdot EF_{\text{GN}} \cdot \Phi_{\text{CBAM},t}$

$C_{3,t} \leftarrow \max(0,\ E_{\text{legal},t} - A_{\text{free},t}) \cdot P_{\text{CO}_2,t}$

$OPEX_t \leftarrow C_{1,t} + C_{2,t} + C_{3,t}$

end for

return $\{C_{1,t},\ C_{2,t},\ C_{3,t},\ OPEX_t,\ \alpha_{\text{bio},t},\ \alpha_{\text{H}_2,t}\}$ for all t

C.4 Physical Compliance Baseline(B0)

for each year $t \in \{2026, \ldots, 2045\}$ **do**

$\alpha_{\text{bio},t} \leftarrow 0 \quad \alpha_{\text{H}_2,t} \leftarrow 0$

$C_{1,t} \leftarrow E_{\text{annual}} \cdot p_{\text{GN},t}$

$E_{\text{legal},t} \leftarrow E_{\text{util}} \cdot EF_{\text{GN}}$

$A_{\text{free},t} \leftarrow E_{\text{util}} \cdot EF_{\text{GN}} \cdot \Phi_{\text{CBAM},t}$

$C_{3,t} \leftarrow \max(0,\ E_{\text{legal},t} - A_{\text{free},t}) \cdot P_{\text{CO}_2,t}$

$OPEX_{B0,t} \leftarrow C_{1,t} + C_{3,t}$

end for

return $OPEX_{B0,t}$ for all t

Key outputs passed to Model 3:

- $C_{1,t}$, $C_{2,\text{bio},t}$, $C_{2,\text{H}_2,t}$, and $C_{3,t}$, corresponding to annual cost layers for NPV and LCDE computation.
- $\alpha_{\text{bio},t}$ and $\alpha_{\text{H}_2,t}$, corresponding to GO coverage fractions for avoided emissions calculation.
- $A_{\text{free},t}$, corresponding to free allowance allocation.
- $EF_{\text{legal},t}$, corresponding to the legally attributed emission factor under GO procurement.

Appendix D– Model 3 Computational Implementation

This appendix presents the core computational logic of Model 3, implemented in `model4.py`. The model aggregates the annual cost and emissions outputs of Model 2 into discounted economic and carbon performance indicators over the full planning horizon. The methodology is formalised in Section 3.6.

D.1 Discount Factor

for $t = 1$ **to** T **do**
    $df_t \leftarrow 1/(1+r)^t$
end for
return $\{df_t\}_{t=1}^{T}$

D.2 Net Present Value

Require: $OPEX_{\text{cen},t}$, $OPEX_{B0,t}$, df_t, $CAPEX_{L1}$
Ensure: NPV [€]

$$NPV \leftarrow \sum_{t=1}^{T} [\Delta EF_t \cdot E_{\text{util}} \cdot P_{\text{CO}_2,t} - C_{2,\text{bio},t} - C_{2,\text{H}_2,t}] \cdot df_t$$

return NPV

D.3 Levelised Cost of Decarbonised Energy

Require: $OPEX_{\text{cen},t}$, $CAPEX_{L1}$, E_{util}, df_t
Ensure: $LCDE$ [€/MWh]

$$CAPEX_{\text{PV}} \leftarrow CAPEX_{L1} \cdot df_{2037}$$

$$OPEX_{\text{PV}} \leftarrow \sum_{t=1}^{T} OPEX_{\text{cen},t} \cdot df_t$$

$$E_{\text{util,PV}} \leftarrow \sum_{t=1}^{T} E_{\text{util}} \cdot df_t$$

$$LCDE \leftarrow (CAPEX_{\text{PV}} + OPEX_{\text{PV}})/E_{\text{util,PV}}$$

return $LCDE$

D.4 Carbon Abatement Cost

Require: $OPEX_{\text{cen},t}$, $OPEX_{B0,t}$, $E_{\text{CO}_2,\text{cen},t}$, $E_{\text{CO}_2,\text{B0},t}$, df_t
Ensure: CAC [€/tCO$_2$]

$$\Delta OPEX_{\text{PV}} \leftarrow \sum_{t=1}^{T} (C_{2,\text{bio},t} + C_{2,\text{H}_2,t} - \Delta C_{3,t}) \cdot df_t$$

2: $\Delta CO_{2,\mathrm{PV}} \leftarrow \sum_{t=1}^{T} \Delta EF_t \cdot E_{\mathrm{util}} \cdot df_t$
3: $CAC \leftarrow \Delta OPEX_{\mathrm{PV}} / \Delta CO_{2,\mathrm{PV}}$
4: **return** CAC

D.5 Avoided Emissions

1: **for** each year t **do**
2: $\quad \Delta EF_t \leftarrow \alpha_{\mathrm{bio},t}(EF_{\mathrm{GN}} - EF_{\mathrm{bio}}) + \alpha_{\mathrm{H_2},t}(EF_{\mathrm{GN}} - EF_{\mathrm{H_2}})$
3: $\quad \Delta CO_{2,t} \leftarrow \Delta EF_t \cdot E_{\mathrm{util}}$
4: **end for**
5: $\Delta CO_{2,\mathrm{total}} \leftarrow \sum_{t=1}^{T} \Delta CO_{2,t}$
6: **return** $\Delta CO_{2,t}$, $\Delta CO_{2,\mathrm{total}}$

D.6 Break-Even Year

1: $S_{\mathrm{acum}} \leftarrow 0$
2: **for** $t = 1$ **to** T **do**
3: $\quad S_{\mathrm{acum}} \leftarrow S_{\mathrm{acum}} + \Delta EF_t \cdot E_{\mathrm{util}} \cdot P_{\mathrm{CO_2},t} \cdot df_t - (C_{2,\mathrm{bio},t} + C_{2,\mathrm{H_2},t}) \cdot df_t$
4: $\quad$ **if** $S_{\mathrm{acum}} \geq 0$ **then**
5: $\quad\quad$ **return** year $t + 2025$ as break-even
6: $\quad$ **end if**
7: **end for**
8: **return** `None`

Key outputs:

- NPV [€], corresponding to the net economic value of GO procurement relative to $B0$.
- $LCDE$ [€/MWh], corresponding to the total discounted cost per unit of useful energy delivered.
- CAC [€/tCO_2], corresponding to the net cost per tonne of CO_2 legally avoided relative to $B0$ [63].
- $\Delta CO_{2,\mathrm{total}}$ [$ktCO_2$], corresponding to cumulative avoided emissions over the 20-year horizon on a book-and-claim basis.

Appendix E– Monte Carlo Computational Implementation

E.1 GBM Carbon Price Path Generation

Require: $P_0 = 65$ EUR/tCO$_2$, $\mu = 5\%$/yr, $\sigma = 35\%$/yr, floor $= 30$, cap $= 200$ EUR/tCO$_2$
Ensure: Stochastic price path $\{P_{\mathrm{CO}_2,t}\}_{t=1}^{T}$

$d \leftarrow \mu - \frac{1}{2}\sigma^2$
$P \leftarrow P_0$
for $t = 1$ **to** T **do**
    $\varepsilon_t \sim \mathcal{N}(0,1)$
    $P \leftarrow P \cdot \exp(d + \sigma\,\varepsilon_t)$
    $P_{\mathrm{CO}_2,t} \leftarrow \min(\max(P,\ \text{floor}),\ \text{cap})$
end for
return $\{P_{\mathrm{CO}_2,t}\}_{t=1}^{T}$

E.2 Per-Iteration OPEX and Decision Logic

for each year t **do**
    $P_{\mathrm{CO}_2,t} \leftarrow$ GBM path from E.1
    $p_{\mathrm{GO,bio},t} \leftarrow$ scenario trajectory ($S1, S2,$ or $S3$)
    $p_{\mathrm{GO},\mathrm{H}_2,t} \leftarrow$ central trajectory
    $\lambda_{\mathrm{bio},t} \leftarrow p_{\mathrm{GO,bio},t}/(EF_{\mathrm{GN}} - EF_{\mathrm{bio}})$
    $\lambda_{\mathrm{H}_2,t} \leftarrow p_{\mathrm{GO},\mathrm{H}_2,t}/(EF_{\mathrm{GN}} - EF_{\mathrm{H}_2})$
    if $P_{\mathrm{CO}_2,t} \geq \lambda_{\mathrm{H}_2,t}$ **then**
        $\alpha_{\mathrm{H}_2,t} \leftarrow \alpha_{\mathrm{H}_2,\max}$
    else
        $\alpha_{\mathrm{H}_2,t} \leftarrow \alpha_{\mathrm{H}_2,\min}$
    end if
    if $P_{\mathrm{CO}_2,t} \geq \lambda_{\mathrm{bio},t}$ **then**
        $\alpha_{\mathrm{bio},t} \leftarrow \min(1 - \alpha_{\mathrm{H}_2,t},\ 1.0)$
    else
        $\alpha_{\mathrm{bio},t} \leftarrow \alpha_{\mathrm{bio,min},t}$
    end if
    $C_{1,t} \leftarrow E_{\mathrm{annual}} \cdot p_{\mathrm{GN},t}$
    $C_{2,t} \leftarrow \alpha_{\mathrm{bio},t} \cdot E_{\mathrm{util}} \cdot p_{\mathrm{GO,bio},t} + \alpha_{\mathrm{H}_2,t} \cdot E_{\mathrm{util}} \cdot p_{\mathrm{GO},\mathrm{H}_2,t}$
    $C_{3,t} \leftarrow \max(0,\ E_{\mathrm{util}} \cdot EF_{\mathrm{legal},t} - A_{\mathrm{free},t}) \cdot P_{\mathrm{CO}_2,t}$
    $OPEX_t \leftarrow C_{1,t} + C_{2,t} + C_{3,t}$
end for

22: **return** $\{OPEX_t,\ \alpha_{\text{bio},t},\ \alpha_{\text{H}_2,t},\ EF_{\text{legal},t}\}$

E.3 Main Monte Carlo Loop

Require: $n = 10{,}000$ iterations, scenarios $\{S_1, S_2, S_3\}$, seed $= 42$

▷ Sole stochastic variable: $P_{\text{CO}_2,t}$ via GBM ($P_0 = 75.36$ €/t, $\mu = 5\%$, $\sigma = 35\%$, floor=30, cap=200)

▷ $p_{\text{GO,bio},t}$ deterministic per scenario; $p_{\text{GO,H}_2,t}$ single central trajectory

for scenario $s \in \{S_1, S_2, S_3\}$ **do**

  for iteration $k = 1$ **to** n **do**

    $\{P_{\text{CO}_2,t}\}_{t=1}^{T} \leftarrow$ `sortear_co2`()

    $\{OPEX_t\} \leftarrow$ `opex_ano_mc`() for all t

    $NPV_k \leftarrow \sum_{t=1}^{T} [\Delta EF_t \cdot E_{\text{util}} \cdot P_{\text{CO}_2,t} - C_{2,t}] \cdot df_t$

    $CAC_k \leftarrow \Delta OPEX_{\text{PV},k} / \Delta CO_{2,\text{PV},k}$

    $\Delta CO_{2,k} \leftarrow \sum_{t=1}^{T} \Delta EF_t \cdot E_{\text{util}}$

    Store NPV_k, CAC_k, $\Delta CO_{2,k}$

  end for

  $NPV_{P10}, NPV_{P50}, NPV_{P90} \leftarrow$ percentiles of $\{NPV_k\}$

  $P(\text{NPV} > 0) \leftarrow |\{k : NPV_k > 0\}|/n$

  $P(\text{rational}) \leftarrow |\{k : \exists\, t \mid P_{\text{CO}_2,t} \geq \lambda_{\text{bio},t}\}|/n$

  $\Delta CO_{2,P50} \leftarrow \text{median}\{\Delta CO_{2,k}\}$

end for

return distributions per scenario

Key design decisions:

- $P_{\text{CO}_2,t}$ is the sole stochastic variable. Biomethane GO premium trajectories and green hydrogen costs are deterministic per scenario, with uncertainty captured through scenario contrast rather than stochastic sampling.
- Free allowances $A_{\text{free},t}$ follow the deterministic CBAM phase-out schedule in both the investment scenario and Baseline $B0$, cancelling in the incremental NPV.
- The procurement decision switches between mandatory minimum and maximum voluntary coverage when $P_{\text{CO}_2,t}$ crosses $\lambda_{\text{bio},t}$ or $\lambda_{\text{H}_2,t}$, consistent with the annual spot assumption of Section 3.8.

Appendix F– EU ETS EUA Annual Volatility Statistics

Historical EUA Price Evolution

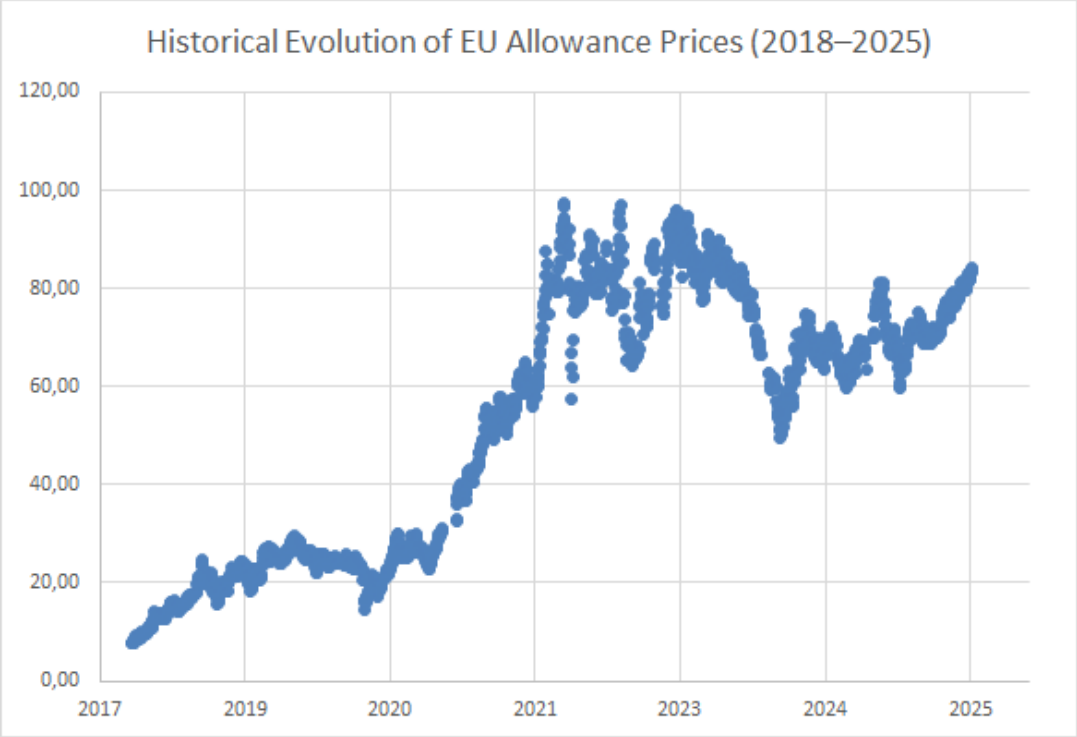


Figure F.1: Historical evolution of EU Allowance prices between 2018 and 2025, based on the daily closing-price series used for the estimation of annualised carbon-price volatility.

Annual EUA Price Statistics and Realised Volatility

Table F.1: Annual EU ETS EUA price statistics and realised volatility from 2018 to 2025 [87].

Year	N	**Mean** [**EUR/tCO$_2$**]	**Minimum** [**EUR/tCO$_2$**]	**Maximum** [**EUR/tCO$_2$**]	$\hat{\sigma}_{\text{annual}}$ [%]
2018	207	15.6	7.7	24.9	55.1
2019	214	24.7	18.3	29.4	43.2
2020	215	24.3	14.5	30.9	58.6
2021	229	54.1	32.6	87.5	39.6
2022	218	80.0	57.5	97.3	55.9
2023	222	83.4	66.4	95.9	32.2
2024	220	64.5	49.5	74.8	36.8
2025	212	73.3	59.7	84.3	28.0

N denotes the number of inter-auction observations available for each year. Annualised realised volatility is calculated from EUA auction settlement price log returns according to Equation 4.5

Appendix G– Deterministic Scenario Outputs

Scenario S_1

S1 — Mercado nascente (90 €/MWh) | Cruzamento: ~2039 | NPV(2045): +535 k€ | ΔCO₂: 568 ktCO₂													
Ano	p_gas €/MWh	p_GO,bio €/MWh	λ_bio €/tCO₂	P_CO₂ €/tCO₂	α_bio% %	α_H₂% %	C2_bio k€/yr	C2_H₂ k€/yr	ΔC3 k€/yr	Poup k€/yr	NPV_cum k€	ΔCO₂ tCO₂/yr	Status
2026	45,0	45,0	247	75,4	0,0	0,0	0	0	0	0	0	0	min
2027	46,4	43,7	240	79,2	1,3	0,0	213	0	70	-142	-132	887	min
2028	47,7	42,3	232	83,3	1,3	1,3	209	380	155	-435	-505	1 856	min
2029	49,2	40,8	224	87,6	2,6	1,3	401	373	240	-534	-929	2 743	min
2030	50,6	39,4	216	92,0	3,9	1,3	578	366	334	-611	-1 378	3 630	min
2031	52,2	37,8	208	96,8	5,4	1,3	775	359	453	-681	-1 841	4 683	min
2032	53,7	36,3	199	101,7	4,8	3,4	663	937	597	-1 003	-2 473	5 873	min
2033	55,3	34,7	190	106,9	6,3	3,4	834	917	741	-1 010	-3 063	6 926	min
2034	57,0	33,0	181	112,4	7,8	3,4	985	896	897	-984	-3 594	7 980	min
2035	58,7	31,3	172	118,2	7,9	4,8	944	1 248	1 079	-1 113	-4 151	9 126	min
2036	60,5	29,5	162	124,2	9,4	4,8	1 061	1 216	1 265	-1 012	-4 620	10 180	min
2037	62,3	27,7	152	130,6	5,0	10,8	523	2 661	1 518	-1 667	-5 335	11 622	min
2038	64,2	25,8	142	137,3	6,5	10,8	638	2 584	1 740	-1 482	-5 923	12 675	min
2039	66,1	23,9	131	144,4	89,2	10,8	8 124	2 505	10 106	-523	-6 115	70 005	VOL✓
2040	68,1	21,9	121	151,8	89,2	10,8	7 450	2 424	10 624	750	-5 860	70 005	VOL✓
2041	70,1	19,9	109	159,5	89,2	10,8	6 757	2 340	11 168	2 072	-5 207	70 005	VOL✓
2042	72,2	17,8	98	167,7	89,2	10,8	6 042	2 253	11 741	3 446	-4 201	70 005	VOL✓
2043	74,4	15,6	86	176,3	89,2	10,8	5 306	2 164	12 343	4 872	-2 884	70 005	VOL✓
2044	76,6	13,4	74	185,4	89,2	10,8	4 548	2 072	12 976	6 355	-1 294	70 005	VOL✓
2045	78,9	11,1	61	194,9	89,2	10,8	3 768	1 978	13 641	7 895	535	70 005	VOL✓
TOTAL 20yr							49 820	27 675			535	568 215	

Figure G.1: Annual deterministic outputs for Scenario S_1.

Scenario S_2

S2 — Mercado em desenvolvimento (75 €/MWh) | Cruzamento: ~2034 | NPV(2045): +18450 k€ | ΔCO₂: 865 ktCO₂													
Ano	p_gas €/MWh	p_GO,bio €/MWh	λ_bio €/tCO₂	P_CO₂ €/tCO₂	α_bio% %	α_H₂% %	C2_bio k€/yr	C2_H₂ k€/yr	ΔC3 k€/yr	Poup k€/yr	NPV_cum k€	ΔCO₂ tCO₂/yr	Status
2026	45,0	30,0	165	75,4	0,0	0,0	0	0	0	0	0	0	min
2027	46,4	28,7	157	79,2	1,3	0,0	140	0	70	-69	-64	887	min
2028	47,7	27,3	150	83,3	1,3	1,3	135	380	155	-361	-373	1 856	min
2029	49,2	25,8	142	87,6	2,6	1,3	254	373	240	-387	-681	2 743	min
2030	50,6	24,4	134	92,0	3,9	1,3	358	366	334	-390	-967	3 630	min
2031	52,2	22,8	125	96,8	5,4	1,3	468	359	453	-374	-1 222	4 683	min
2032	53,7	21,3	117	101,7	4,8	3,4	389	937	597	-729	-1 681	5 873	min
2033	55,3	19,7	108	106,9	6,3	3,4	473	917	741	-649	-2 060	6 926	min
2034	57,0	18,0	99	112,4	96,6	3,4	6 622	896	7 816	298	-1 899	69 523	VOL✓
2035	58,7	16,3	89	118,2	95,2	4,8	5 904	1 248	8 228	1 076	-1 360	69 616	VOL✓
2036	60,5	14,5	80	124,2	95,2	4,8	5 265	1 216	8 650	2 169	-356	69 616	VOL✓
2037	62,3	12,7	70	130,6	89,2	10,8	4 317	2 661	9 144	2 166	573	70 005	VOL✓
2038	64,2	10,8	60	137,3	89,2	10,8	3 682	2 584	9 613	3 346	1 901	70 005	VOL✓
2039	66,1	8,9	49	144,4	89,2	10,8	3 029	2 505	10 106	4 572	3 582	70 005	VOL✓
2040	68,1	6,9	38	151,8	89,2	10,8	2 355	2 424	10 624	5 845	5 572	70 005	VOL✓
2041	70,1	4,9	27	159,5	89,2	10,8	1 662	2 340	11 168	7 167	7 832	70 005	VOL✓
2042	72,2	2,8	15	167,7	89,2	10,8	947	2 253	11 741	8 541	10 325	70 005	VOL✓
2043	74,4	0,6	3	176,3	89,2	10,8	211	2 164	12 343	9 968	13 019	70 005	VOL✓
2044	76,6	0,0	0	185,4	89,2	10,8	0	2 072	12 976	10 903	15 747	70 005	VOL✓
2045	78,9	0,0	0	194,9	89,2	10,8	0	1 978	13 641	11 663	18 450	70 005	VOL✓
TOTAL 20yr							36 210	27 675			18 450	865 397	

Figure G.2: Annual deterministic outputs for Scenario S_2.

Scenario S_3

S3 — Referência Portaria 15/2023 (62 €/MWh) | Cruzamento: ~2028 | NPV(2045): +41864 k€ | ΔCO₂: 1256 ktCO₂													
Ano	p_gas €/MWh	p_GO,bio €/MWh	λ_bio €/tCO₂	P_CO₂ €/tCO₂	α_bio% %	α_H₂% %	C2_bio k€/yr	C2_H₂ k€/yr	ΔC3 k€/yr	Poup k€/yr	NPV_cum k€	ΔCO₂ tCO₂/yr	Status
2026	45,0	17,0	93	75,4	0,0	0,0	0	0	0	0	0	0	min
2027	46,4	15,7	86	79,2	1,3	0,0	76	0	70	-6	-6	887	min
2028	47,7	14,3	78	83,3	98,7	1,3	5 362	380	5 779	37	26	69 387	VOL✓
2029	49,2	12,8	70	87,6	98,7	1,3	4 823	373	6 075	879	724	69 387	VOL✓
2030	50,6	11,4	62	92,0	98,7	1,3	4 268	366	6 387	1 752	2 012	69 387	VOL✓
2031	52,2	9,8	54	96,8	98,7	1,3	3 697	359	6 714	2 658	3 821	69 387	VOL✓
2032	53,7	8,3	45	101,7	96,6	3,4	3 043	937	7 072	3 092	5 769	69 523	VOL✓
2033	55,3	6,7	37	106,9	96,6	3,4	2 449	917	7 435	4 069	8 143	69 523	VOL✓
2034	57,0	5,0	27	112,4	96,6	3,4	1 838	896	7 816	5 082	10 889	69 523	VOL✓
2035	58,7	3,3	18	118,2	95,2	4,8	1 191	1 248	8 228	5 789	13 785	69 616	VOL✓
2036	60,5	1,5	8	124,2	95,2	4,8	552	1 216	8 650	6 881	16 972	69 616	VOL✓
2037	62,3	0,0	0	130,6	89,2	10,8	0	2 661	9 144	6 483	19 752	70 005	VOL✓
2038	64,2	0,0	0	137,3	89,2	10,8	0	2 584	9 613	7 028	22 544	70 005	VOL✓
2039	66,1	0,0	0	144,4	89,2	10,8	0	2 505	10 106	7 600	25 338	70 005	VOL✓
2040	68,1	0,0	0	151,8	89,2	10,8	0	2 424	10 624	8 200	28 130	70 005	VOL✓
2041	70,1	0,0	0	159,5	89,2	10,8	0	2 340	11 168	8 829	30 913	70 005	VOL✓
2042	72,2	0,0	0	167,7	89,2	10,8	0	2 253	11 741	9 488	33 682	70 005	VOL✓
2043	74,4	0,0	0	176,3	89,2	10,8	0	2 164	12 343	10 179	36 433	70 005	VOL✓
2044	76,6	0,0	0	185,4	89,2	10,8	0	2 072	12 976	10 903	39 162	70 005	VOL✓
2045	78,9	0,0	0	194,9	89,2	10,8	0	1 978	13 641	11 663	41 864	70 005	VOL✓
TOTAL 20yr							27 300	27 675			41 864	1 256 281	

Figure G.3: Annual deterministic outputs for Scenario S_3.

Appendix H– Extended Scenario: Technical and Economic Assumptions

H.1 - In-situ Scenario Parameters

Table H.1: Technical and economic parameters adopted in the extended scenario.

Parameter	Value	Source
Electrolyser technology	PEM	[109, 110]
Electrolyser efficiency, η_{elec}	70% (LHV)	[109]
Electrolyser CAPEX	1,200 EUR/kW	[109, 111, 112]
Electrolyser power	5.0 MW	Derived H.5
Total electrolyser CAPEX	6.00 MEUR	Derived H.6
O&M extra cost	3% of CAPEX/yr	[16]
Renewable electricity price (PPA)	45 EUR/MWh	[113, 114]
Combustion retrofit — in-situ pathway	L3 - 586 kEUR	Section 4.2.1
Combustion retrofit — network pathway	L1 - 117 kEUR	Section 4.2.1
Hydrogen energy share in P_3	5.96% of E_{annual}	Derived H.2
Electrolyser installation year	2037	Assumed
$p_{\text{total,H}_2}$ (Initial)	127 EUR/MWh	Section 3.7
Sensitivity variable	Annual decline of $p_{\text{total,H}_2}$	0–8%/yr
WACC	8%	Section 4.2.2
Planning horizon	2026–2045	Section 4.2.2
Biomethane Scenario	S_2 (75 EUR/MWh)	Section 4.2.3

H.2 - Derived Sizing Calculations

$$x_{\mathrm{H}_2,P3} = 0.18 \tag{H.1}$$

$$f_{\mathrm{H}_2} = \frac{x_{\mathrm{H}_2,P3} \cdot LHV_{\mathrm{H}_2}}{LHV_{\mathrm{mix},P3}} = \frac{0.18 \times 10.80}{32.60} \approx 0.0596 = 5.96\% \tag{H.2}$$

$$E_{\mathrm{H}_2} = E_{\mathrm{annual}} \cdot f_{\mathrm{H}_2} = 448{,}000 \times 0.0596 \approx 26{,}715 \text{ MWh/yr} \tag{H.3}$$

$$E_{\mathrm{elec}} = \frac{E_{\mathrm{H}_2}}{\eta_{\mathrm{elec}}} = \frac{26{,}715}{0.70} \approx 38{,}164 \text{ MWh/yr} \tag{H.4}$$

$$P_{\mathrm{elec}} = \frac{E_{\mathrm{elec}} \cdot 10^3}{CF \cdot 8760} = \frac{38{,}164 \times 10^3}{0.872 \times 8760} \approx 4{,}996 \text{ kW} \approx 5.0 \text{ MW} \tag{H.5}$$

$$CAPEX_{\mathrm{elec}} = P_{\mathrm{elec}} \cdot c_{\mathrm{elec}} = 4{,}996 \text{ kW} \times 1{,}200 \text{ EUR/kW} \approx 6.00 \text{ MEUR} \tag{H.6}$$

$$OM_{\mathrm{elec}} = f_{\mathrm{OM}} \cdot CAPEX_{\mathrm{elec}} = 0.03 \times 6.00 \text{ MEUR} = 0.180 \text{ MEUR/yr} = 180 \text{ kEUR/yr} \tag{H.7}$$

Additional O&M costs are represented by an annual allowance equal to 3% of electrolyser CAPEX [16]. This allowance covers routine maintenance, membrane servicing, labour, and ancillary operational requirements not modelled separately.

For the considered in-situ production scale, process water demand is approximately 7,000–8,000 m^3/year. Site-specific elements, such as water supply, compression, buffer storage, grid connection, stack replacement, safety and permitting, and internal pipework adaptations, are not individually costed. These elements are treated as engineering-dependent boundary conditions requiring detailed site-level assessment.

H.3 - Sensitivity Analysis Computational Implementation

Require: Decline rates $g \in \{0\%, 0.5\%, \ldots, 8\%\}$; fixed parameters from Table H.1; design H_2 energy fraction f_{des}; model inputs from Sections 4.2.3 and 4.2.4

Ensure: $\Delta LCDE(g)$ for each decline rate g

Compute fixed CAPEX differential:
$\Delta CAPEX_{PV} \leftarrow (CAPEX_{\text{elec}} + CAPEX_{L3} - CAPEX_{L1}) \cdot DF_{2037}$
for each decline rate g **do**
    $\Delta OPEX_{PV} \leftarrow 0$
    for each year $t \in \{2026, \ldots, 2045\}$ **do**
        $p_{\text{total},H_2}(t) \leftarrow 127 \cdot (1-g)^{t-2026}$
        $p_{\text{GO},H_2,t} \leftarrow \max(p_{\text{total},H_2}(t) - p_{\text{gas},t},\ 0)$
    // Network pathway
        $\alpha_{H_2,r} \leftarrow \texttt{quota_min_rfnbo}(t, x_{H_2,\text{rede}})$
        $\alpha_{\text{bio},r} \leftarrow \max(0,\ \texttt{quota_min_art22}(t) - \alpha_{H_2,r})$
        $\Delta EF_r \leftarrow \alpha_{\text{bio},r}(EF_{\text{GN}} - EF_{\text{bio}}) + \alpha_{H_2,r}(EF_{\text{GN}} - EF_{H_2})$
        $C_{2,H_2,r} \leftarrow E_{\text{util}} \cdot \alpha_{H_2,r} \cdot p_{\text{GO},H_2,t}$
        $C_{3,r} \leftarrow \max(0,\ E_{\text{util}}(EF_{\text{GN}} - \Delta EF_r) - FA_t) \cdot P_{CO_2,t}$
    // In-situ pathway
        if $t \geq 2037$ **then**
            $\alpha_{H_2,i} \leftarrow f_{\text{des}}$
            $ppa_om_t \leftarrow E_{\text{elec}} \cdot p_{\text{PPA}} + OM_{\text{elec}}$
            $poup_gas_t \leftarrow E_{H_2} \cdot p_{\text{gas},t}$
        else
            $\alpha_{H_2,i} \leftarrow 0$
            $ppa_om_t \leftarrow 0;\ poup_gas_t \leftarrow 0$
        end if
        $\alpha_{\text{bio},i} \leftarrow \max(0,\ \min(\texttt{quota_min_art22}(t) - \alpha_{H_2,i},\ 1 - \alpha_{H_2,i}))$
        $\Delta EF_i \leftarrow \alpha_{\text{bio},i}(EF_{\text{GN}} - EF_{\text{bio}}) + \alpha_{H_2,i}(EF_{\text{GN}} - EF_{H_2})$
        $C_{2,H_2,i} \leftarrow 0$
        $C_{3,i} \leftarrow \max(0,\ E_{\text{util}}(EF_{\text{GN}} - \Delta EF_i) - FA_t) \cdot P_{CO_2,t}$
    // Incremental OPEX
        $\Delta OPEX_t \leftarrow (C_{2,H_2,i} - C_{2,H_2,r}) + (C_{3,i} - C_{3,r}) + ppa_om_t - poup_gas_t$
        $\Delta OPEX_{PV} \leftarrow \Delta OPEX_{PV} + \Delta OPEX_t \cdot DF_t$
    end for
    $\Delta LCDE(g) \leftarrow (\Delta CAPEX_{PV} + \Delta OPEX_{PV})/E_{\text{util,PV}}$
end for
Identify break-even g^* by linear interpolation where $\Delta LCDE(g^*) = 0$
return $\{\Delta LCDE(g)\},\ g^*$

Appendix I– Network Injection Perspectives and Deployment Gaps

This appendix reproduces the principal results of the companion study to this dissertation, which was developed from a network-level perspective to assess renewable gas integration trajectories and their implications for the gas distribution system. Put another way, this study estimates the renewable gas injection gap in the Portuguese industrial gas network under alternative biomethane deployment trajectories and hydrogen subscenarios, assessed against the RED III Article 22 minimum industrial renewable-energy obligation.

Three biomethane trajectories are considered. Trajectory C^{-} uses the 0.546 TWh/yr of registered capacity accumulated by 2026 under DL 62/2020 as the maximum deliverable volume in the absence of further policy intervention. It therefore represents a **lower-bound supply case** under policy continuity. Trajectory C^{0} reflects the phased industrial incorporation industrial obligations announced under the PAB in April 2026, namely 1.5% in 2027, 3.0% in 2028, 6.0% in 2029, and 9.0% in 2030 [79]. This trajectory represents a **demand-side** mandate rather than a direct projection of available supply. Trajectory C^{+} assumes full achievement of the PAB 2030 and 2040 **supply targets**, equal to 2.720 TWh/yr and 5.570 TWh/yr, respectively, supported by an instrument with adequate tariff sufficiency, contract horizon, and temporal antecedence.

Two hydrogen subscenarios are also included. For example, Subscenario H_2B follows the conservative RMSA-G 2024 planning fractions,

$$\alpha^{B}_{\mathrm{H_2},t}: \ 0\%\ (2025) \rightarrow 5\%\ (2030) \rightarrow 7.5\%\ (2035) \rightarrow 10\%\ (2040), \tag{I.1}$$

capped at the currently certified 10% transmission-network blending limit. Subscenario H_2A defines an upper-bound pathway in which the transmission-network trajectory converges towards the 20% threshold certified for the distribution network [76]. Injectable hydrogen energy available to the industrial sector is calculated using Equation I.2.

$$E_{\mathrm{H_2},t} = C_{\mathrm{ind},t} \cdot \alpha_{\mathrm{H_2},t} \cdot \frac{LHV_{\mathrm{H_2}}}{LHV_{\mathrm{GN}}} \qquad [\mathrm{TWh/yr}] \tag{I.2}$$

Hydrogen is represented as an additive component above each biomethane trajectory. This allows the relative contribution of biomethane and hydrogen to be distinguished visually, while also making the remaining compliance gap clear for each trajectory-subscenario combination.

I.1 – Injection Capacity vs RED III Obligation

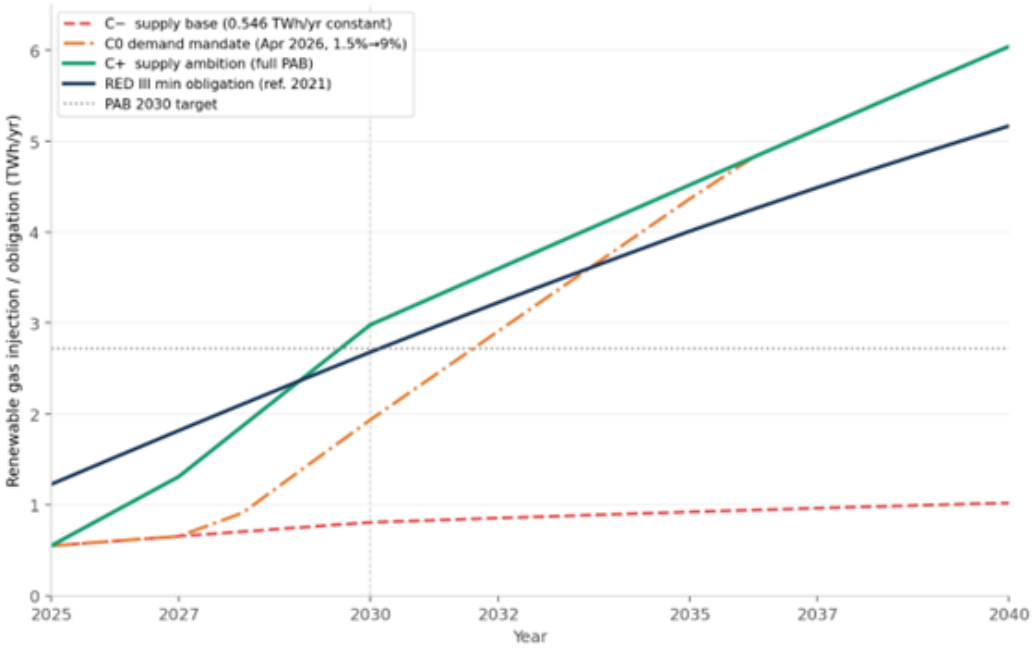


Figure I.1: Injection capacity vs RED III minimum obligation, H_2B subcenario.

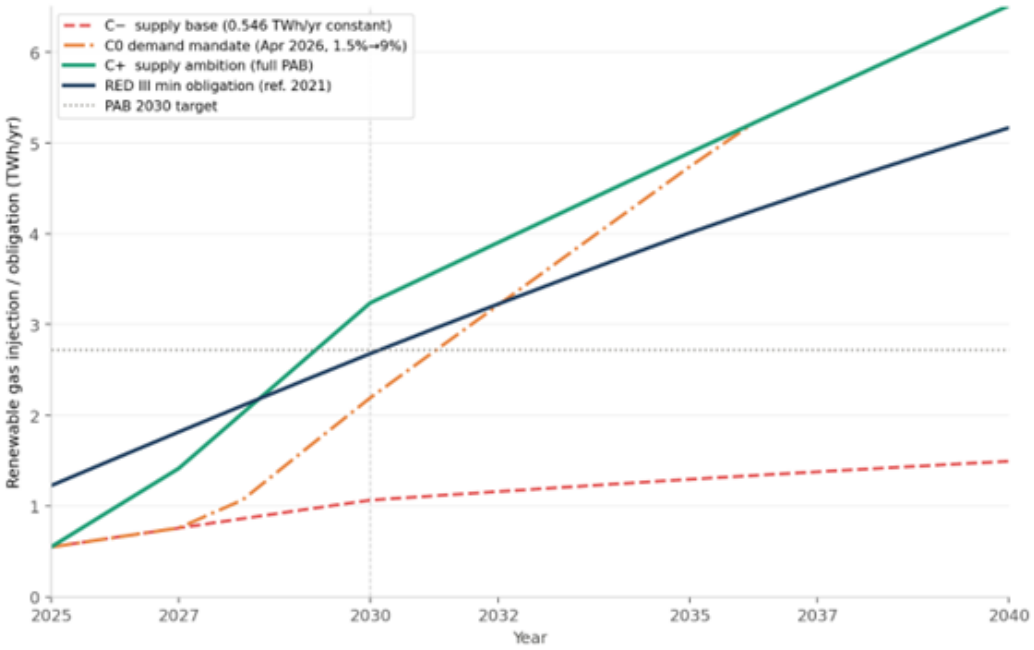


Figure I.2: Injection capacity vs RED III minimum obligation, H_2A subcenario.

I.2 – Supply-Demand Gap Decomposition

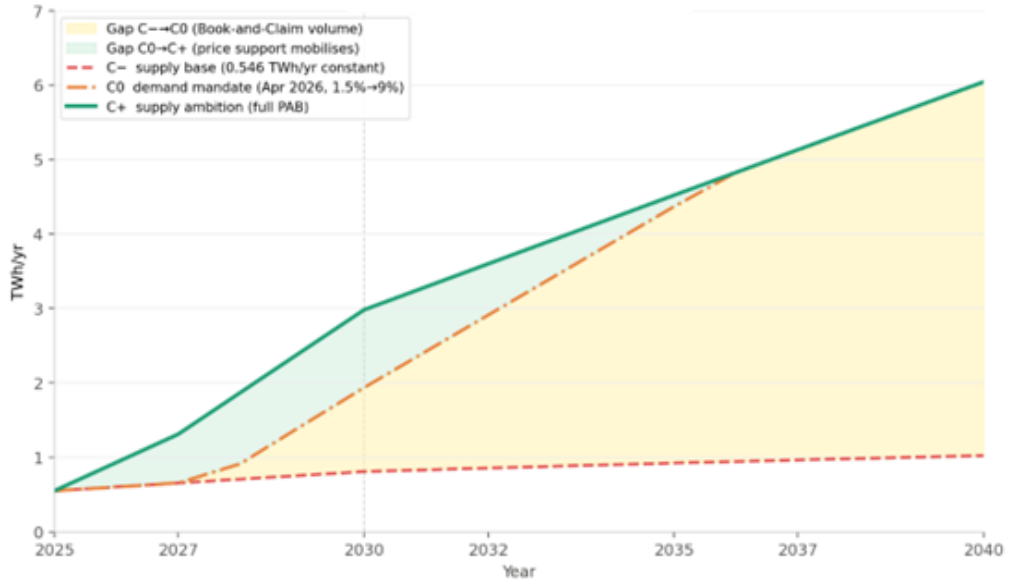


Figure I.3: Supply-demand gap decomposition, H_2B subcenario.

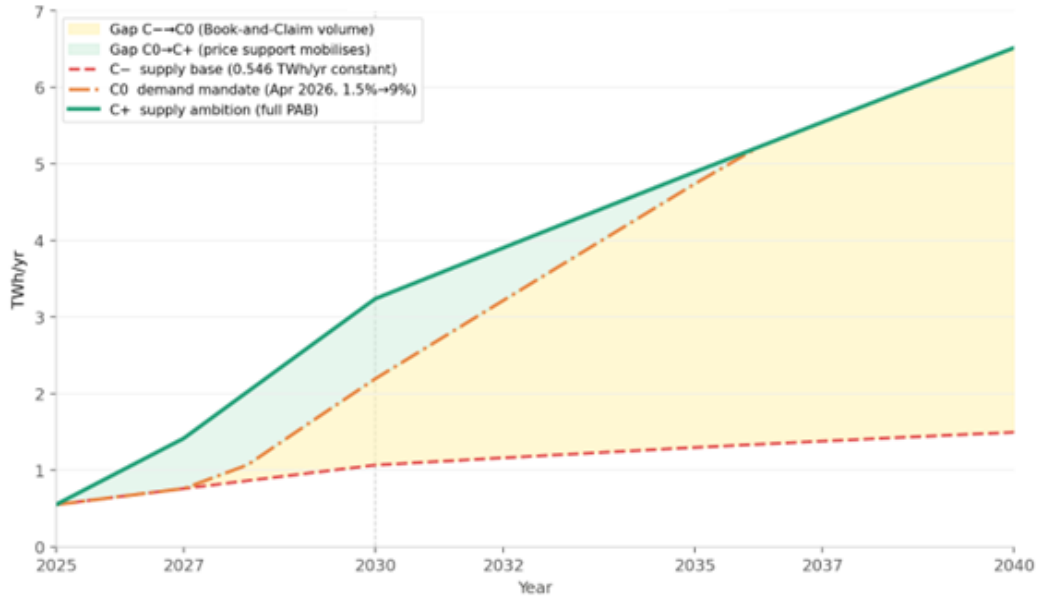


Figure I.4: Supply-demand gap decomposition, H_2A subcenario.

I.3 – Compliance Gap Summary

Four structural patterns emerge consistently from the gap analysis summarised in Figure I.5, remaining robust across all demand-scenario combinations:

- **Trajectory C^+ closes the minimum RED III compliance gap.** Across all scenario combinations and compliance horizons, C^+ is sufficient to meet the minimum obligation, provided that the PAB 2030 and 2040 injection targets are fully materialised through an effective price-support instrument.
- **Trajectory C^0 closes the gap by 2035, but not by 2030.** Under both hydrogen subscenarios, C^0 closes the minimum gap by 2035 across all demand scenarios. In 2030, however, a residual gap of 0.47 to 0.77 TWh/yr remains, depending on the hydrogen subscenario.
- **Trajectory C^- never closes the minimum gap.** Under all scenario and hydrogen-subscenario combinations, C^- remains insufficient. The gap reaches 1.56 to 1.95 TWh/yr in 2030 and continues to increase as the RED III obligation accumulates.
- **Biomethane deployment is the dominant uncertainty.** Results are driven more strongly by the biomethane deployment trajectory than by industrial demand projections. For a given biomethane trajectory and hydrogen subscenario, the spread across the four RMSA-G 2024 demand scenarios remains below 0.15 TWh at the 2030 horizon.

Scenario	H_2	Obligation (TWh)	C– 2030	C^0 2030	C+ 2030	C– 2035	C^0 2035	C+ 2035	C– 2040	C^0 2040	C+ 2040
Central Ambition	H2B	2.68	1.87	0.75	0.00	3.09	0.00	0.00	4.15	0.00	0.00
	H2A	2.68	1.61	0.49	0.00	2.72	0.00	0.00	3.68	0.00	0.00
Central Conservative	H2B	2.69	1.89	0.75	0.00	3.17	0.00	0.00	4.34	0.00	0.00
	H2A	2.69	1.63	0.49	0.00	2.79	0.00	0.00	3.85	0.00	0.00
Supply Ambition	H2B	2.77	1.95	0.77	0.00	3.29	0.00	0.00	4.56	0.00	0.00
	H2A	2.77	1.68	0.50	0.00	2.90	0.00	0.00	4.05	0.00	0.00
Inferior Conservative	H2B	2.61	1.81	0.72	0.00	2.97	0.00	0.00	3.96	0.00	0.00
	H2A	2.61	1.56	0.47	0.00	2.61	0.00	0.00	3.50	0.00	0.00

Figure I.5: Compliance gap summary at key horizons [TWh/yr].

References

[1] Ana Maria Fagetan. Transposition and implementation of european union renewable energy legislation in france, italy, and germany: A regulatory perspective and a comprehensive analysis of opportunities and challenges. *Licensee MDPI, Basel, Switzerland*, 15:3, 12 2025. ISSN 2075471X. doi: 10.3390/laws15010003. URL https://doi.org/10.3390/laws15010003.

[2] European Commission. Repowereu plan. Technical Report COM(2022) 230 final, European Commission, 2022.

[3] European Parliament and the Council of the European Union. Directive (ue) 2023/2413 of the european parliament. *Official Journal of the European Union, Series L*, 10 2023. URL https://eur-lex.europa.eu/eli/dir/2023/2413/oj. RED III.

[4] Silvia Madeddu, Falko Ueckerdt, Michaja Pehl, Juergen Peterseim, Michael Lord, Karthik Ajith Kumar, Christoph Krüger, and Gunnar Luderer. The CO2 reduction potential for the european industry via direct electrification of heat supply (power-to-heat). *Environmental Research Letters*, 15(12):124004, 2020. doi: 10.1088/1748-9326/abbd02. URL https://doi.org/10.1088/1748-9326/abbd02.

[5] Jörg Leicher, Anne Giese, and Christoph Wieland. Electrification or hydrogen? the challenge of decarbonizing industrial (high-temperature) process heat. *J*, 7(4):439–456, 2024. doi: 10.3390/j7040026. URL https://doi.org/10.3390/j7040026.

[6] Michael Zier, Noah Pflugradt, Peter Stenzel, Leander Kotzur, and Detlef Stolten. Industrial decarbonization pathways: The example of the german glass industry. *Energy Conversion and Management: X*, 17, 1 2023. ISSN 25901745. doi: 10.1016/j.ecmx.2022.100336.

[7] Filipe M. Quintino, Nuno Nascimento, and Edgar C. Fernandes. Aspects of hydrogen and biomethane introduction in natural gas infrastructure and equipment. *Hydrogen (Switzerland)*, 2:301–318, 9 2021. ISSN 26734141. doi: 10.3390/hydrogen2030016.

[8] Lucideon (via American Ceramic Society Bulletin). Hydrogen firing: Uk's lucideon works with ceramics industry on hydrogen-firing trials. Technical report, American Ceramic Society Bulletin, 4 2023. URL www.ceramics.org/ceramicandglassmanufacturingwww.ceramics.org/ceramicandglassmanufacturing.

[9] Alexander Shkarovskiy, Anatolii Koliienko, and Vitalii Turchenko. Interchangeability and standardization of the parameters of combustible gases when using hydrogen. *Architecture and Engineering*, 7:33–45, 2022. ISSN 25000055. doi: 10.23968/2500-0055-2022-7-1-33-45.

[10] Jeffrey Rissman, Chris Bataille, Eric Masanet, Nate Aden, William R. Morrow, Nan Zhou, Neal Elliott, Rebecca Dell, Niko Heeren, Brigitta Huckestein, Joe Cresko, Sabbie A. Miller, Joyashree Roy, Paul Fennell, Betty Cremmins, Thomas Koch Blank, David Hone, Ellen D.

Williams, Stephane de la Rue du Can, Bill Sisson, Mike Williams, John Katzenberger, Dallas Burtraw, Girish Sethi, He Ping, David Danielson, Hongyou Lu, Tom Lorber, Jens Dinkel, and Jonas Helseth. Technologies and policies to decarbonize global industry: Review and assessment of mitigation drivers through 2070, 5 2020. ISSN 03062619.

[11] Alessandro Franco and Michele Rocca. Industrial decarbonization through blended combustion of natural gas and hydrogen. *Hydrogen*, 5(3):519–539, 2024. doi: 10.3390/hydrogen5030029. URL https://doi.org/10.3390/hydrogen5030029.

[12] Alessandro Franco. Green hydrogen and the energy transition: Hopes, challenges, and realistic opportunities. *Hydrogen*, 6:28, 2025.

[13] Felipe Solferini de Carvalho, Luiz Carlos Bevilaqua dos Santos Reis, Pedro Teixeira Lacava, Fernando Henrique Mayworm de Araújo, and João Andrade de Carvalho Jr. Substitution of natural gas by biomethane: Operational aspects in industrial equipment. *Energies*, 16(2): 839, 2023. doi: 10.3390/en16020839. URL https://doi.org/10.3390/en16020839.

[14] Domiziana Vespasiano, Antonio Sgaramella, Gianluigi Lo Basso, Livio de Santoli, and Lorenzo Mario Pastore. Hydrogen blending in natural gas grid: Energy, environmental, and economic implications in the residential sector. *Buildings*, 14(8):2284, 2024. doi: 10.3390/buildings14082284. URL https://doi.org/10.3390/buildings14082284.

[15] Carl Philipp Anke, Hannes Hobbie, Steffi Schreiber, and Dominik Möst. Coal phase-outs and carbon prices: Interactions between eu emission trading and national carbon mitigation policies. *Energy Policy*, 144, 9 2020. ISSN 03014215. doi: 10.1016/j.enpol.2020.111647.

[16] International Energy Agency (IEA). Global hydrogen review 2025. Technical report, International Energy Agency (IEA), 9 2025. URL https://www.iea.org/reports/global-hydrogen-review-2025.

[17] Mônica Valéria dos Santos Machado, João Andrade de Carvalho Jr, Ivonete Ávila, Andreas Nascimento, and Felipe Solferini de Carvalho. The substitution of natural gas with biomethane in an industrial fluidized bed sand drying process. *Energies*, 18(6):1364, 2025. doi: 10.3390/en18061364. URL https://doi.org/10.3390/en18061364.

[18] Direção-Geral das Atividades Económicas. Transposição da diretiva red iii. Destaque institucional, November 2024. URL https://www.dgae.gov.pt/comunicacao/destaques/transposicao-da-diretiva-red-iii-.aspx. Accessed: 2026-05-26.

[19] United Nations Industrial Development Organization and International Hydrogen Energy Centre. Global green hydrogen report: Strategic opportunities, market outlook, and case studies towards 2030. Technical report, UNIDO and IHEC, Vienna, Austria, 2024. URL https://www.unido.org. Accessed: 2026-06-01.

[20] Association of Issuing Bodies (AIB). Gos vs. voluntary energy attribute tracking schemes. Official Certification Guidance, AIB Website, 2026. URL https://www.aib-net.org/certification/gos-vs-voluntary-energy-attribute-certification-schemes. Accessed: June 2026. Analysis based on EECS Rules and EU Renewable Energy Directive (RED III).

[21] Matthias Edel, Flore Belin, Stefanie Königsberger, Andreas Wolf, Franz Keuschnig, Katrien Verwimp, Milenko Matosic, Katharina Sailer, Jakob Jegal, and Toni Reinholz. D4.2 technical and operational comparison of the biomethane/renewable gas go system and the electricity go system. Deliverable Report Grant Agreement No. 857796, REGATRACE Project Consortium, European Commission Horizon 2020, February 2021. URL https://www.ergar.org.

[22] Uniaõ Europeia. Parlamento Europeu e Conselho. Diretiva (UE) 2018/2001 do Parlamento Europeu e do Conselho, de 11 de dezembro de 2018, relativa à promoção da utilização de energia de fontes renováveis. URL http://data.europa.eu/eli/dir/2018/2001/oj.

[23] Diana Filipa da Rocha Reis. Produção de hidrogénio verde no contexto do mercado elétrico em portugal. Dissertação de mestrado integrado em engenharia eletrotécnica e de computadores, Faculdade de Engenharia da Universidade do Porto (FEUP), Porto, Portugal, Julho 2022. Disponível no Repositório Aberto da Universidade do Porto.

[24] European Commission. Guidance on the targets for the consumption of renewable fuels of non-biological origin in the industry and transport sectors. Communication from the Commission, C/2025/2983, 2025. URL https://eur-lex.europa.eu/eli/C/2025/2983/oj/eng. Guidance on Articles 22a, 22b and 25 of Directive (EU) 2018/2001, as amended by Directive (EU) 2023/2413.

[25] S&P Global Commodity Insights. Renewable gas tracking systems – Value of biomethane/RNG certificates. White paper / final report, S&P Global, Prepared for EBA, Eurogas, ERGAR and Coalition for Renewable Natural Gas, London, UK, October 2024. URL https://www.spglobal.com/commodityinsights. Support study for the revision of the Greenhouse Gas Protocol (GHGP).

[26] Semra Bakkaloglu and Adam Hawkes. A comparative study of biogas and biomethane with natural gas and hydrogen alternatives. *Energy & Environmental Science*, 17(4):1482–1499, 2024. doi: 10.1039/d3ee02516k. URL https://doi.org/10.1039/d3ee02516k.

[27] Uniaõ Europeia. Comissão Europeia. Regulamento Delegado (UE) 2023/1184 de 10 de fevereiro de 2023 que completa a Diretiva (UE) 2018/2001 do Parlamento Europeu e do Conselho estabelecendo uma metodologia da União que determina regras pormenorizadas aplicáveis à produção de combustíveis líquidos e gasosos renováveis de origem não biológica. URL http://data.europa.eu/eli/reg_del/2023/1184/oj.

[28] European Parliament and Council of the European Union. Directive (EU) 2023/959 of the european parliament and of the council of 10 may 2023 amending directive 2003/87/EC establishing a system for greenhouse gas emission allowance trading within the Union and decision (EU) 2015/1814 concerning the establishment and operation of a market stability reserve for the Union greenhouse gas emission trading system, May 2023. URL http://data.europa.eu/eli/dir/2023/959/oj.

[29] European Commission. Commission delegated regulation (eu) 2023/1185 of 10 february 2023 supplementing directive (eu) 2018/2001 of the european parliament and of the council by establishing a minimum threshold for greenhouse gas emissions savings of recycled carbon fuels and by specifying a methodology for assessing greenhouse gas emissions savings from renewable liquid and gaseous transport fuels of non-biological origin and from recycled carbon fuels. *Official Journal of the European Union, Series L 157*, 6 2023. URL https://eur-lex.europa.eu/eli/reg_del/2023/1185/oj.

[30] Arup. Arup guide to eu carbon legislation. Technical report, Arup, 1 2024. URL https://www.arup.com/globalassets/downloads/insights/arup-guide-to-eu-carbon-legislation.pdf.

[31] Long Chu, Thang Nam Do, Thi Ha Lien Le, Quoc Anh Ho, and Khoi Dang. Carbon border adjustment mechanism, carbon pricing, and within-sector shifts: A partial equilibrium

approach to vietnam's steel sector. *Energy Policy*, 193, 10 2024. ISSN 03014215. doi: 10.1016/j.enpol.2024.114293.

[32] Cecilia Bellora and Lionel Fontagné. Eu in search of a carbon border adjustment mechanism. *Energy Economics*, 123, 7 2023. ISSN 01409883. doi: 10.1016/j.eneco.2023.106673. URL https://doi.org/10.1016/j.eneeco.2023.106673.

[33] Onur Kodak, Farshid Sadeghi-Khaneghah, Alp Er Ş. Konukman, Levent Kılıç, Neşet Arzan, and Gürhan Dural. Energy usage in glass industry: past, today, and tomorrow. *Thermal Science and Engineering Progress*, 49:102450, 2024. doi: 10.1016/j.tsep.2024.102450. URL https://doi.org/10.1016/j.tsep.2024.102450.

[34] Jörg Leicher. Investigations into the use of natural gas / hydrogen blends and hydrogen for decarbonization in the glass industry. In *Proceedings of the Floene Conference: Roadmap for the Introduction of Renewable Gases in the Industrial Sector*, Lisbon, Portugal, December 2022. URL https://www.gwi-essen.de. Presentation on the HYGLAS Project. Gas- und Wärme-Institut Essen e.V. (GWI).

[35] Jörg Leicher, Bledar Islami, Anne Giese, Klaus Görner, and Johann Overath. Investigations into the use of natural gas/hydrogen blends and hydrogen for decarbonization in the glass industry. In *Proceedings of the 13th International Conference on Industrial Furnaces and Boilers (INFUB-13)*, pages 1–12, Algarve, Portugal, April 2022. INFUB. URL https://www.gwi-essen.de.

[36] Bledar Islami, Anne Giese, Marcel Biebl, Bernhard Fleischmann, and Johann Overath. Wasserstoffnutzung in der Glasindustrie als Möglichkeit zur Reduzierung von CO_2-Emissionen und des Einsatzes erneuerbarer Gase – Untersuchung der Auswirkungen auf den Glasherstellungsprozess und Analyse der Potenziale in NRW (Akronym: HyGlass). Abschlussbericht (Final Project Report) PRO 0087 A / PRO 0087 B, Gas- und Wärme-Institut Essen e.V. (GWI) and Hüttentechnische Vereinigung der deutschen Glasindustrie e.V. (HVG) and Bundesverband Glasindustrie e.V. (BV Glas), Essen/Düsseldorf, Germany, December 2021. URL https://www.gwi-essen.de. Funded by the Ministerium für Wirtschaft, Innovation, Digitalisierung und Energie des Landes Nordrhein-Westfalen under the IN4CLIMATE.NRW initiative.

[37] Portgás – Componente de Redes de Gás. Infraestrutura de distribuição e transição para gases renováveis. Website oficial institucional, 2026. URL https://www.portgas.pt/. Acedido em: 1 de junho de 2026.

[38] Portgás – Componente de Redes de Gás. Projeto h2 @ braga: Injeção de hidrogénio verde na rede de distribuição de gás natural. Website oficial do projeto piloto, 2026. URL https://www.portgas.pt/gases-renovaveis/projeto-h2-braga/. Acedido em: 1 de junho de 2026.

[39] Filipe F. Mil-Homens, Alexandre Gamboa, Bruno Gouveia, Henrique Santos, and ; Edgar Fernandes. Estudo sobre o impacto da injecção de hidrogénio no sng em tecnologias de combustão relatório técnico. Technical report, Instituto Superior Técnico (IST) – Laboratory of Combustion, Thermofluids and Energy Systems (IN+), 12 2025. Tenchnical Report- REN (Redes Energéticas Nacionais).

[40] European Commission. Repowereu with clean energy going faster and further with clean energy projects. *Publications Office of the European Union*, pages 1–2, 5 2022. doi: 10.277

5/528866. URL https://ec.europa.eu/commission/presscorner/api/files/attachment/872548/FS_CleanEnergy.pdf.

[41] International Organization for Standardization (ISO). Iso 6976:2016 - natural gas — calculation of calorific values, density, relative density and wobbe indices from composition. Technical report, ISO, 8 2016. URL www.iso.orgiTehSTANDARDPREVIEW.

[42] European Committee for Standardization (CEN). En 437:2021 - test gases - test pressures - appliance categories. Technical report, CEN (European Committee for Standardization), 7 2021.

[43] M. Prussi, M. Padella, M. Conton, E. D. Postma, and L. Lonza. Review of technologies for biomethane production and assessment of eu transport share in 2030. *Journal of Cleaner Production*, 222:565–572, 6 2019. ISSN 09596526. doi: 10.1016/j.jclepro.2019.02.271.

[44] N. Keogh, D. Corr, and R. F. D. Monaghan. An environmental and economic assessment for biomethane injection and natural gas heavy goods vehicles. *Applied Energy*, 360:122800, 2024. doi: 10.1016/j.apenergy.2024.122800. URL https://doi.org/10.1016/j.apenergy.2024.122800.

[45] IEA Bioenergy. Energy from biogas: Iea bioenergy task 37 end of triennium report 2019-2021. Technical report, https://www.ieabioenergy.com/publications/, 2022. URL http://task37.ieabioenergy.com/about-task-37.html.

[46] Abubakar Jibrin Abbas, Hossein Hassani, Martin Burby, and Idoko Job John. An investigation into the volumetric flow rate requirement of hydrogen transportation in existing natural gas pipelines and its safety implications. *Gases*, 1(4):156–179, 2021. doi: 10.3390/gases1040013. URL https://doi.org/10.3390/gases1040013.

[47] Harmen de Vries, Anatoli V. Mokhov, and Howard B. Levinsky. The impact of natural gas/hydrogen mixtures on the performance of end-use equipment: Interchangeability analysis for domestic appliances. *Applied Energy*, 208:1007–1019, 2017. doi: 10.1016/j.apenergy.2017.09.049. URL https://doi.org/10.1016/j.apenergy.2017.09.049.

[48] Mengxiao Sun, Xiaomei Huang, Yelong Hu, and Shan Lyu. Effects on the performance of domestic gas appliances operated on natural gas mixed with hydrogen. *Energy*, 244:122557, 2022. doi: 10.1016/j.energy.2021.122557. URL https://doi.org/10.1016/j.energy.2021.122557.

[49] Yamei Lan, Zheng Wang, Jingxiang Xu, and Wulang Yi. The impact of hydrogen on flame characteristics and pollutant emissions in natural gas industrial combustion systems. *Energies*, 17(19):4959, 2024. doi: 10.3390/en17194959.

[50] Inês. Rondão. Transformação de fornos cerâmicos rumo à transição energética. Technical report, CTCV – Centro Tecnológico da Cerâmica e do Vidro, 2 2023. URL https://www.industriadefuturo.pt/repositorio/.

[51] British Ceramic Confederation. Hydrogen for the ceramics sector: Industrial fuel switching phase 1 final report. Technical report, British Ceramic Confederation, 2023. Industrial Fuel Switching Phase 1 feasibility study.

[52] British Ceramic Confederation. Feasibility study for progreen h2. Technical report, Department for Business, Energy and Industrial Strategy, 2023. URL https://assets.publishing.service.gov.uk/media/648089165f7bb7000c7fa665/iha-2a-cen-cpi-progreen-h2-final-report.pdf. Accessed: 2026-06-13.

[53] Md Monjur Hossain Bhuiyan, Nitesh Subedi, and Zahed Siddique. Material compatibility in hydrogen infrastructure: Challenges, advances, and future prospects, 11 2025. ISSN 03603199. URL https://doi.org/10.1016/j.ijhydene.2024.152138.

[54] Jose M. Chamorro e Mikel Gonzalez-Eguino Luis M. Abadie. Technical and economic report of hydrogen injection in natural gas networks. Technical report, BC3 - Basque Centre for Climate Change, 6 2023. URL https://info.bc3research.org/2021/06/15/technical-and-economic-report-of-hydrogen-injection-in-natural-gas-networks/.

[55] Hydrogen Europe Research. Compatibility of polymer-based materials for the hydrogen transport infrastructure. Position paper, Hydrogen Europe Research, Brussels, Belgium, November 2025. URL https://www.hydrogeneuroperesearch.eu.

[56] Marco Cavana and Pierluigi Leone. Smart gas network with linepack managing to increase biomethane injection at the distribution level. *Energies*, 15(21):8198, 2022. doi: 10.3390/en15218198. URL https://doi.org/10.3390/en15218198.

[57] Giulio Guandalini, Paolo Colbertaldo, and Stefano Campanari. Dynamic quality tracking of natural gas and hydrogen mixture in a portion of natural gas grid. *Energy Procedia*, 75: 1037–1043, 2015. doi: 10.1016/j.egypro.2015.07.473. URL https://doi.org/10.1016/j.egypro.2015.07.473.

[58] Elmer R Weaver. Formulas and graphs for representing the interchange-ability of fuel gases. Technical report, Journal of Research of the National Bureau of Standards, 3 1951.

[59] Anatolii Kolienko, Rasul Ahmednabiev, Oksana Demchenko, Olha Hukasian, and Volodymyr Semko. *Interchangeability of various combustible gases and adaptation of gas-using equipment for their efficient combustion*, volume 1348. IOP Publishing, 2024. doi: 10.1088/1755-1315/1348/1/012048.

[60] Stanislav Honus, Shogo Kumagai, and Toshiaki Yoshioka. Replacing conventional fuels in usa, europe, and uk with plastic pyrolysis gases - part ii: Multi-index interchangeability methods. *Energy Conversion and Management*, 126:1128–1145, 2016. doi: 10.1016/j.enconman.2016.08.061. URL https://doi.org/10.1016/j.enconman.2016.08.061.

[61] Hadhami Bdioui, Hazem Touati, Maher Ben Chiekh, and Angeles López-Agüera. Green hydrogen blending into the tunisian natural gas distributing system. *Hydrogen*, 5(4):1004–1019, 2024. doi: 10.3390/hydrogen5040054. URL https://doi.org/10.3390/hydrogen5040054.

[62] Vanderson Delapedra-Silva, Paula Ferreira, Jorge Cunha, and Herbert Kimura. Methods for financial assessment of renewable energy projects: A review. *Processes*, 10(2):184, 2022. doi: 10.3390/pr10020184. URL https://doi.org/10.3390/pr10020184.

[63] Roxana T. Shafiee and Daniel P. Schrag. Carbon abatement costs of green hydrogen across end-use sectors. *Joule*, 8:3281–3289, 12 2024. ISSN 25424351. doi: 10.1016/j.joule.2024.09.003.

[64] Agora Energiewende, Agora Industry, and Umlaut. Levelised Cost of Hydrogen: Making the Application of the LCOH Concept More Consistent and More Useful. Impulse Study 301/05-I-2023/EN, Agora Energiewende, Berlin, Germany, July 2023. URL https://www.agora-energiewende.de. Developed within the framework of the H2 Trans4Real project.

[65] European Hydrogen Observatory and Clean Hydrogen JU. Levelised cost of hydrogen (lcoh) calculator manual: Update of the may 2024 manual. Technical report / methodology manual,

European Hydrogen Observatory, Clean Hydrogen Joint Undertaking, Brussels, Belgium, May 2025. URL https://www.hydrogen-observatory.ec.europa.eu. Based on research conducted by Hydrogen Europe. Version 3.1.

[66] Tristan Gilbert, Akanksha K. Menon, Chris Dames, and Ravi Prasher. Heat source and application-dependent levelized cost of decarbonized heat. *Joule*, 7:128–149, 1 2023. ISSN 25424351. doi: 10.1016/j.joule.2022.11.006.

[67] Luis M. Abadie and José M. Chamorro. European co2 prices and carbon capture investments. *Energy Economics*, 30:2992–3015, 11 2008. ISSN 01409883. doi: 10.1016/j.eneco.2008.03.008.

[68] International Organization for Standardization. Buildings and constructed assets — service life planning — part 5: Life-cycle costing. Standard ISO 15686-5:2017, International Organization for Standardization, Geneva, Switzerland, 2017. URL https://www.iso.org/standard/61148.html.

[69] Andrea Demurtas, Mohammad Ansarin, Csinszka Bene, Anna Kralli, Timo van Delzen, and Luc van Nuffel. Overview of the diffusion of power purchase agreements and contracts for difference across member states: Existing barriers and tools to favour their uptake. Study requested by the ITRE Committee PE 780.416, European Parliament, Policy Department for Transformation, Innovation and Health, Brussels, Belgium, 2026. URL https://www.europarl.europa.eu.

[70] Wouter Grimme and Gemma Toop S. Alberici. Biomethane production potentials in the eu: Feasibility of repowereu 2030 targets, production potentials in the member states and outlook to 2050. Technical report, Gas for Climate / Guidehouse, 7 2022. URL https://gasforclimate2050.eu/.

[71] Adrian Odenweller and Falko Ueckerdt. The green hydrogen ambition and implementation gap. Technical report, Nature Communications, 2024. URL https://www.nature.com/articles/s41467-023-44414-6.

[72] ENTSOG (European Network of Transmission System Operators for Gas). Report on annual renewable gas injections into gas networks 2026. Technical report, ENTSOG, 2026. URL https://www.entsog.eu/publications.

[73] Sebastian Busch, Ruben Kasdorp, Derck Koolen, Arnaud Mercier, and Magdalena Spooner. The development of renewable energy in the electricity market. Technical Report 187, European Commission, Directorate-General for Economic and Financial Affairs, Brussels, June 2023.

[74] Jonas Meckling, Thomas Sterner, and Gernot Wagner. Policy sequencing toward decarbonization. *Nature Energy*, 2(12):918–922, 2017. doi: 10.1038/s41560-017-0025-8.

[75] Friedemann Polzin, Paschen von Flotow, Michael Migendt, and Florian Täube. Public policy influence on renewable energy investments—a panel data study across OECD countries. *Energy Policy*, 80:98–111, 2015. ISSN 0301-4215. doi: 10.1016/j.enpol.2015.01.026.

[76] Direção-Geral de Energia e Geologia. Relatório de monitorização da segurança de abastecimento do sistema nacional de gás para o período 2025–2040 (rmsa-g 2024). Technical report, Direção-Geral de Energia e Geologia, Lisboa, Portugal, 2025. URL https://www.dgeg.gov.pt/pt/areas-setoriais/energia/planeamento-energetico-e-seguranca-de-abastecimento/seguranca-de-abastecimento/monitorizacao-da-seguranca-de-abastecimento/.

[77] Portugal. Governo. Decreto-lei n. 62/2020, de 28 de agosto. Diario da Republica, 1.a serie, n. 168/2020, August 2020. URL https://diariodarepublica.pt/dr/detalhe/decreto-lei/62-2020-141377978. Estabelece a organizacao e o funcionamento do Sistema Nacional de Gas e procede a transposicao da Diretiva (UE) 2019/692. Accessed: 2026-06-29.

[78] LNEG – Laboratório Nacional de Energia e Geologia. Portal do Biometano. https://biometano.lneg.pt/, 2026. Organização: Ministério do Ambiente e Energia. Acedido em: 29 de junho de 2026.

[79] Portugal. Presidência do Conselho de Ministros. Resolução do Conselho de Ministros n.º 41/2024: Aprova o Plano de Ação para o Biometano 2024-2040. URL https://diariodarepublica.pt.

[80] Volker Krey IIASA, Omar Masera, Geoffrey Blanford USA, Thomas Bruckner, Roger Cooke, Karen Fisher-Vanden, Kornelis Blok, R Pichs-Madruga, Y Sokona, E Farahani, S Kadner, K Seyboth, A Adler, I Baum, S Brunner, P Eickemeier, B Kriemann, J Savolainen, S Schlömer, C von Stechow, T Zwickel, and JC Minx. 2006 ipcc guidelines for national greenhouse gas inventories (volume 2: Energy). Technical report, Stationary Combustion (Chapter 2), 2006. URL https://www.ipcc-nggip.iges.or.jp/public/2006gl/vol2.html.

[81] Comissão Europeia. Regulamento delegado (UE) 2024/873 da Comissão, de 30 de janeiro de 2024, que altera o Regulamento Delegado (UE) 2019/331 no que respeita às regras transitórias da União aplicáveis à atribuição harmonizada de licenças de emissão a título gratuito, apr 2024. URL https://eur-lex.europa.eu/legal-content/PT/TXT/?uri=CELEX:32024R0873. Acedido em: July 20, 2026.

[82] European Commission. Carbon leakage, 2026. URL https://climate.ec.europa.eu/eu-action/carbon-markets/eu-emissions-trading-system-eu-ets/free-allocation/carbon-leakage_en. Accessed: 2026-06-12.

[83] Portugal. Ministério do Ambiente e da Ação Climática. Portaria n.º 15/2023: Estabelece o sistema de compra centralizada de biometano e hidrogénio produzido por eletrólise a partir da água. ´iário da República, 1.ª série, n.º 3, pp. 34–36, 2023. Publicado em 4 de janeiro de 2023. Disponível em: https://diariodarepublica.pt/dr/detalhe/portaria/15-2023-205561081.

[84] Direção-Geral de Energia e Geologia (DGEG). Resultados do 1º leilão eletrónico para a compra centralizada de biometano e hidrogénio produzido por eletrólise a partir da Água. Ministério do Ambiente e Energia, República Portuguesa, Fevereiro 2025. Relatório de Homologação de Resultados assinado a 11 de fevereiro de 2025.

[85] Biomethane Industrial Partnership. Current biomethane production costs from real industry data. Task force 4.2 report, Biomethane Industrial Partnership, November 2023. URL https://bip-europe.eu/2023/11/02/executive-summary-and-slidedeck-available-for-download-task-force-4-2-reveals-current-biomethane-production-costs-from-real-industry-data/. Executive summary and slidedeck on European biomethane production costs based on real industry data.

[86] Maria Olczak. Biomethane in europe: Why scaling up is harder than it looks. OIES Paper NG 203, The Oxford Institute for Energy Studies (OIES), January 2026. URL https://www.oxfordenergy.org/. Analysis of systemic challenges, supply chains, and regulatory barriers in scaling EU renewable gas production.

[87] European Energy Exchange (EEX). EU ETS Auctions: Primary Market Allocation and

Clearing Data. Official Auction Platform, EEX Environmental Markets, 2026. URL https://www.eex.com/en/markets/environmental-markets/eu-ets-auctions. Accessed: June 2026. Common Auction Platform for EU Member States under Directive 2003/87/EC.

[88] Thomas Aspinall, Adrian Gepp, Geoff Harris, Simone Kelly, Colette Southam, and Bruce Vanstone. Estimation of a term structure model of carbon prices through state space methods: The european union emissions trading scheme. *Accounting & Finance*, 61(2):3797–3819, 2021. doi: 10.1111/acfi.12708. URL https://onlinelibrary.wiley.com/doi/abs/10.1111/acfi.12708.

[89] Homaio. A guide to EU ETS assets: EUA futures and EUA spot. Homaio Blog, February 2024. URL https://www.homaio.com/post/a-guide-to-eu-ets-assets-exploring-the-difference-between-eua-futures-and-eua-spot. Explains the distinction between EUA futures and EUA spot contracts.

[90] IEA Bioenergy (ou International Energy Agency). Renewable gas: Deployment, markets and sustainable trade. Technical report, IEA Bioenergy, 2022. URL https://www.ieabioenergy.com/publications/.

[91] Matteo Prussi, Monica Padella, M. Reale, S. Fazio, and P. Costamagna. Biomethane deployment in the european union: A review of production, market status, and support frameworks. *Renewable and Sustainable Energy Reviews*, 173:113113, 2023. doi: 10.1016/j.rser.2022.113113.

[92] British Glass. Glass sector net zero strategy 2050. Sector decarbonisation strategy report, British Glass Manufacturers' Confederation, 2021. URL https://www.britglass.org.uk/. Analysis of alternative low-CO2 raw materials, hydrogen combustion (Hyglass project), and process electrification (VERCANE project).

[93] Progressive Energy. Hynet industrial fuel switching: Phase 3 report. Technical report, Department for Business, Energy & Industrial Strategy (BEIS), 2022. URL https://assets.publishing.service.gov.uk/government/uploads/system/uploads/attachment_data/file/866401/HS42_-Progressive_Energy-_HyNet_Industrial_Fuel_Switching.pdf.

[94] MIBGAS. Mibgas daily prices. Iberian Gas Market, 2026. URL https://www.mibgas.es/en/market-results/daily-price/gnl-tvb. Accessed: 2026-06-30.

[95] Eurostat. Natural gas price statistics: Non-household consumers. Eurostat Statistics Explained, 2026. URL https://ec.europa.eu/eurostat/statistics-explained/index.php/Natural_gas_price_statistics. Accessed: 2026-06-30. Non-household natural gas prices for Portugal, H2 2025.

[96] Gabriel Sousa. Floene vê 50 projetos de biometano gerarem investimento de 1,5 mil milhões até 2030. ECO – Economia Online (Entrevista), January 2026. URL https://eco.sapo.pt/entrevista/floene-ve-50-projetos-de-biometano-gerarem-investimento-de-15-mil-milhoes-ate-2030/.

[97] European Commission. Eu reference scenario 2020: Energy, transport and ghg emissions – trends to 2050, 2021. URL https://op.europa.eu/en/publication-detail/-/publication/96c2ca82-e85e-11eb-93a8-01aa75ed71a1/language-en.

[98] Enerdata. Enerfuture: World energy forecasts and modelling. Enerdata Research, 2024. URL https://www.enerdata.net/research/forecast-enerfuture.html. Cenário EnerBlue (NDC-aligned): preços de gás na Europa projectados em alta até 2040.

[99] European Energy Exchange (EEX). Environmental indices: ECarbix and CBAM reference price market data. Official Market Data Hub, EEX Platform, 2026. URL https://www.eex.com/en/markets/environmentals/environmental-indices. Accessed: June 2026. Spot and futures price references for EU Allowances (EUA) under the EU ETS framework.

[100] Malvika Gurung and Rachael Rajan. Realized volatility: What is it, calculation, importance & limitations. Investing.com Academy Center, Analysis Section, April 2026. URL https://www.investing.com/academy/analysis/realized-volatility-definition/. Accessed: June 2026. Methodology for historical standard deviation and annualization of asset returns.

[101] Clean Hydrogen Joint Undertaking. Hydrogen Valleys. https://www.clean-hydrogen.europa.eu/get-involved/hydrogen-valleys_en, 2026. Accessed: 2026-06-29.

[102] Portgás. RelatÓrio: Indicadores de caracterização da concessão 2025 – municípios. Relatório Técnico REL.AT-038, Portgás – Sociedade de Produção e Distribuição de Gás, S.A., Porto, Portugal, 2025. Dados estatísticos e operacionais da infraestrutura de distribuição de gás natural por concelho.

[103] US Environmental Protection Agency. U.s. container glass industry carbon intensities (2019). Technical Report EPA 430-F-22-005, US EPA, 2022. URL https://www.epa.gov/system/files/documents/2022-06/2019%20Container%20Glass%20Plant%20Carbon%20Intensities%20Fact%20Sheet%20.pdf.

[104] Marex. Europe's biomethane market: 2026 outlook and the road ahead. Marex / CSC Commodities, December 2025. URL https://www.marex.com/news/2025/12/european-biomethane-market-2025-trends-and-2026-outlook/.

[105] Direção-Geral de Energia e Geologia (DGEG). Plano de ação para o biometano (pab) 2024-2040: Rascunho para consulta pública. Relatório técnico, Ministério do Ambiente e da Energia, República Portuguesa, Lisboa, Portugal, 2024. URL https://www.dgeg.gov.pt. Acedido em junho de 2026. Define as metas de incorporação de gases renováveis na Rede Pública de Gás Natural (RPGN).

[106] REN – Redes Energéticas Nacionais. Relatório e contas setembro 2024: Demonstrações financeiras consolidadas. Technical report, REN – Redes Energéticas Nacionais, SGPS, S.A., 2024. URL https://www.ren.pt/media/12abvgtd/relatorio-e-contas-9m2024.pdf.

[107] M. Holst et al. Learning in green hydrogen production: Insights from a novel european dataset, June 2025. URL https://www.sciencedirect.com/science/article/pii/S0360319925027661.

[108] Wood Mackenzie. Enforcement and investment: How red iii is shaping the hydrogen market in the eu. Wood Mackenzie Opinion, August 2025. URL https://www.woodmac.com/news/opinion/enforcement-and-investment-how-red-iii-is-shaping-the-hydrogen-market-in-the-eu/.

[109] International Renewable Energy Agency. Green hydrogen cost reduction: Scaling up electrolysers to meet the 1.5°c climate goal. Technical report, IRENA, Abu Dhabi, 2020. URL https://www.irena.org/-/media/Files/IRENA/Agency/Publication/2020/Dec/IRENA_Green_hydrogen_cost_2020.pdf. Accessed: 2026-07-05.

[110] R. P. Borges et al. Green hydrogen production at the gigawatt scale in portugal: A technical and economic evaluation. *Energies*, 17(7):1638, 2024. doi: 10.3390/en17071638.

[111] International Energy Agency. Global hydrogen review 2024. Technical report, IEA, 2024. URL https://www.iea.org/reports/global-hydrogen-review-2024. Accessed: 2026-07-05.

[112] Hydrogen Europe. Clean hydrogen production pathways report 2024. Technical report, Hydrogen Europe, 2024. URL https://hydrogeneurope.eu/wp-content/uploads/2024/06/2024_H2E_CleanH2ProductionPathwaysReport.pdf. Accessed: 2026-07-05.

[113] APREN. Anuário 2025: Resumo do ano 2024. Technical report, Associação Portuguesa de Energias Renováveis, 2025. URL https://anuario.apren.pt/contents/APREN-ANUARIO_RESUMO_DE_ANO.pdf. Accessed: 2026-07-05.

[114] ERSE. Annual report on the electricity and natural gas markets in 2024. Technical report, Entidade Reguladora dos Serviços Energéticos, 2025. URL https://www.erse.pt/media/w13jyupd/relat%C3%B3rio-ce-2024_en.pdf. Accessed: 2026-07-05.